Mechanistic basis of RHD3 function in formation of interconnected tubular ER network

Jiaqi Sun

Biology Department, McGill University, Montreal

January 2018

A thesis submitted to McGill University in partial fulfillment of the requirements of the degree of Doctor of Philosophy

TABLE OF CONTENTS

LIST OF FIGURES

ABSTRACT

The endoplasmic reticulum (ER) is an interconnected membrane network of tubules and sheets found in all eukaryotic cells. The formation of this interconnected network requires homotypic fusion of ER membranes, which is mediated by a family of dynamin-like large Atlastin GTPases, including mammalian Atlastins, yeast Sey1p and plant RHD3 (ROOT HAIR DEFECTIVE 3). As a plant member of Atlastin GTPases, the mechanistic basis of how RHD3 acts in ER membrane fusion process is largely unknown.

In the first part of the thesis, a systemic structure-function analysis of the action of different RHD3 domains in mediating ER fusion was conducted. Similar to Atlastins in mammalian cells and Sey1p in yeast cells, RHD3 has a GTPase domain in the N-terminus, a 3-helix bundle (3HB) enriched middle domain, two transmembrane domains and amphipathic C-terminal domain. I found that the GTPase domain and the first and second 3HBs in the middle domain promote the dimerization of RHD3. This dimerization of RHD3 is required for efficient ER membrane fusion. On the other hand, the third and fourth 3HBs are required for the protein stability of RHD3. I also found that the transmembrane domains (TMs) of RHD3 not only serve as an ER membrane anchor, but also facilitate the oligomerization of RHD3. In the C-terminal tail of RHD3, there is an amphipathic helix. I revealed that this amphipathic helix has a special membrane anchoring ability and is required for efficient ER membrane fusion. With this work, I contribute to a deeper understanding of the mechanistic basis of action of RHD3 in mediated ER membrane fusion.

To maintain the ER homeostasis, the fusion action of Atlastin GTPases must be regulated and balanced. However, the knowledge of the regulation of action of Atlastin GTPses is very limited.

Lunapark proteins (LNPs), a family of proteins known to be required for maintaining a normal tubular ER morphology, have been recently found to act antagonistically with Sey1p in yeast cells. But the exact molecular mechanisms how LNPs antagonize the action of Atlastin GTPases remain unclear. In the second part of the thesis, I found that there are two LNP homologs, LNP1 and LNP2 in *Arabidopsis*, both of them interact with RHD3 on 3-way junctions of the ER. Loss of LNPs in *Arabidopsis* cause plants to grow short root hairs and to be dwarfed. Additionally, massive sheet ER containing dense 3-way junctions is found in the cells. LNP1 and LNP2 are localized to 3-way-junctions of the ER where they stabilize the newly formed 3-way junctions of the ER. I revealed that LNPs are recruited by RHD3, after the ER membrane fusion, to the newly formed 3-way junctions. They can inhibit the fusion action of RHD3 likely by promoting the protein degradation of RHD3. With this work, I propose a novel post-membrane fusion regulation for RHD3 in which the RHD3 protein is degraded by the action of LNPs to avoid excessive fusion for the generation of an interconnected ER with an open polygonal network.

RÉSUMÉ

Le réticulum endoplasmique est un organite dans les cellules eucaryotes composé de tubules et de plaques membraneuses. Ces tubules et plaques interconnectées sont crée par des fusions homotypiques entre le réticulum endoplasmique, ce qui est contrôlé par une famille de protéines appelés Atlastin GTPases (similaire à la dynamine). Cette famille inclut des Atlastins mammifères, Sey1p des cellules levures, et RHD3 (ROOT HAIR DEFECTIVE 3) des plantes. Le mécanisme dont RHD3 régule la fusion des membranes du réticulum endoplasmique n'est pas connu.

La première partie de cette thèse s'agit d'une analyse systémique de la structure et fonction de chaque domaine protéique de RHD3 par rapport à son rôle dans la fusion des membranes réticulum endoplasmique. Comme les Atlastins (mammifères) et Sey1p (cellules de levure), RHD3 a: une domaine GTPase à son N-terminale, des faisceau de trois hélices dans la milieu domaine protéique, et aussi deux domaines transmembranaire et une domaine amphipathique à son C-terminale. Les donnés démontrent que la domaine GTPase et le premier et deuxième faisceau d'hélices se sont responsables pour la dimérisation de RHD3. La dimérisation de RHD3 est requit pour la fusion du réticulum endoplasmique. Par contre, le troisième et quatrième faisceau d'hélices sont requises pour la stabilité protéique de RHD3. Les domaines transmembranaires contrôlent l'oligomérisation de RHD3, et la domaine amphipathique à la C-terminale est capable d'ancrer RHD3 au réticulum endoplasmique, ce qui est requit pour maximiser la fusion membranaire. Ce travail aide à mieux comprendre les mécanismes par lesquels RHD3 fonctionne pour réguler la fusion membranaire du réticulum endoplasmique.

Pour maintenir l'homéostasie du réticulum endoplasmique, la fonction des Atlastin GTPases doivent être régulés précisément, ce qui n'est pas bien connu. « Lunapark proteins (LNPs) », une famille de protéines qui maintiennent la morphologie tubulaire du réticulum endoplasmique, était récemment démontré d'avoir un effet antagoniste avec Sey1p dans les cellules de levure. Comment LNP fonctionne pour avoir un effet antagoniste avec Atlastin GTPases n'est pas claire. J'ai identifié deux homologues de LNP, LNP1 et LNP2 dans *Arabidopsis*. LNP1 et LNP2 interagirent avec RHD3 aux jonctions de trois surfaces du réticulum endoplasmique. La perte de fonction des LNPs dans *Arabidopsis* résulte dans des plus petites plantes avec des poils racinaires raccourcis, et du réticulum endoplasmique en forme de plaques avec plusieurs jonctions de trois surfaces. LNP1 et LNP2 sont localisés jonctions de trois surfaces du réticulum endoplasmique et jouent un rôle stabilisateur; ils stabilisent les jonctions de trois surfaces qui étaient récemment crée. J'ai démontré que les LNPs sont recrutés aux jonctions après la fusion membranaire du réticulum endoplasmique par RHD3. Avec ces donnés, je propose que RHD3 est régulé par LNP dans le façon suivant: après la fusion membranaire, RHD3 est dégradé (suivant un signal de LNP) pour éviter d'avoir trop de fusion membranaire dans le réticulum endoplasmique, ce qui empêcherait le réticulum de fonctionner comme il faut.

ACKNOWLEDGEMENTS

First of all, I would like to sincerely thank my supervisor Dr. Hugo Zheng for mentoring me over the course of my studies. His patient and relentless guidance take me step into the world of science, where I encountered the wonder of life under microscopy. He gives me not only profound and thoughtful suggestions on the research, but also, more importantly, on how to do a critical thinking and have an overall insight, on how to talk with other scientists and give a concise scientific talk, on how to prepare a high-level manuscript and on how to respond to the comments of the reviewers. Being one of his students, I feel truly honored!

I would like to give my gratitude to my supervisory committee members, Dr. Tamara Western and Dr. Nam-Sung Moon for their valuable and constructive suggestions on my projects in each committee meeting.

I really appreciate the help from my previous lab colleagues Dr. Xingyun Qi and Dr. Mi Zhang. They gave me a lot of useful technical support especially at the early stage of my Ph.D study. I would like to thank Dr. Nooshin Movahed for the transmission electron microscopy analysis of the *lnp1 lnp2* mutant, which showed a new perspective of the function of LNPs.

I would like to thank the Chinese Scholarship Council for financial support of my Ph.D study.

Finally, my deepest and grateful thanks to my family for encouraging and supporting my decisions, and my dear little cat, Yang, for being with me during my hardest time and help me grow up from a boy to a man.

PREFACE AND CONTRIBUTIONS OF AUTHORS

The thesis of my Ph.D study is presented in a manuscript-based format, consisting of an introduction (Chapter I), two research chapters (Chapter II and III) and a conclusion chapter (Chapter IV). Chapter II is a published paper and Chapter III is a submitted manuscript, so these two chapters are simply re-formatted version of the manuscripts, which are composed of abstract, introduction, results, discussion, and methods. Each chapter has their own references. All the chapters in this thesis are written by myself. I design and performed all the experiments in Chapter II and III. My supervisor helped me design experiments in Chapter II and Chapter III, and helped me prepare the writings in all the chapters.

Chapter I is a literature review, giving an introduction on the current knowledge of the interaction between the ER and the other organelles, and the mechanisms of the shaping and regulation of the ER by different factors with a focus on plant cells.

Chapter II is a published manuscript.

This chapter is a re-formatted version of:

Sun, J., and Zheng, H. (2018). Efficient ER Fusion Requires a Dimerization and a C-Terminal Tail Mediated Membrane Anchoring of RHD3. Plant Physiol. 176: 406-417.

Chapter III is a submitted manuscript to Nature Communications.

This chapter is a re-formatted version of:

Sun, J., and Zheng, H. (2018). An inhibition of RHD3 fusion activity by Lunapark is essential for generation of interconnected tubular ER network. Submitted.

ABBREVIATIONS

AD – alzheimer disease

APH – amphipathic helix

ATL - atlastin

ATP – adenosine triphosphate

BiFC – bimolecular florescence complementation

CT – C-terminal tail

Co-IP – co-immunoprecipitation

DNA – deoxyribonucleic acid

EE – early endosome

EMS – ethyl methane sulfonate

ER – endoplasmic reticulum

ERAD – ER-associated degradation

ERES – endoplasmic reticulum exit site

ERMES – ER-mitochondria encounter structure

EPCS – ER-PM contact site

FLS2 – flagellin-sensitive2

GD – GTPase domain

GDP – guanosine diphosphate

GDI – GDP-dissociation inhibitor

GEF – guanine nucleotide exchange factor

GFP – green fluorescent protein

GMP-PNP – 5'-guanylyl imidodiphosphate

GTP – guanosine triphophate

HSP – hereditary spastic paraplegia

LatB – latrunculin B

LE – late endosome

LNP - lunapark

MFN - mitofusion

MVB – multi-vesicular bodies

ORF – open reading frame

PI – phosphatidylinositol

PIS – phosphatidylinositol synthase

PLAM – plastid associated membrane

PM – plasma membrane

PVC – prevacuolar compartments

REEP – receptor expression enhancing protein

RFP – red fluorescent protein

RHD3 – root hair defective 3

RL1 – RHD3-like1

RL2 – RHD3-like2

RNA – ribonucleic acid

RNAi – RNA interference

RTN – reticulon

RTNLB – reticulon like protein subfamily B

SCLIM – super-resolution confocal live imaging microscopy

Sey1p – synthetic enhancer of Yop1

SNARE – soluble N-ethylmaleimide-sensitive factor attachment protein receptor

SUS – split ubiquitin system

SYT – synaptotagmin

TAC – tip attachment complex

T-DNA – transfer DNA

TEM – transmission electron microscopy

TGD4 - trigalactosyldiacylglycerol4

TGN – trans-Golgi network

TM – transmembrane domain

TSWV – tomato spotted wilt tospovirus

UPR – unfolded protein response

VAP – vesicle-associated membrane protein-associated protein

VTC – vesicular tubular complex

WT – wild type

YFP – yellow fluorescent protein

3HB – three helix bundle

CHAPTER I:

INTRODUCTION

The endoplasmic reticulum (ER) is an interconnected membrane network, composed of tubules and sheets that span from the outer nuclear envelop to the cell periphery. This structure was first discovered by Keith R. Porter using the electron microscope, and was described as “a lace-like reticulum” (Porter et al., 1945). The ER is necessary for many key cell functions including the biosynthesis, folding, modification, and trafficking of proteins (Shibata et al., 2010), the biosynthesis of phospholipids (Bessoule and Moreau, 2004) and the maintenance of the calcium homoeostasis (Berridge, 2002; Hong et al., 1999; Somlyo et al., 1985). Traditionally the ER is classified into two major forms, the rough and smooth ER based on the presence and absence of ribosomes attached to its surface. The rough ER usually has a sheet-like morphology and is responsible for the biosynthesis of proteins. Conversely, the smooth ER tends to be more tubular in structure and is involved in lipid metabolism, and calcium storage (Carrasco and Meyer, 2011; Chen et al., 2012a). The ER also frequently contacts with other organelles including plasma membrane (PM), Golgi, endosomes, mitochondria, peroxisomes and chloroplasts as well as the cytoskeleton. It has been shown that the ER is a very dynamic membrane network, which undergoes continual remodeling, changing between sheet-like and tubular structures and extension and retraction of tubules in living cells (Nixon-Abell et al., 2016; Sparkes et al., 2009b). Many studies on the ER morphology defective mutants convincingly demonstrate that a correct shape of the ER is crucial in many intracellular events and pathogenesis, for example about 60% of hereditary spastic paraplegias (HSPs), a class of neurologic disorders characterized with a defective lower motor neuron cell development and degeneration from the spinal cord, results from mutations in three ER shaping proteins: spastin (SPG4), atlastin (SPG3A) and REEP1 (SPG31) (Blackstone et al., 2011). The generation and maintenance of an architecture of the ER require the contributions from the cytoskeleton, ER membrane fusogens

and membrane-bending proteins (Westrate et al., 2015). In this chapter, I will focus on the new understandings of how the ER contacts with other organelles and how the structure of ER is shaped and regulated by different factors with a focus on plant cells.

1.1. The ER interconnects with other membrane organelles and cytoskeleton

1.1.1. The ER-Golgi interaction

The Golgi apparatus was first discovered by Camillo Golgi in the Purkinje cells of the cerebellum and was described as "apparato reticolare interno (internal reticular apparatus)" (Golgi, 1898). There was an intense debate regarding the existence of the Golgi apparatus in mammalian cells (Bentivoglio, 1998). In 1951, with the application of electron microscopy, the Golgi apparatus in intestinal epithelium cells was observed (Dalton, 1951). Soon after, the Golgi apparatus was found in all eukaryotic cells, including plant cells (Beams and Kessel, 1968).

In mammalian cells, the Golgi apparatus typically exhibits as stacks of flattened cisternal membranes that are connected to form a ribbon and positioned close to the centrosome, which is usually clustered near the nucleus (Lowe, 2011; Rios and Bornens, 2003). The Golgi is physically separated from the ER but is functionally linked by the presence of an intermediate compartment (ERGIC) or Vesicular Tubular Complex (VTC) that is believed to be formed through the homotypic fusion of transport carriers originated from the ER (Palmer et al., 2009; Zeuschner et al., 2006).

The discrete stacked structure of the Golgi is thought to be evolutionally conserved among eukaryotes, however there are some exceptions in yeast (Ito et al., 2014). In *Schizosaccharomyces pombe* and *Pichia pastoris*, the Golgi apparatus is a stacked cisternae membrane structure, while in *Saccharomyces cerevisiae*, the Golgi membrane scatters in the cytoplasm as individual cisternae, which exhibits tubular network-like structure. The different cisternae are defined as *cis*, *medial*, and *trans* by the localization of the marker proteins (Matsuura-Tokita et al., 2006; Preuss et al., 1992; Rambourg et al., 1993).

In higher plant cells, the Golgi stacks are discrete and mobile. Golgi moves (several micrometers per second) in a stop-and-go fashion along the surface of the ER (Boevink et al., 1998), while in mammalian cells, the Golgi stacks are more or less stationary. The ER and the Golgi stacks are believed to be physically connected in plant cells (Sparkes et al., 2009c). Sparkes et al. (2009c) demonstrated that, after the actin was depolymerized to inhibit Golgi movement, the ER network can be dragged and remodelled in living cells by movement of artificially laser trapped Golgi. This strongly suggests that at least a part of the Golgi stacks are physically linked with the ER membranes in plant cells (Chen et al., 2012a; Sparkes et al., 2009c). In addition, a plant golgin protein AtCASP was found to have a tethering role at the ER-Golgi interface (Osterrieder et al., 2017).

The Golgi apparatus plays central roles in transport and sorting of proteins and lipids that are synthesized in the ER, to their final destinations. An active exchange of membrane and soluble cargos between the ER and Golgi, is believed to be important for their functions and their physical separation (Brandizzi, 2017). There is a general consensus that in mammals and in

yeasts, anterograde protein transport out of the ER to the Golgi is largely dependent on Coat Protein II (COPII) vesicles and the retrograde transport from the Golgi back to the ER is mainly COPI vesicle dependent (Robinson et al., 2015). In plants, the sites marked by COPII coat components (Sec13, Sec23, Sec24 and Sec31) are commonly considered as ER exit sites (ERESs), associated with the ER moving together with the Golgi stacks. Therefore, the ERESs and the Golgi may behave as a single secretory unit that is motile along the ER in plant cells (DaSilva et al., 2004; Stefano et al., 2006). Intriguingly, in plants, there are relatively few reports of vesicles budding from the ER or existing at the interface between the ER and Golgi, which raised a question that whether vesicles are really the vectors of bidirectional traffic between the two organelles in plant cells (Robinson et al., 2015). In contrast, tubular connections between the ER and cis-Golgi is observed in tomograms of osmium-impregnated root material (Robinson et al., 2015), which suggests that tubular-like structures may be used for the trafficking between the ER and Golgi in plant cells. More recently, using an extremely high speed and high resolution microscopy technique, super-resolution confocal live imaging microscopy (SCLIM), a "Hug-and-kiss" action for protein transport out the ER was observed in yeast (*S. cerevisiae*) (Kurokawa et al., 2014). The cargo protein synthesized in the ER is found to be loaded to the ERES first. Then *cis*-Golgi takes a hug-and-kiss action towards the ERES. During the contact between COPII buds/vesicles and *cis*-Golgi, the COPII coat cargo collapses. Then *cis*-Golgi receives cargo and leaves the ERES (Kurokawa et al., 2014). The "Hug-and-Kiss" action is believed, compared to releasing free COPII vesicles into the cytosol, to be a safer and more efficient way to send cargos. This 'Hug-and-kiss' action may also explain why it has been so difficult to observe COPII vesicles in yeast cells by electron microscopy, because the vesicles

stay with the ERES instead of being released into the cytosol (Kurokawa et al., 2014). It will be interesting to see if a similar mechanism exists in plant cells.

1.1.2. The ER-endosome interaction

The internalization of different contents at the plasma membrane is carried out by various endocytic trafficking pathways. The endosomes function in the sorting and delivery of internalized material from the cell surface and the transport of materials from the Golgi to the lysosome or vacuole (Contento and Bassham, 2012). The early endosome (EE) is defined as the first endocytic compartment to accept incoming cargo internalized from the PM. In plant cells, the Trans-Golgi Network (TGN) is the first place that receive endocytic cargo after internalization from the cell surface, and is labeled rapidly by FM4-64, an endocytic tracer that first appears at the PM and then internalized into endosomal structures (Tse et al., 2004). So the TGN is regarded as the plant early endosomes (EE) (Bolte et al., 2004; Viotti et al., 2010). The material endocytosed to the EEs might be recycled back to the plasma membrane, or sorted to the late endosomes (LEs), which will deliver the cargos to the lysosome or vacuole for degradation. In plant cells, as the LEs have multi-vesicular structures, multi-vesicular bodies (MVB) or prevacuolar compartments (PVC) are equivalent to LEs (Contento and Bassham, 2012).

In mammalian cells, contacts between the endosomes and the ER are very pervasive during trafficking (Friedman et al., 2013; Rowland et al., 2014). The endosomes become more tightly associated with the ER through a maturation progress (Friedman et al., 2013). The ER-endosome contact sites also define the position and time of endosome fission (Rowland et al., 2014). The

contacts may be involved in regulating cholesterol sensing and lipid transfer (Rocha et al., 2009). The LEs may take up Ca^{2+} from the ER stores during their maturation (Kilpatrick et al., 2013; Lopez-Sanjurjo et al., 2013; Morgan et al., 2013). In addition, a growing number of proteins that tether endosome with the ER or function at the ER-endosome contact sites have been identified in mammalian cells (Dong et al., 2016; Phillips and Voeltz, 2016; Raiborg et al., 2015). However, there are only few studies on the ER-endosome contacts in plant cells. Recently, the ER network was found to be required for maintaining the spatial distribution and dynamics of endosomes, as well as for proper endocytic traffic (Stefano et al., 2015). Overexpression of RTNLB (a reticulon protein involved in the tubulation of the ER (see next section 2)), which causes extensive remodeling of ER tubules, significantly decreased the dynamics of endosomes (Stefano et al., 2015). In a mutant of *ROOT HAIR DEFECTIVE 3* (*rhd3*), a critical ER membrane fusogen in plant, the spatiotemporal distribution of endosome and endocytosis are compromised, probably due to less-branched ER structure (Stefano et al., 2015).

1.1.3. The ER-Mitochondria interaction

Mitochondria are double-membrane bound organelles, which are best known for their role in the generation of ATP to supply the cellular needs (Roger et al., 2017). In mammalian cells, the ER-mitochondria contacts are ~10 nm at the smooth ER and ~25nm at the rough ER determined using electron tomography (Csordas et al., 2006). This distance is close enough to suspect that the two organelles are tethered by proteins located on the two opposing membranes (Rowland and Voeltz, 2012). Live confocal fluorescence microscopy also revealed that the ER and mitochondria exhibit tightly coupled dynamics and have extensive contacts. Furthermore, ER tubules are suggested to play an important role in marking the mitochondrial division sites

(Friedman et al., 2011). The contacts between ER and mitochondria facilitate inter-organelle calcium and phospholipid exchange (Kornmann et al., 2009). Notably, mitochondria-associated ER membrane related functions are perturbed in Alzheimer disease (AD) (Area-Gomez and Schon, 2016). Several proteins have been identified and proposed to function as the tethering factors of the ER and mitochondria. In a synthetic biology screen, the ER-mitochondria encounter structure (ERMES), which consists of Mmm1, Mdm10, Mdm12 and Mdm34, was identified as a molecular tether between the ER and mitochondria in the yeast (Kornmann et al., 2009). Recently in mammalian cells, the PDZD8 protein was proved to be a functional homolog of the Mmm1 protein, which is essential for regulating Ca^{2+} dynamics in neurons (Hirabayashi et al., 2017). Both mitofusion 1 (MFN1) and MFN2 are known to tether two mitochondria together to direct their fusion (Chen et al., 2003), while MFN2 also tethers mitochondria with the ER, an unusual quality that requires its localization to both organelles (de Brito and Scorrano, 2008).

In plant cells, the knowledge of the contacts between ER and mitochondria is very limited, and there was no ER-mitochondria tethering factor reported yet, but contacts between the ER and mitochondria were also observed in onion stem cells through electron microscopy (Morre et al., 1971). Recently, time-lapse imaging of living cells revealed that contortions and fission of elongated mitochondria occur through physical interactions with the ER mesh (Jaipargas et al., 2015). The mitochondrial morphology may change in response to light and cytosolic sugar levels in an ER mediated manner (Jaipargas et al., 2015).

1.1.4. The ER-Chloroplast interaction

In addition to being the site for photosynthesis, chloroplasts are the hub of plant metabolism (e.g., the synthesis of fatty acids, amino acids, tocophrols and carotenoids), providing biochemical building blocks and energy for the cell (Mehrshahi et al., 2014). The continuity between the ER and chloroplast was found frequently through electron microscopy in different plant cells, such as in green alga, *Chara globularis var. capillacea*, in the lower vascular plant, *Equisetum telmateia*, and in embryonic pea leaf cells (Kaneko and Keegstra, 1996; Mclean et al., 1988). With confocal microscopy imaging and manipulation with a laser scalpel and optical tweezers, strong attracting forces (up to 400 picoNewtons) at the membrane contact sites between the ER and chloroplasts (Plastid associated membranes, PLAMs) were revealed (Andersson et al., 2007). In plant cells, chloroplasts are interconnected by stromules, which are stroma-filled tubular protrusions extended from the outer membranes of the chloroplasts. Stromules also connect chloroplasts with the nucleus, plasma membrane and the ER (Kwok and Hanson, 2004; Schattat et al., 2011). Live imaging and 3D or 4D projection in diverse cell types suggested that the stromule branching correlates with the dynamic rearrangement of cortical ER tubules, possibly through multiple membrane contact sites (Schattat et al., 2011).

The plastid-ER contact sites are proposed to be hemifused-membranes, which can facilitate direct or transporter-independent access of enzymes to the nonpolar compounds in ER and plastids (Mehrshahi et al., 2014). In a transorganellar complementation assay (Mehrshahi et al., 2013), mutations disrupting plastid-resident enzymes in tocopherol and carotenoid synthesis were complemented by retargeting the enzymes to the ER, suggesting at least seven nonpolar, plastid envelope-localized substrates can be accessed from the ER lumen possibly through

PLAMs (Mehrshahi et al., 2013). In addition, the extraplastidic trigalactosyldiacylglycerol4 (TGD4) protein could facilitate the lipid trafficking between the ER and plastid (Xu et al., 2008).

1.1.5. The ER-Peroxisome interaction

Peroxisomes (POs) are single membrane bound organelles, playing pivotal roles in the metabolism of reactive oxygen species and lipid synthesis. Real-time fluorescence microscopy showed that peroxisomal membrane proteins are initially inserted into the ER membrane, subsequently bud off from the ER and mature into the fully functional peroxisomes in yeast (Hoepfner et al., 2005). It has been shown that trafficking of lipids and proteins between the ER and peroxisomes are through vesicles (Agrawal et al., 2011; Lam et al., 2010) or direct membrane contact transfer mechanism (Raychaudhuri and Prinz, 2008; Shai et al., 2016). Isolated highly purified peroxisomes were found to be associated ER membranes through ultrastructural examination in bovine kidney cells (Zaar et al., 1987). In yeast, the contacts between ER and peroxisomes are mediated by Pex30p, Pex31p, Pex3p and Inp1p, which are required for proper peroxisome inheritance (Knoblach et al., 2013; Raychaudhuri and Prinz, 2008). In human cells, ER-peroxisome contact sites were tethered by VAPA/B (vesicle-associated membrane protein-associated protein A/B) and ACBD5 (acyl Co-A binding protein 5) (Costello et al., 2017; Hua et al., 2017). In plant cells, the ER and peroxisomes are also connected to each other, but there may be no luminal continuity between the two organelles (Barton et al., 2013; Sinclair et al., 2009). The change of the redox state can promote the formation of peroxules (extensions from peroxisomes) which connect the peroxisomes with the other organelles including the ER membranes (Sinclair et al., 2009). But the potential ER-peroxisome tethers in plant cells are still unknown.

1.1.6. The ER-PM junctions

In eukaryotic cells, the ER anchors to the plasma membrane (PM) without membrane fusion through largely static structures called ER-PM contact sites (EPCSs) (Bayer et al., 2017). EPCSs were first found by electron microscopy in muscle cells (Porter and Palade, 1957). The existence of EPCSs in plant cells was also observed through electron microscopy (Hepler et al., 1990). EPCSs can be defined as ribosome excluded regions where the ER and PM are closely attached (less than 10nm apart) (Wang et al., 2017a). Time series imaging of the ER structure showed that despite most ER membranes are very quickly moving and remodeling, some ER nodes are relatively stable over time (Sparkes et al., 2009a; Wang et al., 2014). With optical tweezer, the ER tubules could be dragged and moved around some anchoring points, which are believed to be EPCSs (Bayer et al., 2017; Sparkes et al., 2009c). With quantitative live imaging and transmission electron microscopy (TEM) in multiple Arabidopsis tissues, young growing cells are found to have a denser EPCSs than that in the mature cells (McFarlane et al., 2017).

The structure and functions of EPCSs are believed to be regulated and maintained by tethering complexes. In yeast, several protein families are identified as the EPCS tethers, including Ist2 (a member of the TMEM16 ion channel family), the tricalbins (Tcb1/2/3, orthologs of the extended synaptotagmins), vesicle-associated membrane protein-associated protein (VAP) orthologs Scs2 and Scs22 (Manford et al., 2012; Zhang et al., 2012). Loss of these six tethering proteins results in a separation of the ER from the PM and an accumulation of cytoplasmic ER, which leads to a mis-regulated phosphoinositide signaling at the PM, and a constitutively activated unfolded protein response in the ER (Manford et al., 2012). In mammalian cells, the

synaptotagmins are also proposed to mediate the formation of EPCSs, which is PI(4,5)P_2-dependent and Ca^{2+}-regulated (Giordano et al., 2013). Studies have suggested that EPCSs are important for Ca^{2+} level regulation, phosphatidylinositol (PI) metabolism, and lipid transfer (Dickson et al., 2016; Jing et al., 2015; Stefan et al., 2011).

In plant cells, a complex composed of VAP27-1 (a plant homology of VAP proteins), NET protein NET3C, microtubules, and actin filaments, has been proposed to mediate the formation of EPCSs (Wang et al., 2014). The NET superfamily are plant-specific actin binding proteins, which link different endomembrane systems with actin (Hawkins et al., 2014). The functional significance of the EPCSs in Arabidopsis has been suggested (Wang et al., 2016a). For example, the pollen grains of the double mutant *NET3C RNAi*/*net3b-1* were abnormal and unable to germinate (Wang et al., 2014). Either VAP27-1 RNAi mutant or VAP27-1-GFP overexpressing lines are defective in root hair development (Wang et al., 2016a). In Arabidopsis, there are five Synaptotag/min (SYT) proteins, homologs of mammalian extended synaptotagmins and yeast tricalbin proteins (Perez-Sancho et al., 2016). The most well characterized SYT protein is SYT1, which labels distinct EPCSs that are physically separated from NET3C-VAP27-1 enriched EPCSs (Siao et al., 2016). The existence of different EPCSs indicates that there are diverse EPCSs with possible different functions in plant cells. In the absence of SYT1, plants are defective in endocytosis (Kim et al., 2016; Lewis and Lazarowitz, 2010) with a disassembled cortical ER network (Siao et al., 2016). SYT1 is required for tolerance to abiotic stresses, such as salt stress (Schapire et al., 2008), cold stress (Yamazaki et al., 2008) and mechanical stress (Perez-Sancho et al., 2015). Interestingly, SYT1 negatively regulates plant immune responses through endocytosis or plasmodesmata (Levy et al., 2015; Lewis and Lazarowitz, 2010).

Another synaptotagmin protein, SYT2, is found to regulate pollen germination and pollen tube growth, and is involved in conventional exocytosis (Wang et al., 2015). These accumulating evidences indicate that EPCSs in plant cells may be involved in plant cell development and stress response and the remodelling of the ER network (Bayer et al., 2017).

1.1.7. The ER-actin interaction

It is well known that in both animals and plants, the remodeling of the ER network is cytoskeleton-dependent. In animal cells the ER structure is highly dependent on microtubules (Terasaki et al., 1986), however in plant cells, the main contributors to the ER structure are actin filaments (Ueda et al., 2010). *In vitro* and *in vivo* systems showed that the tips of ER tubules move along filamentous actin during tubule elongation (Hamada et al., 2014; Yokota et al., 2011). The ER dynamics was inhibited by the treatments of latrunculin B (Lat B) or cytochalasin B, the actin polymerization inhibitor, or 2,3-butanedione monoxime (BDM), a myosin activity inhibitor (Runions et al., 2006; Sparkes et al., 2009a; Ueda et al., 2010). These treatments produced a more persistent network of ER tubules and larger persistent cisternae (Sparkes et al., 2009a), which suggested that the actomyosin system is not only required for cytoplasmic ER movement, but also the establishment and the maintenance of the ER network structure.

It was proposed that ER tubules may be attached on the anchor points and that actin polymerization can drive the ER tubule growth (Sparkes et al., 2009a). However, the molecular mechanism of the formation of the ER-myosin-actin complex is still not very clear (Buchnik et al., 2015; Chen et al., 2012a; Wang et al., 2017b). The electron micrographs of epidermal cells of *Drosera* suggested a direct attachment of the plant ER to the actin (Lichtscheidl et al., 1990;

Staehelin, 1997). Recently SYP73 was identified as a plant specific and novel ER-associated actin binding protein that is required for normal ER morphology and streaming, as well as plant growth at early stages of development (Cao et al., 2016). Loss of SYP73 would lead to increased ER area and reduced streaming due to depletion of anchoring points between the ER and actin filaments (Cao et al., 2016). In cotton, a novel protein family containing GhCFE1A and GhCFE5 was found to reside on both ER and actin, playing an important role in cotton fibre cell development (Lv et al., 2016; Lv et al., 2015). In *Arabidopsis*, members of the plant-specific Networked (NET) superfamily of actin-binding proteins, are found to localize to the actin filaments and link actin with different membrane compartment, including ER membranes (Deeks et al., 2012; Wang and Hussey, 2017). A NET protein, NET3C, forms homodimers/oligomers with VAP27, which together form complexes with actin and microtubules, anchoring to the ER-PM contact sites (EPCS) (Wang et al., 2014).

1.1.8. The ER-microtubule interaction

In animal cells, the ER is believed to be distributed mainly by microtubules in living cells using two distinct mechanisms, the motor based membrane sliding mechanism and the tip attachment complex (TAC) mechanism (Waterman-Storer et al., 1995; Waterman-Storer and Salmon, 1998). In the motor based membrane sliding model, microtubule motors, kinesin and dynein, drive ER tubule extension towards the cell periphery and in the direction of the cell center, respectively (Wozniak et al., 2009). The TAC model proposed that an ER tubule attaches to and elongates together with the EB1-STIM1 positive end of a growing microtubule, therefore ER tubules grow and shrink with the microtubules (Grigoriev et al., 2008). The interaction between microtubules and the ER is important for the formation and maintaining of the tubular ER network in cells,

because a disruption of microtubules with nocodazole (microtubule depolymerizing drug) causes collapse of the ER via retraction from the cell periphery and conversion of tubules to sheet-like structures (Terasaki and Reese, 1994).

In plant cells, although actin-dependent ER formation and movement predominates, in the dividing and elongating cells, ER movement may be microtubule-dependent. Foissner et al. (2009) observed that at the onset of cell elongation, the cortical ER tubules situated near the plasma membrane frequently co-align with microtubules (Foissner et al., 2009). Recently, the slow extension of the ER tubules was observed after treatment with the actin-depolymerizing drug Latrunculin B (Hamada et al., 2014). It has been suggested that ER tubules may elongate along microtubules in both directions, and microtubules may also provide anchoring points to the ER in the absence of actin filaments (Hamada et al., 2014). Most recently, with a live imaging and pharmacologic modification of root hair growth in the *rhd3-1* mutant, an interplay between the ER and microtubules in the polarized cell growth of root hairs was observed (Qi et al., 2016). The molecular basis of the interaction of the ER and microtubules in plant cells is still poorly understood, except the fact that VAP27 and NET3c work together to link actin, microtubules, ER and PM together at the EPCS (Wang et al., 2014).

1.2. Shaping the ER membranes

Although it is generally accepted that the cytoskeleton plays important roles in regulating ER dynamics and morphology *in vivo*, it is interesting to note that an interconnected tubular ER network can be generated from a *Xenopus* microsomal membrane fraction in a GTP-dependent manner in the absence of microtubules or actin filaments (Dreier and Rapoport, 2000). This

suggested that the cytoskeleton is not absolutely required for ER tubule formation, at least at *in vitro* conditions. Indeed, a dynamic tubular ER membrane structure can be reconstituted by mixing proteoliposomes with purified ER proteins, like Sey1p and Yop1p from yeast in a GTP hydrolysis dependent manner (Powers et al., 2017). In the following sections, I will highlight the action of these ER membrane proteins in the formation of interconnected ER network of tubules and sheets.

1.2.1. ER proteins involved in tubule generation

The diameters of ER tubules are relatively small, ~30 nm in yeast and ~ 60 nm in mammals. Because lipid membranes are typically 5-10 nm in thickness, these extremely curved ER tubular membranes must be stabilized by some mechanisms in this high-energy state (Hu et al., 2011).

With an *in vitro* system, the reticulons (RTNs) and DP1/Yop1p proteins are the first identified proteins involved in the generation of ER tubules as overexpression of these proteins induce tubular membrane structures in the mammalian cells (Voeltz et al., 2006). Conversely, deletion these proteins in yeast or in mammalian cells caused the expansion of ER sheets (Anderson and Hetzer, 2008; Voeltz et al., 2006). Their roles in ER tubulation is verified by experiments that show the purified Rtn1p and Yop1p can deform proteoliposomes into narrow tubules (Hu et al., 2008). Furthermore, RTNs and Yop1p have been proposed to be able to maintain high membrane curvature, whose abundance determines the ratio of the tubules to sheets in the cells (Shibata et al., 2010). *In vivo*, the RTNs and DP1/Yop1p localize preferentially to the ER tubules and the edges of ER sheets (Shibata et al., 2010; Voeltz et al., 2006).

The RTNs and DP1/Yop1p are highly conserved ER membrane proteins with two transmembrane segments that form a wedge-shaped hairpin in the membrane (Hu et al., 2008). It has been revealed that, with this special hairpin conformation, RTNs and DP1/Yop1p occupy more space in the outer leaflet of a membrane bilayer, which produces a local curvature (Hu et al., 2011; Zhang and Hu, 2016). In addition to this unusual hairpin-like transmembrane domain, a C-terminal conserved amphipathic helix (APH) near to the end of the transmembrane domains is also identified to be functionally important for Yop1p in forming ER tubules in yeast (Brady et al., 2015). With the solution NMR, the secondary structure and dynamics of Yop1p were revealed, and an APH was identified. The isolated APH of Yop1p could interact with negatively charged membrane, consistent with the high pI of the helix, which is important for the function of Yop1p in forming ER tubules *in vivo* and *in vitro* (Brady et al., 2015). Consistent with this notion, purified Yop1p form less tubules in neutral lipids, dioleoylphosphatidylcholine (DOPC), than in other lipid mixtures containing significant amounts of anionic lipids (Hu et al., 2008).

In mammals, RTN4A was suggested to inhibit neurite outgrowth after spinal cord injury (Chen et al., 2000; Prinjha et al., 2000) and RTN4b might also inhibit axonal growth (GrandPre et al., 2000). In addition, the RTNs have been linked to Alzheimer's disease (AD), which is always associated with the accumulation of extracellular neuritic plaques composed of β-amyloid and of intracellular neurofibrillary tangles containing hyperphosphorylated microtubule-associated protein tau (Area-Gomez and Schon, 2016). The reticulon family members are binding partners of β-amyloid converting enzyme 1 (BACE1), which reduces the production of β-amyloid (He et al., 2004). Overexpression any of the reticulon proteins reduces the production of β-amyloid. Conversely, reducing the expression of RTN3 increased the secretion of β-amyloid (He et al.,

2004). Mutations in RTN2 cause the hereditary spastic paraplegia (HSP), a group of genetically heterogeneous neurodegenerative conditions (Montenegro et al., 2012). *REEP1*, belonging to the same family of REEP5/DP1, is another commonly mutated gene in HSP. Loss of REEP1 in mice showed severe motor defects and the neurons showed reduced complexity of the peripheral ER (Beetz et al., 2013).

In plants, homologs of RTNs and Yop1 also exists. In *Arabidopsis*, there are 21 RTNLB (for Reticulon Like Protein subfamily B) genes (Nziengui and Schoefs, 2009; Tolley et al., 2008). Overexpression of RTNLB13 and RTNLB1-4 constricts ER membranes and remodels the ER lumen (Sparkes et al., 2010; Tolley et al., 2008). All these five RTNs are preferentially localized on ER tubules and excluded from ER sheets (Sparkes et al., 2010). With Forster resonance energy transfer (FRET) and fluorescence lifetime imaging microscopy, the RTNs are found to interact with themselves and each other (Sparkes et al., 2010). Similar to Yop1p, there is also an APH in the C-terminal region of RTNLB13 and it was found that deletion of the APH or introducing mutations into the hydrophobic face of the APH to disrupt the helix structure abolished the ability of RTN13 to remodel the ER membrane (Breeze et al., 2016). However, APH was not necessarily required for the homotypic interactions or the ER membrane localization of RTNLB13 (Breeze et al., 2016).

RTNLB1 and RTNLB2 are also implicated in defence against pathogens. Both of them interact with FLAGELIN-SENSITIVE2 (FLS2) receptor, which is the cellular surveillance element that triggers a defense response to pathogen attacks (Lee et al., 2011). *rtnlb1 rtnlb2* mutants or RTNLB1 overexpressing lines exhibited reduced activation of FLS2-dependent signaling and

increased susceptibility to pathogens. In *rtnlb1 rtnlb2* mutants or RTNLB1 overexpressing lines, the accumulation of FLS2 at the plasma membrane was significantly affected, suggesting that RTNLB1 and RTNLB2 regulate the transport of newly synthesized FL2 to the plasma membrane (Lee et al., 2011). *HVA22*, the plant Yop1p homolog, was first identified as an abscisic acid (ABA), and stress-inducible gene in barley (*Hordeum vulgare* L.) (Shen et al., 1993). ABA is a phytohormone playing important roles in plant development and plant responses to environmental stresses. Interestingly, the *HVA22* family as well as *Yop1p* may function as a suppressor of autophagy in both plants and yeast (Chen et al., 2009). The HVA22d RNA interference (RNAi) mutant showed elevated autophagy, indicated by increased number of autophagosomes. The yeast *yop1* mutant showed increased autophagy as well (Chen et al., 2009). Recently, a seed-specific isoform, HVA22b, was found to label the ER in tobacco leaves, but its overexpression did not alter ER morphology (Lee et al., 2013).

1.2.2. Proteins involved in the formation of the ER sheets

In mammals, the size of the peripheral ER sheets varies in different cell types, but it is particularly prominent in cells that are highly specialized in secretion (Shibata et al., 2009). The ER sheets consist of two closely apposed membranes and in secretory cells, like pancreatic or plasma cells, these membranes are studded with ribosomes. With improved staining and automated ultrathin sectioning electron microscopy, the stacked ER sheets are found to be continuously connected by twisted membrane surfaces with edges of left or right handedness (Terasaki et al., 2013).

The ER membranes at the edge of ER sheets are highly bended with high curvatures, where reticulons and DP1/Yop1p are found to be enriched (Shibata et al., 2010). Recently, with a help from superresolution imaging technologies, some sheet-like ER structures within the thin periphery cells were found to be in fact dense tubular matrices, which could be labeled by both RTN4 and Climp63 (Nixon-Abell et al., 2016). It is possible that the edge and inner tubules of the dense tubular matrices are enriched with different RTNs, which determine the area of the dense tubular matrices. These dense tubular ER matrices are also a fact of so called sheet proliferation after overexpression of the ER tubular fusion protein Atlastin (the role of Atlastin will be discussed the following section) (Nixon-Abell et al., 2016). The exist of these dense tubular ER matrices suggests that there may be two different kinds of ER sheets in the cells. One group of sheets is conventional flat and stacked sheets, and another kind of sheets is densely clustered tubules with interconnecting junctions.

Climp63, a coiled-coil ER membrane protein is also suggested to play an important role in the formation of the ER sheets (Shibata et al., 2010). Climp63 is upregulated in mammalian cells with proliferated ER sheets. Overexpression of Climp63 converted the tubules into sheets, although deletion of Climp63 did not decrease the sheet area, but the luminal width of the sheets is decreased (from ~50 to ~30 nm (Shibata et al., 2010). It has been suggested that Climp63 is not essential for sheet formation per se, but for bridging the two apposed membranes (Shibata et al., 2010). In plants, no homolog of Climp63 has been identified, whether or not such dense tubular ER matrices exist still needs to be explored.

1.2.3. Building an interconnected network of ER by homotypic membrane fusion

1.2.3.1. Atlastin protein family

1.2.3.1.1. Atlastin

ER tubules are built by curvature-stabilizing proteins, but to establish and maintain a tubular ER network, these ER tubules need to be connected by some membrane fusogens. Recently, a family of dynamin-like large GTPases, including mammalian Atlastins (ATLs), yeast Sey1p and plant RHD3 (ROOT HAIR DEFECTIVE3), were found to function as the ER membrane fusogens (Hu et al., 2009; Orso et al., 2009; Zhang et al., 2013). ATLs localize to the ER membrane and interact with RTNs and DP1 (Hu et al., 2009). In *Drosophila* neurons, the loss of Atlastin causes fragementation and discontinuity of the ER (Orso et al., 2009). In Hela cells, depletion of ATL2 and ATL3 with RNAi, or expression of GTPase defective ATL1 mutant protein, lead to unbranched ER tubules (Hu et al., 2009). In addition, Atlastin antibodies inhibit the ER network formation in an *in vitro* system (Hu et al., 2009). These ER morphological defects are all due to a lack of ER tubular connections caused by defective tubule fusion. Conversely, overexpression of ATL1 leads to visible aberrant ER sheets, which are in fact tubular ER matrices with dense tubular junctions in super-resolution microscopy (Hu et al., 2009; Nixon-Abell et al., 2016). *In vitro*, purified Atlastin could mediate proteoliposome fusion in a GTP binding and hydrolysis manner, directly supporting its role in the fusion of ER tubules (Orso et al., 2009).

ATL1 plays important roles in cell and organ development, because mutations in *ATL1* cause the most common early-onset HSP (Blackstone, 2012). ATL1 interacts with the other proteins related to HSP, such as REEP1 (SPG31) or Spastin (SPG4). Both of them are found to be

involved in the formation of the ER network (Park et al., 2010). SPG3A, SPG4 and SPG31 account for over 50% of all HSP cases (Blackstone, 2012). This indicates that the neuron development is very sensitive to the defects in the ER network formation (Hu et al., 2009).

The overall structure of Atlastin proteins is conserved (Stefano and Brandizzi, 2014). The N-terminus of ATL1 contains a globular GTPase domain, a middle domain folding into a three-helix bundle (3HB), two transmembrane domains and an amphipathic C-terminus. Recently, the crystal structures of the cytosolic N-terminus of human ATL1 is revealed (Bian et al., 2011; Byrnes and Sondermann, 2011). Two different distinct crystal forms are reported in the presence of GDP. In both forms, the N-terminus of ATL1 forms dimers through the globular GTPase domain, but they are strikingly different in the relative orientation of the GTPase domain and middle domain. In form 1, the nucleotide binding sites of the GTPase domains face to each other and the liner regions twist through one another, allowing the 3HBs to cross and run parallel to one another. The C-terminus of the two ATL1 molecules are only ~ 10 Å apart, suggesting that the following transmembrane domains in the full-length protein would probably sit in the same membrane (Bian et al., 2011). The form 2 structure is obtained with GDP and high concentrations of inorganic phosphate (P_i). In contrast to form 1, in form 2, the 3HBs are associated with the GTPase domain of the same molecules and point in two different directions, although the GTPase domains are facing to each other in a similar way as in form 1. The form 2 structure would represent the situation that two full-length proteins sitting in different membranes, are tethering the two membranes together. Therefore, the form 1 and form 2 structures are proposed as “postfusion” and “prefusion” states, respectively (Figure 1.1) (Bian et al., 2011).

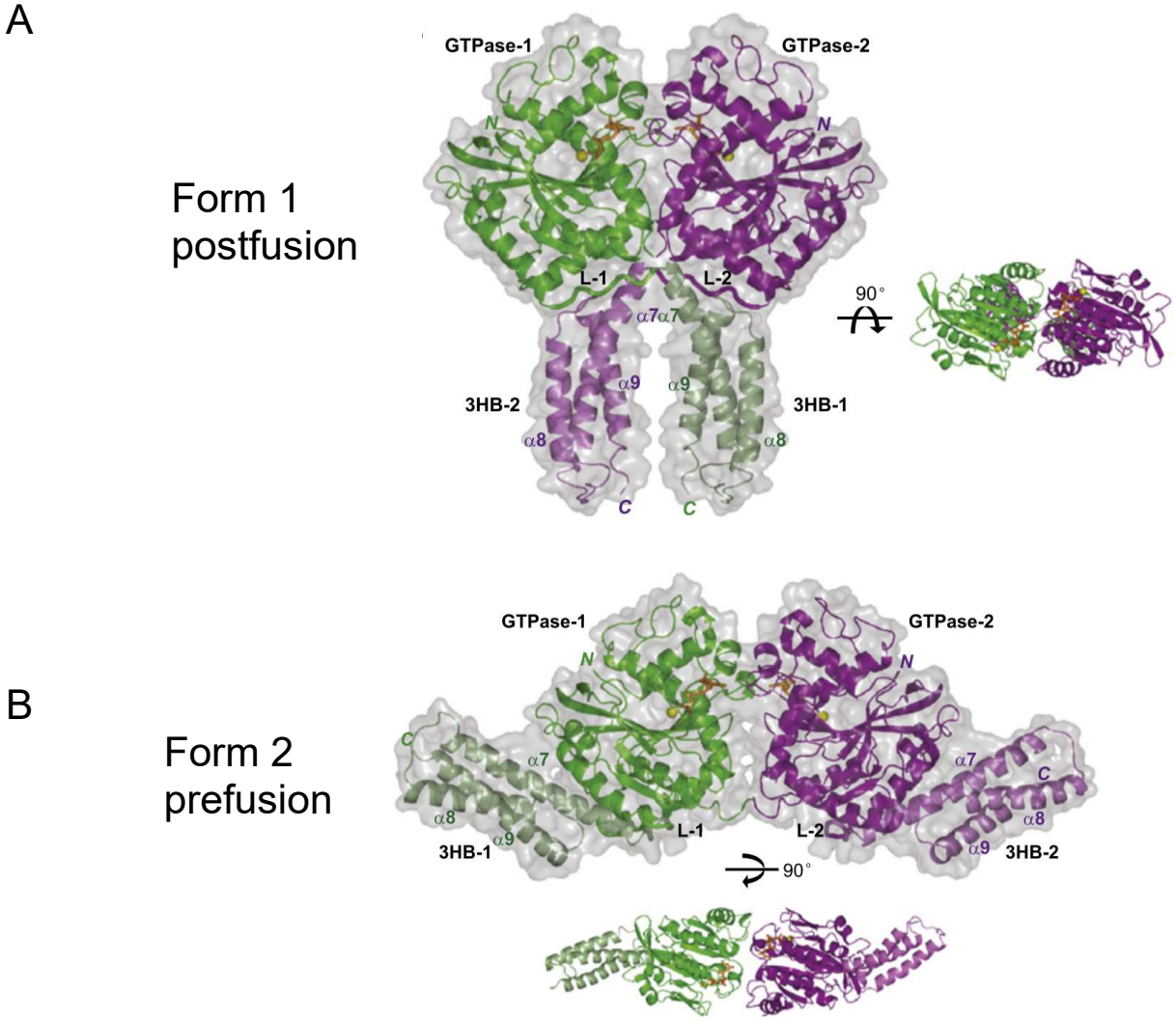

Figure 1.1. Crystal structure of the cytosolic domain of ATL1. A. The structure of Form 1 cytosolic domain of ATL1, corresponding to the post fusion state. The right shows a different view of the dimer after 90 degree rotation. B. The structure of Form 2 cytosolic domain of ATL1, corresponding to the prefusion state. The lower shows a different view of the dimer after 90 degree rotation. (Adopted from (Bian et al., 2011))

The lipid bilayer experiments conducted by Liu et al. (2015) show that ATL molecules sitting on the same membrane (cis) can also undergo nucleotide-dependent dimerization, and that GTP hydrolysis is also required to dissociate the cis-dimers and generate a pool of ATL monomers that can interact with molecules on the different membranes (trans) (Liu et al., 2015). The transmembrane domains of ATL do not only serve as membrane anchors, but also mediate the nucleotide independent oligomerization of ATL in the same membrane (Liu et al., 2012). Following the transmembrane domains, an APH in the C-terminal tail of ATL was found to bind and perturb the membrane bilayers, which could lower the energy barrier to facilitate the membrane fusion (Faust et al., 2015; Liu et al., 2012). Without the C-terminal tail, ATL molecules have very low fusion activity, but the fusion efficiency can be restored by adding a synthetic peptide corresponding to the APH (Liu et al., 2012).

Based on the known fact about ATL described above, a comprehensive model for ATL mediated membrane fusion was proposed by (Hu and Rapoport, 2016; Liu et al., 2015). It is believed that, at first, ATL monomers can bind GTP and form dimers rapidly. These dimers are relatively unstable and transient. Subsequent GTP hydrolysis would trigger a conformational change of the dimers, which eventually makes two 3HBs tightly associate with each other. After P_i and GDP are released, the dimers will be dissociated into monomers. This transition cycle can occur with ATL molecules in the same membranes (cis interaction) or in different membranes (trans interactions), but membrane tethering and fusion can only take place with trans interactions. It is believed that GTP hydrolysis triggered conformational change of the dimers that sit in different membranes would pull and fuse the two membranes together. The cooperation of

several ATL molecules in each membrane mediated by the transmembrane domains of ATL and multiple rounds of GTP hydrolysis are required for a successful fusion event (Liu et al., 2015).

1.2.3.1.2. Sey1p

Sey1p is a functional ortholog of the Atlastin protein in yeast, but the middle domain of Sey1 is longer than that of ATLs (Yan et al., 2015). Sey1p was initially identified in a screen for synthetic genetic interaction for *Yop1p* (Brands and Ho, 2002; Schuldiner et al., 2005). Sey1p localizes to the ER and is enriched in punctae along the ER tubules, sometimes at three-way junctions of ER tubules (Hu et al., 2009). Sey1p interacts and cooperates with Rtn1p/Yop1p in maintaining the ER morphology. Although the morphology of the ER appears normal in the *sey1p* mutant, in double mutant *sey1p rtn1p* or *sey1p yop1p*, the cortical ER was severely disrupted (Hu et al., 2009). Despite the normal ER morphology in *sey1p* mutant cells, in the yeast ER fusion assay, the absence of Sey1p significantly reduced the fusion efficiency (Anwar et al., 2012). *In vitro*, purified Sey1p promote the fusion of proteoliposomes in a GTP hydrolysis dependent manner (Anwar et al., 2012). *In vivo*, Sey1p could partially rescue ATL1 defects, strongly suggests that Sey1p is a functional ATL homolog in yeast and it serves as an ER membrane fusogen (Anwar et al., 2012).

Sep1p contains an N-terminal GTPase domain and a long and helical middle domain connected by a linker region, following by two transmembrane domains and the C-terminus (Yan et al., 2015). The crystal structure of the N-terminal cytosolic domains (cytSey1p) of Sey1p from *C. albicans* (caSey1p) has been determined in the presence of GDP/AlF_4^- or GDP (Yan et al., 2015). It is revealed that, in the presence of GDP/AlF_4^- , cytSey1p molecules form dimers, but with

GDP, cytSey1p molecules are in the monomer state. In the sytSey1p dimer, similar to the form 1 state of ATL1, the nucleotide binding sites of the GTPase domains of Sey1p face each other, and the linker regions of the molecules cross one another. The middle domain following the linker regions consist of four 3HBs, and form a twist arm in the dimer. Interestingly, membrane fusion mediated by Sey1p was observed in the presence of GMP-PNP, indicating that without GTP hydrolysis, Sey1p can still mediate membrane fusion. It is possible that Sey1p forms a tight dimer in the GTP-bound state, which is different from the transition state of ATL1 dimers (Hu and Rapoport, 2016; Yan et al., 2015).

1.2.3.1.3. RHD3

RHD3 (ROOT HAIR DEFECTIVE3) is a plant homolog of the Atlastin protein. *RHD3* was originally identified in a genetic screening for root hair defective mutants after ethyl methane sulfonate (EMS) treatment (Schiefelbein and Somerville, 1990). The *rhd3* mutant shows short and wavy root hairs, and is defective in cell enlargement, rather than cell division (Wang et al., 1997). In addition to RHD3, there are two RHD3-like proteins in *Arabidopsis*, RHD3-like1 (RL1) and RHD3-like2 (RL2) (Chen et al., 2011; Hu et al., 2003). Unlike *RHD3* that is ubiquitously expressed (Wang et al., 2002), *RL1* is only expressed in pollen and *RL2* is ubiquitously expressed in different tissues at very low levels (Chen et al., 2011). Although *RL1* or *RL2* knock out mutants do not produce any visible developmental phenotype, when *rhd3-8* crossed with *rl1* or *rl2* mutant, in the F2 populations no *rhd3 rl1* or *rhd3 rl2* homologous double mutants can be recovered, suggesting that double mutant *rhd3 rl1* or *rhd3 rl2* are likely lethal (Zhang et al., 2013). Furthermore, overexpression of *RL2* rescued the *rhd3-1* mutant phenotype (Chen et al.,

2011). Taken together, these three RHD3 proteins probably play similar roles in plant cell development (Zhang et al., 2013).

In *rhd3-1* mutant cells, the ER is less branched (Zheng et al., 2004). Using a dominant negative approach, Chen et al. (2011) demonstrated that RHD3 is required for the generation of tubular ER network (Chen et al., 2011). In an *in vitro* lipid mixing experiment, Zhang et al., 2013 revealed that RHD3 and RL2 are capable of mediating membrane fusion (Zhang et al., 2013). In addition, driven by the Sey1p promoter, RHD3 could complement the ER morphology defects in *Δsey1Δyop1* cells and enhance the ER fusion efficiency in *Δsey1* cells (Zhang et al., 2013). In addition, RHD3 molecules form homotypic interactions at 3-way junctions of the ER (Chen et al., 2011). Furthermore, similar to Sey1p that interacts with RTNs and Yop1p in yeast, and ATLs that interact with reticulons and REEPs in mammalian cells, RL2 was found to interact with RTNLB13 in plant (Lee et al., 2013). All these results indicated that RHD3 and RHD3-like proteins are the functional homologs of Sey1p and ATLs in plants.

The overall structure of RHD3 is predicted to be closer to Sey1p, consisting of a GTPase domain, a long middle domain, two transmembrane domains and a C-terminal tail (Stefano and Brandizzi, 2014). Although the crystal structure of RHD3 is not determined, mutations in the GTPase binding pocket of RHD3, such as S51N, T75A (Chen et al., 2011) and K50A (Zhang et al., 2013) made RHD3 defective *in vivo* and *in vitro*. However, two genetic mutants, *rhd3-2* and *rhd3-5*, have mutations (D185N and I134T, respectively) in the GTPase domain (Wang et al., 1997), but not in the conserved binding pockets, suggesting that there may be other functions rather than GTP binding and hydrolysis for the GTPase domain. *rhd3-1* has an A575V mutation in the

middle domain, which destabilize the RHD3 protein, implying that the middle domain of RHD3 may play a role in protein stability (Zhang et al., 2013). The mutation P701S between the two transmembrane domains, changes the localization of RHD3, implicating that the two transmembrane domains play a role in the ER membrane anchoring of RHD3 (Stefano et al., 2012). Recently, the phosphorylation of the C-terminal of RHD3 was reported to be important for the oligomerization of RHD3 (Ueda et al., 2015).

In addition to its primary function in the fusion of ER tubules, the other cellular functions of RHD3 that are probably related to its primary role in the generation of tubular ER network are also revealed. For example, Lai et al. (2014) found that a loss of RHD3 compromised the unfolded protein response (UPR), possibly by an interfering with the mRNA splicing ability of IRE1, which is a major ER stress sensor and transducer in both animal and plant (Lai et al., 2014). It is interesting to note that in yeast, loss of six ER-PM tethering proteins constitutively activated UPR (Manford et al., 2012). These results imply that the different parts of the ER network may have different functions in regulating the UPR. Furthermore, in *rhd3* mutant cells, the organelle streaming during cell expansion is slowed down and endocytosis is impaired (Stefano et al., 2015). A loss of RHD3 also influences the nuclear size and movement in the root hairs, possibly due to the close linkage between ER and nuclear outer membrane (Sliwinska et al., 2015). In addition, in the *rhd3* mutant, the targeting of secretory vesicles and plasma membrane protein to the apical dome in growing root hairs is altered (Qi et al., 2016), suggesting that RHD3 or RHD3-mediated generation of the ER network plays a role in targeted secretion. In the *rhd3* mutant, *Tomato spotted wilt tospovirus* (TSWV) cell-to-cell spread is delayed, whereas viral replication is not reduced (Feng et al., 2016). This indicated that RHD3 or RHD3-

mediated generation of the ER network is also required for the viral systemic infection (Feng et al., 2016).

1.2.3.2. SNARE

In addition to the atlastin protein family, it has been found that some ER-associated soluble N-ethylmaleimide-sensitive factor activating protein receptor (SNARE) proteins are also involved in ER membrane fusion in yeast (Anwar et al., 2012; Patel et al., 1998). SNAREs are transmembrane proteins acting as key elements in membrane fusion (Jahn and Scheller, 2006). In yeast, through the genetic screen for synthetic enhancer of *sey1* mutant, SNAREs Sec20p, Ufe1p and Use1p that are involved in retrograde transport of COPI-coated vesicles from the Golgi to the ER were found to be involved in a Sey1p-indepdendent homotypic ER fusion, which requires the Dsl1 tethering complex (Anwar et al., 2012; Rogers et al., 2013; Rogers et al., 2014). The Dsl1 tethering complex is a CATCHR (complex associated with tethering containing helical rods) family member consisting of three subunits (Tip10p, Dsl1p and Sec39p/Dsl3) (Rogers et al., 2014). This complex is thought to mediate the initial connection between the ER membrane and an incoming vesicle (Zink et al., 2009). This result suggests that there may be at least two parallel, Sey1p-dependent and SNARE-dependent pathways, involved in homotypic ER fusion in yeast. Conversely, Lee et al. (2015), suggested a different model for SNARE mediated homotypic fusion in yeast (Lee et al., 2015). Lee et al. (2015), established a split luciferase based ER microsome *in vitro* assay to investigate homotypic ER membrane fusion. With this assay, they found that instead of mediating a Sey1p-independent homotypic membrane fusion, the ER SNAREs Sec22p and Ufe1p support Sey1p-dependent ER fusion by the physical interaction with Sey1p (Lee et al., 2015). This discrepancy may be a result of different experiments systems.

Nevertheless, SNAREs are demonstrated to play a role in mediating ER membrane fusion in yeast cells. SNARE mediated ER fusion has been not found in mammalian and plant cells. This raised a question whether there is a highly conserved SNARE based mechanism for ER membrane fusion in all eukaryotic cells.

1.2.4. The other regulating proteins

In addition to the protein families discussed above, there are several other protein families, including Rabs, protrudin and Lunapark that have been found to be involved in shaping the interconnected tubular ER network, although their exact molecular mechanisms remain unclear.

1.2.4.1. Rab GTPases

Rab GTPases are a family of small GTPases that are known to be required for accurate and efficient tethering and fusion of vesicles at various vesicle transport steps in the endomembrane system (Schwartz et al., 2007). In a quantitative *in vitro* enzyme-linked immunosorbent assay, the homotypic fusion of mammalian ER microsomes could be blocked by adding a general Rab GDP-dissociation inhibitor (GDI), suggesting that a Rab GTPase(s) could be involved in the ER membrane fusion (Turner et al., 1997). To explore the potential roles of Rab GTPases in the ER network formation, Audhya et al. (2007) depleted all 29 Rab GTPases in *Caenorhabditis elegans* embryos by RNAi and found that RAB-5 is essential for the formation of the ER network (Audhya et al., 2007). In addition, a proteomics based *in vitro* assay conducted with *Xenopus* egg microsomes identified RAB10 as an ER localized Rab GTPase, regulating the ER structure and dynamics (English and Voeltz, 2013). Depletion of Rab10 or expression of a Rab10 GDP-locked mutant alters the ER morphology, resulting in expanded ER sheets. A discrete ER domain

at the leading edge of almost half of all dynamic ER tubules, was marked by Rab10, phosphatidylinositol synthase (PIS) and choline/ethanolamine phosphotransferase (CERPT1) (English and Voeltz, 2013).

In addition to Rab5 and Rab10, disruption of Rab18 or Rab3GAP complex, a Rab18 specific guanine nucleotide exchange factor (GEF) can also lead an expansion of ER sheets (Gerondopoulos et al., 2014). Rab18 is found to be targeted to the ER by Rab3GAP complex (Gerondopoulos et al., 2014). Furthermore, genetic mutations of Rab18 and Rab3GAP were found to be involved in the neurological and developmental disorder Warburg Micro syndrome (Bem et al., 2011; Handley and Aligianis, 2012; Handley et al., 2013).

In a large screening of the interacting proteins of Rab GTPases, with affinity chromatography followed by mass spectrometry, the subunits of the Dsl1 tethering complex (NRZ in mammals), which regulates the assembly of ER SNAREs, were found to bound with high specificity to Rab18 (Gillingham et al., 2014), suggesting that Rab18 may be involved in ER fusion via an ER SNARE-mediated mechanism.

1.2.4.2. Protrudin

Protrudin is a protein with three hydrophobic segments, a Rab-binding domain (RBD), two phenylalanines in an acidic tract (FFAT) domain, and a noncanonical FYVE (Fab-1, YGL023, Vps27, and EEA1) domain (Chang et al., 2013b). Protrudin (SPG33) was originally identified as a HSP locus (Mannan et al., 2006) in humans. It was reported that Protrudin is an ER

membrane bound and oligomeric protein, interacting with REEP1(SPG31) or Spastin (SPG4), and Atlastins with its N-terminal transmembrane domain (Chang et al., 2013a).

Chang et al. revealed that upon suppressing the expression of Protrudin by RNAi in the Hela cells, ER sheets labelled by CLIMP63 are expanded. They thus suggested that Protrudin plays a role in the ER tubular network formation (Chang et al., 2013a). Yet, the homologs of Protrudin have not been described in yeast and plant cells, thus whether or not this Protrudin-mediated ER network formation is conserved remains as a question.

1.2.4.3. Lunapark

Recently, a protein called Lunapark (Lnp) has been added to the list of proteins that regulate the formation of tubular ER network (Chen et al., 2015; Chen et al., 2012b; Wang et al., 2016b). In a screen of mutants with disrupted cortical ER network in yeast Lnp1p was identified (Chen et al., 2012b). Loss of Lnp1p in yeast resulted in a collapsed and densely reticulated ER network (Chen et al., 2012b). In mammalian cells, a depletion of mLnp1 in Cos-7 cells also shifts the morphology of the ER from tubular to more sheet-like (Chen et al., 2015). These two results indicated that Lnp proteins are evolutionally conserved and play a role in the formation of the tubular ER network. Lnp has two transmembrane domains and a zinc finger motif. Recently, a novel ubiquitin ligase binding motif was also identified in the N-terminus of mLnp1(Zhao et al., 2016).

Lnp is found to localize to 3-way junctions of the ER in both yeast and mammalian cells (Chen et al., 2015; Chen et al., 2012b). With time series live imaging and *in vitro* ER reconstitution,

mLnp1 has been found to be required for stabilizing nascent 3-way junctions of the ER (Chen et al., 2015; Wang et al., 2016b). In yeast, based on the synthetic genetic relationship of Lnp1p with reticulon and yop1, and the suppression relationship between Lnp1p and Sey1p in yeast, Lnp1p has been proposed to work synergistically with the reticulons and Yop1p, but in antagonism to Sey1p (Chen et al., 2012b). Although Lnp1p physically interacts with Sey1p, reticulons and Yop1p, the exact molecular mechanism of how Lunapark work together with Reticulon and Sey1p is unclear.

1.3. Rationale and objectives of the thesis

1.3.1. Systemic structure-function analyses of roles of different RHD3 domains

RHD3 has been demonstrated to be a functional ER membrane fusogen. Purified RHD3 can mediate the fusion of proteoliposomes in a GTP hydrolysis dependent manner *in vitro* (Zhang et al., 2013). In the *rhd3* mutant, due to the loss of ER tubular fusion mediated by RHD3, thick, bundled and unbranched ER tubules are visible (Zheng et al., 2004). Mutations in the GTPase domain (Chen et al., 2011; Wang et al., 1997; Zhang et al., 2013), middle domain (Wang et al., 1997) and two transmembrane domains (Stefano et al., 2012) of RHD3 all can make RHD3 defective, implying that RHD3-mediated ER membrane fusion is a dedicated process that require the cooperation of different domains of RHD3. However, how exactly the different domains of RHD3 cooperate and function in mediating ER membrane fusion is not very clear.

In the first part of this thesis, I studied how RHD3 works on mediating ER membrane fusion through its different domains. With the simulated RHD3 structure, functional analyses of various mutated versions of RHD3 including their subcellular localization, dominant negative effects on

the formation of the tubular ER network, protein interaction and ER fusion efficiency were conducted. I showed that RHD3 forms a dimer, and likely the dimerization of RHD3 is required for efficient ER fusion as various point mutations that affect the dimerization also affect the ER fusion efficiency. In addition to its GTPase activity, the GTPase domain of RHD3 can promote the dimerization of RHD3. RHD3 has a 3HBs enriched middle domain which is much longer than that of Atlastin. I showed that the first and second 3HBs in the middle domain, are involved in the dimerization of RHD3, while the third and four 3HB3 are important for the protein stability. The transmembrane domains of RHD3 not only serve as the ER membrane anchor, but also facilitate the oligomerization of RHD3. Finally, the amphipathic helix in the CT of RHD3 has a membrane anchoring ability, playing an important role in the efficient ER membrane fusion mediated by RHD3.

1.3.2. The regulation of fusion activity of RHD3 by Lunapark proteins

The Lunapark proteins are required in yeast and mammalian cells for the maintenance of the tubular ER network and they can stabilize 3-way junctions of the ER (Chen et al., 2015; Chen et al., 2012b). Although it has been proposed that in yeast Lnp1p acts antagonizingly with Sey1p (Chen et al., 2012b), the exact molecular mechanism of how the LNP proteins act together with Atlastin or Sey1p to stabilize 3-way junctions of the ER is unclear. In yeast, Lnp1p physically interacts with Sey1p (Chen et al., 2012b), but in mammalian cells, no interaction between mLnp1 and Atlastin is demonstrated (Wang et al., 2016b). In plants, no research on the Lnp proteins has been conducted and the existence of Lnp1 homologs is questioned (Stefano and Brandizzi, 2017).

In the second part of my thesis, I showed that there are two functional Lunapark homologs in *Arabidopsis*, LNP1 and LNP2. Both of them physically interact with RHD3 on 3-way junctions of the tubular ER network. Both LNP1 and LNP2 are ubiquitous expressed in Arabidopsis. Single *lnp1* or *lnp2* mutants had subtle but short root hairs, while the double mutant of *lnp1 lnp2* exhibited enhanced defects in root hair growth as well as other pleiotropic developmental growth defects with massive sheet-like ER with dense 3-way junctions in the cells, suggesting that LNP1 and LNP2 has an overlapped function in the formation of the tubular ER network. Similar to Lnp1p in yeast cells or Lnp1 in mammalian cells, I showed that Arabidopsis LNP2 is also required for stabilizing the newly formed 3-way junctions of the ER. Both LNP1 and LNP2 are recruited by RHD3 to 3-way junctions of the ER. I showed that LNP2 inhibits the fusion activity of RHD3 with molecular and genetic evidence, and that in *lnp1 lnp2* mutant, the protein level of RHD3 is higher than that in wild type plants. I thus proposed that LNPs antagonize the action of RHD3 by inhibiting the fusion activity of RHD3, probably through promoting the protein degradation of RHD3 after the formation of 3-way junctions of the ER by fusion.

1.4. REFERENCES

Agrawal, G., Joshi, S., and Subramani, S. (2011). Cell-free sorting of peroxisomal membrane proteins from the endoplasmic reticulum. P Natl Acad Sci USA *108*, 9113-9118.

Anderson, D.J., and Hetzer, M.W. (2008). Reshaping of the endoplasmic reticulum limits the rate for nuclear envelope formation. Journal of Cell Biology *182*, 911-924.

Andersson, M.X., Goksor, M., and Sandelius, A.S. (2007). Optical manipulation reveals strong attracting forces at membrane contact sites between endoplasmic reticulum and chloroplasts. Journal of Biological Chemistry *282*, 1170-1174.

Anwar, K., Klemm, R.W., Condon, A., Severin, K.N., Zhang, M., Ghirlando, R., Hu, J., Rapoport, T.A., and Prinz, W.A. (2012). The dynamin-like GTPase Sey1p mediates homotypic ER fusion in S. cerevisiae. J Cell Biol *197*, 209-217.

Area-Gomez, E., and Schon, E.A. (2016). Mitochondria-associated ER membranes and Alzheimer disease. Curr Opin Genet Dev *38*, 90-96.

Audhya, A., Desai, A., and Oegema, K. (2007). A role for Rab5 in structuring the endoplasmic reticulum. J Cell Biol *178*, 43-56.

Barton, K., Mathur, N., and Mathur, J. (2013). Simultaneous live-imaging of peroxisomes and the ER in plant cells suggests contiguity but no luminal continuity between the two organelles. Front Physiol *4*, 196.

Bayer, E.M., Sparkes, I., Vanneste, S., and Rosado, A. (2017). From shaping organelles to signalling platforms: the emerging functions of plant ER-PM contact sites. Curr Opin Plant Biol *40*, 89-96.

Beams, H.W., and Kessel, R.G. (1968). The Golgi apparatus: structure and function. Int Rev Cytol *23*, 209-276.

Beetz, C., Koch, N., Khundadze, M., Zimmer, G., Nietzsche, S., Hertel, N., Huebner, A.K., Mumtaz, R., Schweizer, M., Dirren, E.*, et al.* (2013). A spastic paraplegia mouse model reveals REEP1-dependent ER shaping. J Clin Invest *123*, 4273-4282.

Bem, D., Yoshimura, S., Nunes-Bastos, R., Bond, F.C., Kurian, M.A., Rahman, F., Handley, M.T., Hadzhiev, Y., Masood, I., Straatman-Iwanowska, A.A.*, et al.* (2011). Loss-of-function mutations in RAB18 cause Warburg micro syndrome. American journal of human genetics *88*, 499-507.

Bentivoglio, M. (1998). 1898: the Golgi apparatus emerges from nerve cells. Trends Neurosci *21*, 195-200.

Berridge, M.J. (2002). The endoplasmic reticulum: a multifunctional signaling organelle. Cell calcium *32*, 235-249.

Bessoule, J.-J., and Moreau, P. (2004). 2 Phospholipid synthesis and dynamics in plant cells. In Lipid Metabolism and Membrane Biogenesis, G. Daum, ed. (Berlin, Heidelberg: Springer Berlin Heidelberg), pp. 89-124.

Bian, X., Klemm, R.W., Liu, T.Y., Zhang, M., Sun, S., Sui, X., Liu, X., Rapoport, T.A., and Hu, J. (2011). Structures of the atlastin GTPase provide insight into homotypic fusion of endoplasmic reticulum membranes. Proc Natl Acad Sci U S A *108*, 3976-3981.

Blackstone, C. (2012). Cellular pathways of hereditary spastic paraplegia. Annu Rev Neurosci *35*, 25-47.

Blackstone, C., O'Kane, C.J., and Reid, E. (2011). Hereditary spastic paraplegias: membrane traffic and the motor pathway. Nature Reviews Neuroscience *12*, 31-42.

Boevink, P., Oparka, K., Santa, C.S., Martin, B., Betteridge, A., and Hawes, C. (1998). Stacks on tracks: the plant Golgi apparatus traffics on an actin/ER network. Plant J *15*, 441-447.

Bolte, S., Talbot, C., Boutte, Y., Catrice, O., Read, N.D., and Satiat-Jeunemaitre, B. (2004). FM-dyes as experimental probes for dissecting vesicle trafficking in living plant cells. Journal of microscopy *214*, 159-173.

Brady, J.P., Claridge, J.K., Smith, P.G., and Schnell, J.R. (2015). A conserved amphipathic helix is required for membrane tubule formation by Yop1p. P Natl Acad Sci USA *112*, E639-E648.

Brandizzi, F. (2017). Transport from the endoplasmic reticulum to the Golgi in plants: Where are we now? Seminars in Cell & Developmental Biology.

Brands, A., and Ho, T.H. (2002). Function of a plant stress-induced gene, HVA22. Synthetic enhancement screen with its yeast homolog reveals its role in vesicular traffic. Plant Physiol *130*, 1121-1131.

Breeze, E., Dzimitrowicz, N., Kriechbaumer, V., Brooks, R., Botchway, S.W., Brady, J.P., Hawes, C., Dixon, A.M., Schnell, J.R., Fricker, M.D.*, et al.* (2016). A C-terminal amphipathic helix is necessary for the in vivo tubule-shaping function of a plant reticulon. P Natl Acad Sci USA *113*, 10902-10907.

Buchnik, L., Abu-Abied, M., and Sadot, E. (2015). Role of plant myosins in motile organelles: is a direct interaction required? J Integr Plant Biol *57*, 23-30.

Byrnes, L.J., and Sondermann, H. (2011). Structural basis for the nucleotide-dependent dimerization of the large G protein atlastin-1/SPG3A. Proc Natl Acad Sci U S A *108*, 2216-2221.

Cao, P., Renna, L., Stefano, G., and Brandizzi, F. (2016). SYP73 Anchors the ER to the Actin Cytoskeleton for Maintenance of ER Integrity and Streaming in Arabidopsis. Curr Biol.

Carrasco, S., and Meyer, T. (2011). STIM proteins and the endoplasmic reticulum-plasma membrane junctions. Annu Rev Biochem *80*, 973-1000.

Chang, J., Lee, S., and Blackstone, C. (2013a). Protrudin binds atlastins and endoplasmic reticulum-shaping proteins and regulates network formation. P Natl Acad Sci USA *110*, 14954-14959.

Chang, J., Lee, S., and Blackstone, C. (2013b). Protrudin binds atlastins and endoplasmic reticulum-shaping proteins and regulates network formation. Proc Natl Acad Sci U S A *110*, 14954-14959.

Chen, C.N., Chen, H.R., Yeh, S.Y., Vittore, G., and Ho, T.H. (2009). Autophagy is enhanced and floral development is impaired in AtHVA22d RNA interference Arabidopsis. Plant Physiol *149*, 1679-1689.

Chen, H., Detmer, S.A., Ewald, A.J., Griffin, E.E., Fraser, S.E., and Chan, D.C. (2003). Mitofusins Mfn1 and Mfn2 coordinately regulate mitochondrial fusion and are essential for embryonic development. J Cell Biol *160*, 189-200.

Chen, J., Doyle, C., Qi, X., and Zheng, H. (2012a). The endoplasmic reticulum: a social network in plant cells(f). J Integr Plant Biol *54*, 840-850.

Chen, J., Stefano, G., Brandizzi, F., and Zheng, H. (2011). Arabidopsis RHD3 mediates the generation of the tubular ER network and is required for Golgi distribution and motility in plant cells. J Cell Sci *124*, 2241-2252.

Chen, M.S., Huber, A.B., van der Haar, M.E., Frank, M., Schnell, L., Spillmann, A.A., Christ, F., and Schwab, M.E. (2000). Nogo-A is a myelin-associated neurite outgrowth inhibitor and an antigen for monoclonal antibody IN-1. Nature *403*, 434-439.

Chen, S., Desai, T., McNew, J.A., Gerard, P., Novick, P.J., and Ferro-Novick, S. (2015). Lunapark stabilizes nascent three-way junctions in the endoplasmic reticulum. Proceedings of the National Academy of Sciences *112*, 418-423.

Chen, S., Novick, P., and Ferro-Novick, S. (2012b). ER network formation requires a balance of the dynamin-like GTPase Sey1p and the Lunapark family member Lnp1p. Nat Cell Biol *14*, 707-716.

Contento, A.L., and Bassham, D.C. (2012). Structure and function of endosomes in plant cells. J Cell Sci *125*, 3511-3518.

Costello, J.L., Castro, I.G., Hacker, C., Schrader, T.A., Metz, J., Zeuschner, D., Azadi, A.S., Godinho, L.F., Costina, V., Findeisen, P.*, et al.* (2017). ACBD5 and VAPB mediate membrane associations between peroxisomes and the ER. Journal of Cell Biology *216*, 331-342.

Csordas, G., Renken, C., Varnai, P., Walter, L., Weaver, D., Buttle, K.F., Balla, T., Mannella, C.A., and Hajnoczky, G. (2006). Structural and functional features and significance of the physical linkage between ER and mitochondria. J Cell Biol *174*, 915-921.

Dalton, A.J. (1951). Observations of the Golgi substance with the electron microscope. Nature *168*, 244-245.

DaSilva, L.L.P., Snapp, E.L., Denecke, J., Lippincott-Schwartz, J., Hawes, C., and Brandizzi, F. (2004). Endoplasmic reticulum export sites and golgi bodies behave as single mobile secretory units in plant cells. Plant Cell *16*, 1753-1771.

de Brito, O.M., and Scorrano, L. (2008). Mitofusin 2 tethers endoplasmic reticulum to mitochondria. Nature *456*, 605-610.

Deeks, M.J., Calcutt, J.R., Ingle, E.K.S., Hawkins, T.J., Chapman, S., Richardson, A.C., Mentlak, D.A., Dixon, M.R., Cartwright, F., Smertenko, A.P.*, et al.* (2012). A Superfamily of Actin-Binding Proteins at the Actin-Membrane Nexus of Higher Plants. Curr Biol *22*, 1595-1600.

Dickson, E.J., Jensen, J.B., Vivas, O., Kruse, M., Traynor-Kaplan, A.E., and Hille, B. (2016). Dynamic formation of ER-PM junctions presents a lipid phosphatase to regulate phosphoinositides. J Cell Biol *213*, 33-48.

Dong, R., Saheki, Y., Swarup, S., Lucast, L., Harper, J.W., and De Camilli, P. (2016). Endosome-ER Contacts Control Actin Nucleation and Retromer Function through VAP-Dependent Regulation of PI4P. Cell *166*, 408-423.

Dreier, L., and Rapoport, T.A. (2000). In vitro formation of the endoplasmic reticulum occurs independently of microtubules by a controlled fusion reaction. J Cell Biol *148*, 883-898.

English, A.R., and Voeltz, G.K. (2013). Rab10 GTPase regulates ER dynamics and morphology. Nat Cell Biol *15*, 169-178.

Faust, J.E., Desai, T., Verma, A., Ulengin, I., Sun, T.L., Moss, T.J., Betancourt-Solis, M.A., Huang, H.W., Lee, T., and McNew, J.A. (2015). The Atlastin C-terminal Tail Is an Amphipathic Helix That Perturbs the Bilayer Structure during Endoplasmic Reticulum Homotypic Fusion. J Biol Chem *290*, 4772-4783.

Feng, Z.K., Xue, F., Xu, M., Chen, X.J., Zhao, W.Y., Garcia-Murria, M.J., Mingarro, I., Liu, Y., Huang, Y., Jiang, L.*, et al.* (2016). The ER-Membrane Transport System Is Critical for Intercellular Trafficking of the NSm Movement Protein and Tomato Spotted Wilt Tospovirus. PLoS pathogens *12*.

Foissner, I., Menzel, D., and Wasteneys, G.O. (2009). Microtubule-Dependent Motility and Orientation of the Cortical Endoplasmic Reticulum in Elongating Characean Internodal Cells. Cell Motil Cytoskel *66*, 142-155.

Friedman, J., Lackner, L., West, M., DiBenedetto, J., Nunnari, J., and Voeltz, G. (2011). ER tubules mark sites of mitochondrial division. Molecular Biology of the Cell *22*.

Friedman, J.R., DiBenedetto, J.R., West, M., Rowland, A.A., and Voeltz, G.K. (2013). Endoplasmic reticulum-endosome contact increases as endosomes traffic and mature. Molecular Biology of the Cell *24*, 1030-1040.

Gerondopoulos, A., Bastos, R.N., Yoshimura, S., Anderson, R., Carpanini, S., Aligianis, I., Handley, M.T., and Barr, F.A. (2014). Rab18 and a Rab18 GEF complex are required for normal ER structure. J Cell Biol *205*, 707-720.

Gillingham, A.K., Sinka, R., Torres, I.L., Lilley, K.S., and Munro, S. (2014). Toward a comprehensive map of the effectors of rab GTPases. Dev Cell *31*, 358-373.

Giordano, F., Saheki, Y., Idevall-Hagren, O., Colombo, S.F., Pirruccello, M., Milosevic, I., Gracheva, E.O., Bagriantsev, S.N., Borgese, N., and De Camilli, P. (2013). PI(4,5)P(2)-dependent and Ca(2+)-regulated ER-PM interactions mediated by the extended synaptotagmins. Cell *153*, 1494-1509.

Golgi, C. (1898). Sur la structure des cellules nerveuses. Arch Ital Biol *30*, 60-71.

GrandPre, T., Nakamura, F., Vartanian, T., and Strittmatter, S.M. (2000). Identification of the Nogo inhibitor of axon regeneration as a Reticulon protein. Nature *403*, 439-444.

Grigoriev, I., Gouveia, S., Van der Vaart, B., Demmers, J., Smyth, J.T., Honnappa, S., Splinter, D., Steinmetz, M.O., Putney, J.W., Hoogenraad, C.C.*, et al.* (2008). STIM1 is a MT-plus-end-tracking protein involved in remodeling of the ER. Curr Biol *18*, 177-182.

Hamada, T., Ueda, H., Kawase, T., and Hara-Nishimura, I. (2014). Microtubules contribute to tubule elongation and anchoring of endoplasmic reticulum, resulting in high network complexity in Arabidopsis. Plant Physiol *166*, 1869-1876.

Handley, M.T., and Aligianis, I.A. (2012). RAB3GAP1, RAB3GAP2 and RAB18: disease genes in Micro and Martsolf syndromes. Biochem Soc Trans *40*, 1394-1397.

Handley, M.T., Morris-Rosendahl, D.J., Brown, S., Macdonald, F., Hardy, C., Bem, D., Carpanini, S.M., Borck, G., Martorell, L., Izzi, C.*, et al.* (2013). Mutation spectrum in RAB3GAP1, RAB3GAP2, and RAB18 and genotype-phenotype correlations in warburg micro syndrome and Martsolf syndrome. Hum Mutat *34*, 686-696.

Hawkins, T.J., Deeks, M.J., Wang, P., and Hussey, P.J. (2014). The evolution of the actin binding NET superfamily. Front Plant Sci *5*, 254.

He, W., Lu, Y., Qahwash, I., Hu, X.Y., Chang, A., and Yan, R. (2004). Reticulon family members modulate BACE1 activity and amyloid-beta peptide generation. Nat Med *10*, 959-965.

Hepler, P.K., Palevitz, B.A., Lancelle, S.A., Mccauley, M.M., and Lichtscheidl, I. (1990). Cortical Endoplasmic-Reticulum in Plants. Journal of Cell Science *96*, 355-373.

Hirabayashi, Y., Kwon, S.-K., Paek, H., Pernice, W.M., Paul, M.A., Lee, J., Erfani, P., Raczkowski, A., Petrey, D.S., Pon, L.A.*, et al.* (2017). ER-mitochondria tethering by PDZD8 regulates Ca²⁺ dynamics in mammalian neurons. Science *358*, 623-630.

Hoepfner, D., Schildknegt, D., Braakman, I., Philippsen, P., and Tabak, H.F. (2005). Contribution of the endoplasmic reticulum to peroxisome formation. Cell *122*, 85-95.

Hong, B.M., Ichida, A., Wang, Y.W., Gens, J.S., Pickard, B.C., and Harper, J.F. (1999). Identification of a calmodulin-regulated Ca2+-ATPase in the endoplasmic reticulum. Plant Physiology *119*, 1165-1175.

Hu, J., Prinz, W.A., and Rapoport, T.A. (2011). Weaving the web of ER tubules. Cell *147*, 1226-1231.

Hu, J., and Rapoport, T.A. (2016). Fusion of the endoplasmic reticulum by membrane-bound GTPases. Semin Cell Dev Biol *60*, 105-111.

Hu, J., Shibata, Y., Voss, C., Shemesh, T., Li, Z., Coughlin, M., Kozlov, M.M., Rapoport, T.A., and Prinz, W.A. (2008). Membrane proteins of the endoplasmic reticulum induce high-curvature tubules. Science *319*, 1247-1250.

Hu, J., Shibata, Y., Zhu, P.P., Voss, C., Rismanchi, N., Prinz, W.A., Rapoport, T.A., and Blackstone, C. (2009). A class of dynamin-like GTPases involved in the generation of the tubular ER network. Cell *138*, 549-561.

Hu, Y., Zhong, R., Morrison, W.H.R., and Ye, Z.H. (2003). The Arabidopsis RHD3 gene is required for cell wall biosynthesis and actin organization. Planta *217*, 912-921.

Hua, R., Cheng, D., Coyaud, E., Freeman, S., Di Pietro, E., Wang, Y., Vissa, A., Yip, C.M., Fairn, G.D., Braverman, N.*, et al.* (2017). VAPs and ACBD5 tether peroxisomes to the ER for peroxisome maintenance and lipid homeostasis. J Cell Biol *216*, 367-377.

Ito, Y., Uemura, T., and Nakano, A. (2014). Formation and maintenance of the Golgi apparatus in plant cells. Int Rev Cell Mol Biol *310*, 221-287.

Jahn, R., and Scheller, R.H. (2006). SNAREs--engines for membrane fusion. Nature reviews Molecular cell biology *7*, 631-643.

Jaipargas, E.A., Barton, K.A., Mathur, N., and Mathur, J. (2015). Mitochondrial pleomorphy in plant cells is driven by contiguous ER dynamics. Front Plant Sci *6*, 783.

Jing, J., He, L., Sun, A.M., Quintana, A., Ding, Y.H., Ma, G.L., Tan, P., Liang, X.W., Zheng, X.L., Chen, L.Y.*, et al.* (2015). Proteomic mapping of ER-PM junctions identifies STIMATE as a regulator of Ca2+ influx. Nature Cell Biology *17*, 1339-+.

Kaneko, Y., and Keegstra, K. (1996). Plastid biogenesis in embryonic pea leaf cells during early germination. Protoplasma *195*, 59-67.

Kilpatrick, B.S., Eden, E.R., Schapira, A.H., Futter, C.E., and Patel, S. (2013). Direct mobilisation of lysosomal Ca2+ triggers complex Ca2+ signals. J Cell Sci *126*, 60-66.

Kim, H., Kwon, H., Kim, S., Kim, M.K., Botella, M.A., Yun, H.S., and Kwon, C. (2016). Synaptotagmin 1 Negatively Controls the Two Distinct Immune Secretory Pathways to Powdery Mildew Fungi in Arabidopsis. Plant Cell Physiol *57*, 1133-1141.

Knoblach, B., Sun, X., Coquelle, N., Fagarasanu, A., Poirier, R.L., and Rachubinski, R.A. (2013). An ER-peroxisome tether exerts peroxisome population control in yeast. EMBO J *32*, 2439-2453.

Kornmann, B., Currie, E., Collins, S.R., Schuldiner, M., Nunnari, J., Weissman, J.S., and Walter, P. (2009). An ER-mitochondria tethering complex revealed by a synthetic biology screen. Science *325*, 477-481.

Kurokawa, K., Okamoto, M., and Nakano, A. (2014). Contact of cis-Golgi with ER exit sites executes cargo capture and delivery from the ER. Nature communications *5*, 3653.

Kwok, E.Y., and Hanson, M.R. (2004). Plastids and stromules interact with the nucleus and cell membrane in vascular plants. Plant Cell Rep *23*, 188-195.

Lai, Y.S., Stefano, G., and Brandizzi, F. (2014). ER stress signaling requires RHD3, a functionally conserved ER-shaping GTPase. J Cell Sci.

Lam, S.K., Yoda, N., and Schekman, R. (2010). A vesicle carrier that mediates peroxisome protein traffic from the endoplasmic reticulum. P Natl Acad Sci USA *107*, 21523-21528.

Lee, H., Sparkes, I., Gattolin, S., Dzimitrowicz, N., Roberts, L.M., Hawes, C., and Frigerio, L. (2013). An Arabidopsis reticulon and the atlastin homologue RHD3-like2 act together in shaping the tubular endoplasmic reticulum. New Phytol *197*, 481-489.

Lee, H.Y., Bowen, C.H., Popescu, G.V., Kang, H.G., Kato, N., Ma, S.S., Dinesh-Kumar, S., Snyder, M., and Popescu, S.C. (2011). Arabidopsis RTNLB1 and RTNLB2 Reticulon-Like Proteins Regulate Intracellular Trafficking and Activity of the FLS2 Immune Receptor. Plant Cell *23*, 3374-3391.

Lee, M., Ko, Y.J., Moon, Y., Han, M., Kim, H.W., Lee, S.H., Kang, K., and Jun, Y. (2015). SNAREs support atlastin-mediated homotypic ER fusion in Saccharomyces cerevisiae. J Cell Biol.

Levy, A., Zheng, J.Y., and Lazarowitz, S.G. (2015). Synaptotagmin SYTA Forms ER-Plasma Membrane Junctions that Are Recruited to Plasmodesmata for Plant Virus Movement. Curr Biol.

Lewis, J.D., and Lazarowitz, S.G. (2010). Arabidopsis synaptotagmin SYTA regulates endocytosis and virus movement protein cell-to-cell transport. Proc Natl Acad Sci U S A *107*, 2491-2496.

Lichtscheidl, I.K., Lancelle, S.A., and Hepler, P.K. (1990). Actin-Endoplasmic Reticulum Complexes in Drosera - Their Structural Relationship with the Plasmalemma, Nucleus, and Organelles in Cells Prepared by High-Pressure Freezing. Protoplasma *155*, 116-126.

Liu, T.Y., Bian, X., Romano, F.B., Shemesh, T., Rapoport, T.A., and Hu, J. (2015). Cis and trans interactions between atlastin molecules during membrane fusion. Proc Natl Acad Sci U S A.

Liu, T.Y., Bian, X., Sun, S., Hu, X., Klemm, R.W., Prinz, W.A., Rapoport, T.A., and Hu, J. (2012). Lipid interaction of the C terminus and association of the transmembrane segments facilitate atlastin-mediated homotypic endoplasmic reticulum fusion. Proc Natl Acad Sci U S A *109*, E2146-2154.

Lopez-Sanjurjo, C.I., Tovey, S.C., Prole, D.L., and Taylor, C.W. (2013). Lysosomes shape Ins(1,4,5)P3-evoked Ca2+ signals by selectively sequestering Ca2+ released from the endoplasmic reticulum. J Cell Sci *126*, 289-300.

Lowe, M. (2011). Structural organization of the Golgi apparatus. Curr Opin Cell Biol *23*, 85-93.

Lv, F., Li, P., Zhang, R., Li, N., and Guo, W. (2016). Functional divergence of GhCFE5 homoeologs revealed in cotton fiber and Arabidopsis root cell development. Plant Cell Rep *35*, 867-881.

Lv, F., Wang, H., Wang, X., Han, L., Ma, Y., Wang, S., Feng, Z., Niu, X., Cai, C., Kong, Z.*, et al.* (2015). GhCFE1A, a dynamic linker between the ER network and actin cytoskeleton, plays an important role in cotton fibre cell initiation and elongation. J Exp Bot *66*, 1877-1889.

Manford, A.G., Stefan, C.J., Yuan, H.L., Macgurn, J.A., and Emr, S.D. (2012). ER-to-plasma membrane tethering proteins regulate cell signaling and ER morphology. Dev Cell *23*, 1129-1140.

Mannan, A.U., Krawen, P., Sauter, S.M., Boehm, J., Chronowska, A., Paulus, W., Neesen, J., and Engel, W. (2006). ZFYVE27 (SPG33), a novel spastin-binding protein, is mutated in hereditary spastic paraplegia. American journal of human genetics *79*, 351-357.

Matsuura-Tokita, K., Takeuchi, M., Ichihara, A., Mikuriya, K., and Nakano, A. (2006). Live imaging of yeast Golgi cisternal maturation. Nature *441*, 1007-1010.

McFarlane, H.E., Lee, E.K., van Bezouwen, L.S., Ross, B., Rosado, A., and Samuels, A.L. (2017). Multiscale Structural Analysis of Plant ER-PM Contact Sites. Plant Cell Physiol *58*, 478-484.

Mclean, B., Whatley, J.M., and Juniper, B.E. (1988). Continuity of Chloroplast and Endoplasmic-Reticulum Membranes in Chara and Equisetum. New Phytologist *109*, 59-65.

Mehrshahi, P., Johnny, C., and DellaPenna, D. (2014). Redefining the metabolic continuity of chloroplasts and ER. Trends Plant Sci *19*, 501-507.

Mehrshahi, P., Stefano, G., Andaloro, J.M., Brandizzi, F., Froehlich, J.E., and DellaPenna, D. (2013). Transorganellar complementation redefines the biochemical continuity of endoplasmic reticulum and chloroplasts. Proc Natl Acad Sci U S A *110*, 12126-12131.

Montenegro, G., Rebelo, A.P., Connell, J., Allison, R., Babalini, C., D'Aloia, M., Montieri, P., Schule, R., Ishiura, H., Price, J.*, et al.* (2012). Mutations in the ER-shaping protein reticulon 2 cause the axon-degenerative disorder hereditary spastic paraplegia type 12. J Clin Invest *122*, 538-544.

Morgan, A.J., Davis, L.C., Wagner, S.K.T.Y., Lewis, A.M., Parrington, J., Churchill, G.C., and Galione, A. (2013). Bidirectional Ca2+ signaling occurs between the endoplasmic reticulum and acidic organelles. Journal of Cell Biology *200*, 789-805.

Morre, D.J., Merritt, W.D., and Lembi, C.A. (1971). Connections between Mitochondria and Endoplasmic Reticulum in Rat Liver and Onion Stem. Protoplasma *73*, 43-&.

Nixon-Abell, J., Obara, C.J., Weigel, A.V., Li, D., Legant, W.R., Xu, C.S., Pasolli, H.A., Harvey, K., Hess, H.F., Betzig, E.*, et al.* (2016). Increased spatiotemporal resolution reveals highly dynamic dense tubular matrices in the peripheral ER. Science *354*.

Nziengui, H., and Schoefs, B. (2009). Functions of reticulons in plants: What we can learn from animals and yeasts. Cell Mol Life Sci *66*, 584-595.

Orso, G., Pendin, D., Liu, S., Tosetto, J., Moss, T.J., Faust, J.E., Micaroni, M., Egorova, A., Martinuzzi, A., McNew, J.A.*, et al.* (2009). Homotypic fusion of ER membranes requires the dynamin-like GTPase atlastin. Nature *460*, 978-983.

Osterrieder, A., Sparkes, I.A., Botchway, S.W., Ward, A., Ketelaar, T., de Ruijter, N., and Hawes, C. (2017). Stacks off tracks: a role for the golgin AtCASP in plant endoplasmic reticulum-Golgi apparatus tethering. J Exp Bot.

Palmer, K.J., Hughes, H., and Stephens, D.J. (2009). Specificity of cytoplasmic dynein subunits in discrete membrane-trafficking steps. Mol Biol Cell *20*, 2885-2899.

Park, S.H., Zhu, P.P., Parker, R.L., and Blackstone, C. (2010). Hereditary spastic paraplegia proteins REEP1, spastin, and atlastin-1 coordinate microtubule interactions with the tubular ER network. J Clin Invest *120*, 1097-1110.

Patel, S.K., Indig, F.E., Olivieri, N., Levine, N.D., and Latterich, M. (1998). Organelle membrane fusion: a novel function for the syntaxin homolog Ufe1p in ER membrane fusion. Cell *92*, 611-620.

Perez-Sancho, J., Tilsner, J., Samuels, A.L., Botella, M.A., Bayer, E.M., and Rosado, A. (2016). Stitching Organelles: Organization and Function of Specialized Membrane Contact Sites in Plants. Trends Cell Biol *26*, 705-717.

Perez-Sancho, J., Vanneste, S., Lee, E., McFarlane, H.E., del Valle, A.E., Valpuesta, V., Friml, J., Botella, M.A., and Rosado, A. (2015). The Arabidopsis Synaptotagmin1 Is Enriched in Endoplasmic Reticulum-Plasma Membrane Contact Sites and Confers Cellular Resistance to Mechanical Stresses. Plant Physiology *168*, 132-U837.

Phillips, M.J., and Voeltz, G.K. (2016). Structure and function of ER membrane contact sites with other organelles. Nature reviews Molecular cell biology *17*, 69-82.

Porter, K.R., Claude, A., and Fullam, E.F. (1945). A Study of Tissue Culture Cells by Electron Microscopy : Methods and Preliminary Observations. J Exp Med *81*, 233-246.

Porter, K.R., and Palade, G.E. (1957). Studies on the endoplasmic reticulum. III. Its form and distribution in striated muscle cells. J Biophys Biochem Cytol *3*, 269-300.

Powers, R.E., Wang, S., Liu, T.Y., and Rapoport, T.A. (2017). Reconstitution of the tubular endoplasmic reticulum network with purified components. Nature *advance online publication*.

Preuss, D., Mulholland, J., Franzusoff, A., Segev, N., and Botstein, D. (1992). Characterization of the Saccharomyces Golgi-Complex through the Cell-Cycle by Immunoelectron Microscopy. Molecular Biology of the Cell *3*, 789-803.

Prinjha, R., Moore, S.E., Vinson, M., Blake, S., Morrow, R., Christie, G., Michalovich, D., Simmons, D.L., and Walsh, F.S. (2000). Inhibitor of neurite outgrowth in humans. Nature *403*, 383-384.

Qi, X.Y., Sun, J.Q., and Zheng, H.Q. (2016). A GTPase-Dependent Fine ER Is Required for Localized Secretion in Polarized Growth of Root Hairs. Plant Physiology *171*, 1996-2007.

Raiborg, C., Wenzel, E.M., Pedersen, N.M., Olsvik, H., Schink, K.O., Schultz, S.W., Vietri, M., Nisi, V., Bucci, C., Brech, A.*, et al.* (2015). Repeated ER-endosome contacts promote endosome translocation and neurite outgrowth. Nature *520*, 234-238.

Rambourg, A., Clermont, Y., and Kepes, F. (1993). Modulation of the Golgi-Apparatus in Saccharomyces-Cerevisiae Sec7 Mutants as Seen by 3-Dimensional Electron-Microscopy. Anat Rec *237*, 441-452.

Raychaudhuri, S., and Prinz, W.A. (2008). Nonvesicular phospholipid transfer between peroxisomes and the endoplasmic reticulum. P Natl Acad Sci USA *105*, 15785-15790.

Rios, R.M., and Bornens, M. (2003). The Golgi apparatus at the cell centre. Current Opinion in Cell Biology *15*, 60-66.

Robinson, D.G., Brandizzi, F., Hawes, C., and Nakano, A. (2015). Vesicles versus Tubes: Is Endoplasmic Reticulum-Golgi Transport in Plants Fundamentally Different from Other Eukaryotes? Plant Physiol *168*, 393-406.

Rocha, N., Kuijl, C., van der Kant, R., Janssen, L., Houben, D., Janssen, H., Zwart, W., and Neefjes, J. (2009). Cholesterol sensor ORP1L contacts the ER protein VAP to control Rab7-RILP-p150 Glued and late endosome positioning. J Cell Biol *185*, 1209-1225.

Roger, A.J., Munoz-Gomez, S.A., and Kamikawa, R. (2017). The Origin and Diversification of Mitochondria. Curr Biol *27*, R1177-R1192.

Rogers, J.V., Arlow, T., Inkellis, E.R., Koo, T.S., and Rose, M.D. (2013). ER-associated SNAREs and Sey1p mediate nuclear fusion at two distinct steps during yeast mating. Molecular Biology of the Cell *24*, 3896-3908.

Rogers, J.V., McMahon, C., Baryshnikova, A., Hughson, F.M., and Rose, M.D. (2014). ER-associated retrograde SNAREs and the Dsl1 complex mediate an alternative, Sey1p-independent homotypic ER fusion pathway. Mol Biol Cell *25*, 3401-3412.

Rowland, A.A., Chitwood, P.J., Phillips, M.J., and Voeltz, G.K. (2014). ER contact sites define the position and timing of endosome fission. Cell *159*, 1027-1041.

Rowland, A.A., and Voeltz, G.K. (2012). Endoplasmic reticulum-mitochondria contacts: function of the junction. Nature reviews Molecular cell biology *13*, 607-625.

Runions, J., Brach, T., Kuhner, S., and Hawes, C. (2006). Photoactivation of GFP reveals protein dynamics within the endoplasmic reticulum membrane. J Exp Bot *57*, 43-50.

Schapire, A.L., Voigt, B., Jasik, J., Rosado, A., Lopez-Cobollo, R., Menzel, D., Salinas, J., Mancuso, S., Valpuesta, V., Baluska, F.*, et al.* (2008). Arabidopsis Synaptotagmin 1 Is Required for the Maintenance of Plasma Membrane Integrity and Cell Viability. Plant Cell *20*, 3374-3388.

Schattat, M., Barton, K., Baudisch, B., Klosgen, R.B., and Mathur, J. (2011). Plastid Stromule Branching Coincides with Contiguous Endoplasmic Reticulum Dynamics. Plant Physiology *155*, 1667-1677.

Schiefelbein, J.W., and Somerville, C. (1990). Genetic Control of Root Hair Development in Arabidopsis thaliana. Plant Cell *2*, 235-243.

Schuldiner, M., Collins, S.R., Thompson, N.J., Denic, V., Bhamidipati, A., Punna, T., Ihmels, J., Andrews, B., Boone, C., Greenblatt, J.F.*, et al.* (2005). Exploration of the function and organization of the yeast early secretory pathway through an epistatic miniarray profile. Cell *123*, 507-519.

Schwartz, S.L., Cao, C., Pylypenko, O., Rak, A., and Wandinger-Ness, A. (2007). Rab GTPases at a glance. J Cell Sci *120*, 3905-3910.

Shai, N., Schuldiner, M., and Zalckvar, E. (2016). No peroxisome is an island - Peroxisome contact sites. Bba-Mol Cell Res *1863*, 1061-1069.

Shen, Q., Uknes, S.J., and Ho, T.H. (1993). Hormone response complex in a novel abscisic acid and cycloheximide-inducible barley gene. J Biol Chem *268*, 23652-23660.

Shibata, Y., Hu, J., Kozlov, M.M., and Rapoport, T.A. (2009). Mechanisms shaping the membranes of cellular organelles. Annu Rev Cell Dev Biol *25*, 329-354.

Shibata, Y., Shemesh, T., Prinz, W.A., Palazzo, A.F., Kozlov, M.M., and Rapoport, T.A. (2010). Mechanisms Determining the Morphology of the Peripheral ER. Cell *143*, 774-788.

Siao, W., Wang, P., Voigt, B., Hussey, P.J., and Baluska, F. (2016). Arabidopsis SYT1 maintains stability of cortical endoplasmic reticulum networks and VAP27-1-enriched endoplasmic reticulum-plasma membrane contact sites. J Exp Bot *67*, 6161-6171.

Sinclair, A.M., Trobacher, C.P., Mathur, N., Greenwood, J.S., and Mathur, J. (2009). Peroxule extension over ER-defined paths constitutes a rapid subcellular response to hydroxyl stress. Plant J *59*, 231-242.

Sliwinska, E., Mathur, J., and Bewley, J.D. (2015). On the relationship between endoreduplication and collet hair initiation and tip growth, as determined using six Arabidopsis thaliana root-hair mutants. Journal of Experimental Botany *66*, 3285-3295.

Somlyo, A.P., Bond, M., and Somlyo, A.V. (1985). Calcium content of mitochondria and endoplasmic reticulum in liver frozen rapidly in vivo. Nature *314*, 622-625.

Sparkes, I., Runions, J., Hawes, C., and Griffing, L. (2009a). Movement and remodeling of the endoplasmic reticulum in nondividing cells of tobacco leaves. Plant Cell *21*, 3937-3949.

Sparkes, I., Tolley, N., Aller, I., Svozil, J., Osterrieder, A., Botchway, S., Mueller, C., Frigerio, L., and Hawes, C. (2010). Five Arabidopsis reticulon isoforms share endoplasmic reticulum location, topology, and membrane-shaping properties. Plant Cell *22*, 1333-1343.

Sparkes, I.A., Frigerio, L., Tolley, N., and Hawes, C. (2009b). The plant endoplasmic reticulum: a cell-wide web. The Biochemical journal *423*, 145-155.

Sparkes, I.A., Ketelaar, T., de Ruijter, N.C., and Hawes, C. (2009c). Grab a Golgi: laser trapping of Golgi bodies reveals in vivo interactions with the endoplasmic reticulum. Traffic *10*, 567-571.

Staehelin, L.A. (1997). The plant ER: A dynamic organelle composed of a large number of discrete functional domains. Plant J *11*, 1151-1165.

Stefan, C.J., Manford, A.G., Baird, D., Yamada-Hanff, J., Mao, Y.X., and Emr, S.D. (2011). Osh Proteins Regulate Phosphoinositide Metabolism at ER-Plasma Membrane Contact Sites. Cell *144*, 389-401.

Stefano, G., and Brandizzi, F. (2014). Unique and conserved features of the plant ER-shaping GTPase RHD3. Cellular logistics *4*, e28217.

Stefano, G., and Brandizzi, F. (2017). Advances in plant ER architecture and dynamics. Plant Physiol.

Stefano, G., Renna, L., Chatre, L., Hanton, S.L., Moreau, P., Hawes, C., and Brandizzi, F. (2006). In tobacco leaf epidermal cells, the integrity of protein export from the endoplasmic reticulum and of ER export sites depends on active COPI machinery. Plant J *46*, 95-110.

Stefano, G., Renna, L., Lai, Y., Slabaugh, E., Mannino, N., Buono, R.A., Otegui, M.S., and Brandizzi, F. (2015). ER network homeostasis is critical for plant endosome streaming and endocytosis. Cell Discovery *1*, 15033.

Stefano, G., Renna, L., Moss, T., McNew, J.A., and Brandizzi, F. (2012). In Arabidopsis, the spatial and dynamic organization of the endoplasmic reticulum and Golgi apparatus is influenced by the integrity of the C-terminal domain of RHD3, a non-essential GTPase. Plant J *69*, 957-966.

Terasaki, M., Chen, L.B., and Fujiwara, K. (1986). Microtubules and the Endoplasmic-Reticulum Are Highly Interdependent Structures. Journal of Cell Biology *103*, 1557-1568.

Terasaki, M., and Reese, T.S. (1994). Interactions among Endoplasmic-Reticulum, Microtubules, and Retrograde Movements of the Cell-Surface. Cell Motil Cytoskel *29*, 291-300.

Terasaki, M., Shemesh, T., Kasthuri, N., Klemm, R.W., Schalek, R., Hayworth, K.J., Hand, A.R., Yankova, M., Huber, G., Lichtman, J.W.*, et al.* (2013). Stacked Endoplasmic Reticulum Sheets Are Connected by Helicoidal Membrane Motifs. Cell *154*, 285-296.

Tolley, N., Sparkes, I.A., Hunter, P.R., Craddock, C.P., Nuttall, J., Roberts, L.M., Hawes, C., Pedrazzini, E., and Frigerio, L. (2008). Overexpression of a plant reticulon remodels the lumen of the cortical endoplasmic reticulum but does not perturb protein transport. Traffic *9*, 94-102.

Tse, Y.C., Mo, B., Hillmer, S., Zhao, M., Lo, S.W., Robinson, D.G., and Jiang, L. (2004). Identification of multivesicular bodies as prevacuolar compartments in Nicotiana tabacum BY-2 cells. Plant Cell *16*, 672-693.

Turner, M.D., Plutner, H., and Balch, W.E. (1997). A Rab GTPase is required for homotypic assembly of the endoplasmic reticulum. J Biol Chem *272*, 13479-13483.

Ueda, H., Yokota, E., Kutsuna, N., Shimada, T., Tamura, K., Shimmen, T., Hasezawa, S., Dolja, V.V., and Hara-Nishimura, I. (2010). Myosin-dependent endoplasmic reticulum motility and F-actin organization in plant cells. P Natl Acad Sci USA *107*, 6894-6899.

Ueda, H., Yokota, E., Kuwata, K., Kutsuna, N., Mano, S., Shimada, T., Tamura, K., Stefano, G., Fukao, Y., Brandizzi, F.*, et al.* (2015). Phosphorylation of the C-terminus of RHD3 Has a Critical Role in Homotypic ER Membrane Fusion in Arabidopsis. Plant Physiol.

Viotti, C., Bubeck, J., Stierhof, Y.D., Krebs, M., Langhans, M., van den Berg, W., van Dongen, W., Richter, S., Geldner, N., Takano, J.*, et al.* (2010). Endocytic and secretory traffic in Arabidopsis merge in the trans-Golgi network/early endosome, an independent and highly dynamic organelle. Plant Cell *22*, 1344-1357.

Voeltz, G.K., Prinz, W.A., Shibata, Y., Rist, J.M., and Rapoport, T.A. (2006). A class of membrane proteins shaping the tubular endoplasmic reticulum. Cell *124*, 573-586.

Wang, H., Han, S., Siao, W., Song, C., Xiang, Y., Wu, X., Cheng, P., Li, H., Jasik, J., Micieta, K.*, et al.* (2015). Arabidopsis Synaptotagmin 2 Participates in Pollen Germination and Tube Growth and Is Delivered to Plasma Membrane via Conventional Secretion. Mol Plant *8*, 1737-1750.

Wang, H., Lee, M.M., and Schiefelbein, J.W. (2002). Regulation of the cell expansion gene RHD3 during Arabidopsis development. Plant Physiol *129*, 638-649.

Wang, H., Lockwood, S.K., Hoeltzel, M.F., and Schiefelbein, J.W. (1997). The ROOT HAIR DEFECTIVE3 gene encodes an evolutionarily conserved protein with GTP-binding motifs and is required for regulated cell enlargement in Arabidopsis. Genes Dev *11*, 799-811.

Wang, P., Hawes, C., and Hussey, P.J. (2017a). Plant Endoplasmic Reticulum-Plasma Membrane Contact Sites. Trends Plant Sci *22*, 289-297.

Wang, P., Hawkins, T.J., and Hussey, P.J. (2017b). Connecting membranes to the actin cytoskeleton. Curr Opin Plant Biol *40*, 71-76.

Wang, P., Hawkins, T.J., Richardson, C., Cummins, I., Deeks, M.J., Sparkes, I., Hawes, C., and Hussey, P.J. (2014). The Plant Cytoskeleton, NET3C, and VAP27 Mediate the Link between the Plasma Membrane and Endoplasmic Reticulum. Curr Biol *24*, 1397-1405.

Wang, P., and Hussey, P.J. (2017). NETWORKED 3B: a novel protein in the actin cytoskeleton-endoplasmic reticulum interaction. J Exp Bot *68*, 1441-1450.

Wang, P., Richardson, C., Hawkins, T.J., Sparkes, I., Hawes, C., and Hussey, P.J. (2016a). Plant VAP27 proteins: domain characterization, intracellular localization and role in plant development. New Phytologist, n/a-n/a.

Wang, S., Tukachinsky, H., Romano, F.B., and Rapoport, T.A. (2016b). Cooperation of the ER-shaping proteins atlastin, lunapark, and reticulons to generate a tubular membrane network. eLife *5*, e18605.

Waterman-Storer, C.M., Gregory, J., Parsons, S.F., and Salmon, E.D. (1995). Membrane/microtubule tip attachment complexes (TACs) allow the assembly dynamics of plus ends to push and pull membranes into tubulovesicular networks in interphase Xenopus egg extracts. J Cell Biol *130*, 1161-1169.

Waterman-Storer, C.M., and Salmon, E.D. (1998). Endoplasmic reticulum membrane tubules are distributed by microtubules in living cells using three distinct mechanisms. Curr Biol *8*, 798-806.

Westrate, L.M., Lee, J.E., Prinz, W.A., and Voeltz, G.K. (2015). Form follows function: the importance of endoplasmic reticulum shape. Annu Rev Biochem *84*, 791-811.

Wozniak, M.J., Bola, B., Brownhill, K., Yang, Y.C., Levakova, V., and Allan, V.J. (2009). Role of kinesin-1 and cytoplasmic dynein in endoplasmic reticulum movement in VERO cells. J Cell Sci *122*, 1979-1989.

Xu, C.C., Fan, J.L., Cornish, A.J., and Benning, C. (2008). Lipid trafficking between the endoplasmic reticulum and the plastid in Arabidopsis requires the extraplastidic TGD4 protein. Plant Cell *20*, 2190-2204.

Yamazaki, T., Kawamura, Y., Minami, A., and Uemura, M. (2008). Calcium-Dependent Freezing Tolerance in Arabidopsis Involves Membrane Resealing via Synaptotagmin SYT1. Plant Cell *20*, 3389-3404.

Yan, L., Sun, S., Wang, W., Shi, J., Hu, X., Wang, S., Su, D., Rao, Z., Hu, J., and Lou, Z. (2015). Structures of the yeast dynamin-like GTPase Sey1p provide insight into homotypic ER fusion. The Journal of Cell Biology *210*, 961-972.

Yokota, E., Ueda, H., Hashimoto, K., Orii, H., Shimada, T., Hara-Nishimura, I., and Shimmen, T. (2011). Myosin XI-Dependent Formation of Tubular Structures from Endoplasmic Reticulum Isolated from Tobacco Cultured BY-2 Cells. Plant Physiology *156*, 129-143.

Zaar, K., Volkl, A., and Fahimi, H.D. (1987). Association of Isolated Bovine Kidney Cortex Peroxisomes with Endoplasmic-Reticulum. Biochimica Et Biophysica Acta *897*, 135-142.

Zeuschner, D., Geerts, W.J., van Donselaar, E., Humbel, B.M., Slot, J.W., Koster, A.J., and Klumperman, J. (2006). Immuno-electron tomography of ER exit sites reveals the existence of free COPII-coated transport carriers. Nat Cell Biol *8*, 377-383.

Zhang, D., Vjestica, A., and Oliferenko, S. (2012). Plasma membrane tethering of the cortical ER necessitates its finely reticulated architecture. Curr Biol *22*, 2048-2052.

Zhang, H., and Hu, J. (2016). Shaping the Endoplasmic Reticulum into a Social Network. Trends in Cell Biology *26*, 934-943.

Zhang, M., Wu, F., Shi, J., Zhu, Y., Zhu, Z., Gong, Q., and Hu, J. (2013). RHD3 family of dynamin-like GTPases mediates homotypic endoplasmic reticulum fusion and is essential for Arabidopsis development. Plant Physiol.

Zhao, Y., Zhang, T., Huo, H., Ye, Y., and Liu, Y. (2016). Lunapark Is a Component of a Ubiquitin Ligase Complex Localized to the Endoplasmic Reticulum Three-way Junctions. Journal of Biological Chemistry.

Zink, S., Wenzel, D., Wurm, C.A., and Schmitt, H.D. (2009). A link between ER tethering and COP-I vesicle uncoating. Dev Cell *17*, 403-416.

CHAPTER II:

EFFICIENT ER FUSION REQUIRES A DIMERIZATION AND A C-TERMINAL TAIL MEDIATED MEMBRANE ANCHORING OF RHD3

Jiaqi Sun, Hugo Zheng

Plant Physiology, January 2018, Vol. 176, pp. 406–417

ABSTRACT

The endoplasmic reticulum (ER) is a network of tubules and sheets stretching throughout eukaryotic cells. The formation of the ER requires homotypic membrane fusion, which is mediated by a family of Dynamin-like Atlastin GTPase proteins. The Arabidopsis member ROOT HAIR DEFECTIVE3 (RHD3) has been demonstrated to mediate ER membrane fusion, but how exactly RHD3 is involved in the process is still unknown. Here we conducted systemic structure-function analyses of roles of different RHD3 domains in mediating ER fusion. We showed that efficient ER membrane fusion mediated by RHD3 requires a proper dimerization of RHD3 through the GTPase domain (GD) and the first and second three helix bundles (3HBs) in the middle domain. RHD3 has a 3HB-enriched middle domain longer than that of Atlastins, and we revealed that the third and fourth 3HBs are required for the stability of RHD3. The transmembrane segments (TMs) of RHD3 are essential for targeting and retention of RHD3 in the ER and can also facilitate an oligomerization of RHD3. Furthermore, we showed that an amphipathic helix in the C-terminal cytosolic tail (CT) of RHD3 has a membrane anchoring ability that is required for efficient ER membrane fusion mediated by RHD3. This work contributes to a better understanding of a coordinated action of RHD3 in the fusion of ER membranes.

2.1. INTRODUCTION

The endoplasmic reticulum (ER) is a highly conserved, continuous and interconnected membrane network, composed of smooth tubules and sheet-like cisternae that extend throughout the cytoplasm. The ER plays vital roles in protein synthesis, folding and transport, mitochondrial division, calcium regulation, and lipid synthesis and transport in eukaryotic cells including plant cells. Live-cell imaging revealed that the ER is a highly dynamic organelle, showing continuous growth, retraction, sliding and fusion of tubules to form strands, cisternae and polygons (Sparkes et al., 2011). This dynamic is important for the ER to perform its diverse functions. It is known that the ER shaping proteins, reticulons and DP1/Yop1p, play key roles in generating and maintaining the unique reticular morphology of the ER in plant, yeast and mammalian cells (Hu et al., 2008; Sparkes et al., 2010; Voeltz et al., 2006). It is assumed that these proteins can induce and stabilize a membrane curvature of the tubules and edges of the sheet, through their two sets of closely spaced TMs and a C-terminal amphipathic helix (Brady et al., 2015; Breeze et al., 2016; Voeltz et al., 2006). Connecting ER tubules into the polygonal network requires membrane fusion, which is mediated by a family of Dynamin-like Atlastin GTPase proteins, including Atlastins in metazoans, Sey1p in yeast and RHD3 (ROOT HAIR DEFECTIVE3) in plants (Anwar et al., 2012; Chen et al., 2011; Hu et al., 2009; Orso et al., 2009; Zhang et al., 2013). The deletion of Atlastin-1 leads to long and nonbranched ER tubules in mammalian cells and ER fragmentation in Drosophila (Hu et al., 2009; Orso et al., 2009). In plants, the loss of RHD3 leads to thick and bundled ER tubules (Zheng et al., 2004). These ER fusogens also play critical physiological roles. In human, mutations in Atlastin-1 cause a neurodegenerative disease called hereditary spastic paraplegia (Zhao et al., 2001). In yeast *Candida albicans*, deletions of Sey1p lead to attenuated virulence in mice as well as increased susceptibility to cycloheximide (Yamada-Okabe and

Yamada-Okabe, 2002). In plants, mutations in RHD3 result in short and wavy root hair growth (Schiefelbein and Somerville, 1990).

Atlastins, Sey1p and RHD3 are all ER membrane-bound GTPases and share a conserved protein structure. They all have a cytosolic N-terminal GTPase domain (GD), a three helix bundles (3HB)-enriched middle domain and two transmembrane segments (TMs) and a cytosolic C-terminal tail (CT) (Liu et al., 2012; Stefano and Brandizzi, 2014). The mechanistic basis of the action of Atlastins and Sey1p in ER membrane fusion has been studied (Hu and Rapoport, 2016). Based on the revealed homotypic interaction and the crystal structure of the cytosolic N-terminus of Atlastin-1 (Bian et al., 2011), it was proposed that two Atlastin-1 molecules in different membranes bind GTP and form a dimer. The GTP hydrolysis and phosphate release trigger a conformational change of the dimer, leading to the membrane fusion (Bian et al., 2011). Because the two TMs are also involved in homotypic interaction of Atlastin-1, it is believed that several Atlastin-1 molecules in the same membrane could also associate with each other through their TMs and multiple cycles of GTP hydrolysis occur before a successful fusion event (Liu et al., 2015; Liu et al., 2012). It is believed that Sey1p mediates the homotypic ER membrane fusion by a similar paradigm (Yan et al., 2015).

Despite what is unveiled in mammalian and yeast cells, the mechanistic basis of the action of RHD3 in the ER membrane fusion has not been well studied. It is known that overexpression of GDP-locked RHD3 mutant (S51N) and GTP-locked RHD3 mutant (T75A) could exert a dominant-negative effect on the ER morphology and root hair growth (Chen et al., 2011). Also *in vitro* membrane fusion mediated by RHD3 requires GTP hydrolysis (Zhang et al., 2013). Moreover, it has been shown that RHD3 can undergo a GTP-dependent homotypic interaction in yeast 2-hybrid (Y2H) and bi-molecular fluorescent complementation (BiFC) systems (Chen et al., 2011;

Zheng and Chen, 2011). Previous studies indicated that mutations in the GD (Chen et al., 2011; Wang et al., 2015; Zhang et al., 2013), the middle domain (Zhang et al., 2013), two TMs (Stefano et al., 2012) all can make RHD3 defective, suggesting that the RHD3-mediated ER fusion is a delicate process, that may require a coordinated action from different domains of RHD3. However, how the different domains of RHD3 are involved in the RHD3-mediated ER fusion is still not known.

Here, we studied the roles of different RHD3 domains in mediating ER membrane fusion. Our data suggests that, in addition to its GTPase activity, the GD of RHD3 is involved in a dimerization of RHD3 for an efficient ER membrane fusion. Whilst the first and second 3HBs of the middle domain of RHD3 are also involved in the dimerization of RHD3, the third and fourth 3HBs of RHD3 are required for the stability of RHD3. The TMs of RHD3 are essential for the targeting and retention of RHD3 in the ER and can facilitate an oligomerization of RHD3. Furthermore, we showed that an amphipathic helix in the CT of RHD3 has a membrane anchoring ability that is required for efficient ER membrane fusion mediated by RHD3.

2.2. RESULTS

2.2.1. Dimerization of RHD3 through GTPase interface is required for an efficient ER fusion mediated by RHD3

Although the overall structure of the Dynamin-like Atlastin GTPase proteins is conserved, the predicted three helical bundle (3HB)-enriched middle domain of RHD3 and Sey1p is much longer than that of Atlastin-1 (Stefano and Brandizzi, 2014) (Supplemental Fig. S2.1A, Fig. 2.1A). To understand the mechanistic basis of RHD3, we simulated the structure of the cytosolic N-terminus of RHD3 based on the crystal structure of the cytosolic N-terminus of *Candida albicans* Sey1p (Yan et al., 2015). The side view of the simulated structure suggested that, like Sey1p, the cytosolic N-terminus of RHD3 formed a dimer (Fig. 2.1B1, one RHD3 monomer is colored, another one is in grey). The GDs of two RHD3 molecules were facing to each other and the middle domains, composed of four 3HBs, form a twisted arm (Fig. 2.1B1). In the interface of the two GDs, there were three potential polar contacts between Asp-185 (D185) of one RHD3 molecule and Arg-101 (R101) of another (Supplemental Fig. S2.1B, arrowheads). When the simulated structure of RHD3 was viewed from the top (Fig.2.1B2), there were two potential D185-R101 salt bridge sites in the interface of RHD3 (Fig.2.1B2). We noted that, *rhd3-2*, an *RHD3* mutant allele with a point mutation (D185N) grows short and wavy root hairs (Wang et al., 1997). We first wondered if this point mutation in RHD3 could affect the function of RHD3 in the formation of the ER. To this end, we transiently expressed YFP-RHD3(D185N) together with an ER marker RFP-HDEL in tobacco leaves. Transient expression of wild type RFP-RHD3 did not change the interconnected polygonal ER network (Fig.2.1C), while expressing YFP-RHD3(D185N) made thick and unbranched ER bundles (Fig.2.1D, arrowheads). This result suggests that RHD3(D185N) has a negative effect on the formation of the polygonal ER network *in vivo*.

According to the simulated structure, the D185N mutation could potentially reduce the polar contacts between Asp-185 (D185) of one RHD molecule and Arg-101 (R101) of another in the dimerization of RHD3 (Supplemental Fig.S2.1C, arrowhead). As previously reported, RHD3 undergoes a homotypic interaction in both Y2H and BiFC assays (Chen et al., 2011; Zheng and Chen, 2011), and RHD3 is functional in yeast cells (Zhang, et al., 2013), we thus tested if there is a reduced interaction when D185 or R101 is mutated using yeast mating based split-ubiquitin system (SUS) (Grefen et al., 2007). A full length RHD3 could interact with a full length RHD3 (Fig.2. 1E, row 1), more importantly, we found that a full length RHD3 could also interact with the GD of RHD3 (Fig.2. 1E, row 3), indicating that the dimerization of RHD3 via the GDs, suggested by the simulated structure is likely. When D185 was mutated to N (Fig.2. 1E, row 4), or R101 was mutated to E (Fig.2. 1E, row 5), either mutation reduced the interaction between the full-length RHD3 and its GD. Strikingly, the double mutant (R101E, D185N) had a much weaker homotypic interaction than either D185N or R101E mutation (Fig.2. 1E, row 6). In addition, when the interaction between RHD3 and its GD domain with the reciprocal mutation (R101D, D185R) was tested, the interaction between RHD3 and its GD was restored (Fig.2. 1E, row 7). These results confirmed the interaction linkage between D185 and R101 in the simulated RHD3 dimerization. while there was a reduced interaction when either of the amino acids was mutated, interestingly, no significant reduction was found in the interaction between RHD3(R101E) and GD(D185N) compared with the interaction between RHD3 and its GD (Fig.2. 1E, compare row 8 with row 3). As mentioned, there were two potential D185-R101 salt bridge sites in the interface of RHD3 dimer (Fig.2. 1B2), Likely, between RHD3(R101E) and GD(D185N), only one of two salt bridge sites will be affected. This could be a reason we did not detect a significant reduction to the level that was visible in SUS.

The dimerization of Atlastin-1 or Sey1p plays an important role in efficient ER membrane fusion. We thus wondered if RHD3(D185N) or RHD3(R101E) is defective in mediating ER fusion. Because RHD3 is able to rescue the ER fusion deficiency of *Δsey1p* yeast cells (Zhang et al., 2013), we therefore used a *Δsey1p*-based yeast ER fusion assay to quantify the ER fusion efficiency (Anwar et al., 2012). Consistent with the previous report, the *Δsey1p* mutant cells took approximately 28 mins to finish the ER fusion (Fig.2. 2, column 1), while expressing Sey1p and RHD3 in the *Δsey1p* mutant cells could significantly reduce the fusion time to approximately 9 mins and 13 mins, respectively (Fig.2. 2, column 2 and 3). Such a rescue was compromised to approximately 21 mins and 20 mins with the D185N and R101E mutations, respectively (Fig.2. 2, column 4 and column 5). The double mutant RHD3(R101E, D185N) had an enhanced ER fusion deficiency compared to RHD3(R101E) or RHD3(D185N) in rescuing the ER fusion defects of *Δsey1p* mutant (Fig.2. 2, column 6). Interestingly, the reciprocal mutant, RHD3(R101D, D185R) has much more efficient ER fusion (Fig.2. 2, column 7) than double mutant RHD3 (R101R, D185N), as well as single mutants RHD3(R101E) and RHD3(D185N). This was likely due to the restored interaction in the reciprocal mutant RHD3(R101D, D185R) revealed in Fig 1E. Taken all together, the dimerization through D185 and R101 in the GD is required for the efficient ER fusion mediated by RHD3.

2.2.2. The first and second 3HBs are also involved in RHD3 dimerization for efficient ER fusion, whilst the third and fourth 3HBs are required for the protein stability of RHD3

The simulated structure for the cytosolic N-terminus of RHD3 suggests that there are four different 3HBs in the middle domain (Figure 1B1). To gain the insight into the roles of the four 3HBs in the middle domain may play, two different conserved hydrophobic residues in each 3HB were

replaced by proline to disrupt the α-helix structure. The mutated versions of RHD3 were fused with YFP and then transiently expressed in tobacco leaves with an ER marker RFP-HDEL to assess their action in the formation of the ER. The expression of 3HB-1 mutants, RHD3(A285P) and RHD3(L355P), created thick and unbranched ER bundles (Fig.2. 3B; Supplemental Fig.S2.2B, arrows), while the expression of 3HB-2 mutants, RHD3(F382P) and RHD3(L434P), produced aggregations of ER tubules (Fig.2. 3C； Supplemental Fig.S2.2C, arrowheads). On the other hand, transient expression of 3HB-3 mutants, RHD3(L461P) and RHD3(L465P), and 3HB-4 mutants, RHD3(A575P) and RHD3(L580P), including RHD3-1 with a point mutation (A575V) in 3HB-4, had no obvious negative effect on the formation of the polygonal tubular ER network (Fig.2. 3D-E; Supplemental Fig.S2.2D-F). Interestingly, while 3HB-1 mutants, RHD3(A285P) and RHD3(L355P), and 3HB-2 mutants, RHD3(F382P) and RHD3(L434P), were still targeted to the ER (Fig.2. 3B-C; Supplemental Fig.S2.2B-C), all 3HB-3 mutants, RHD3(L461P) and RHD3(L465P), and 3HB-4 mutants, RHD3(A575P), RHD3(L580P) and RHD3-1, had only a faint YFP signal in the form of small punctates (Fig.2. 3D-E; Supplemental Fig.S2.2D-F).

According to the simulated dimerization of RHD3, the first two 3HBs of different RHD3 monomers may hold each other tightly in the dimerization of RHD3. Consistent with this hypothesis, our SUS assay showed that there was an interaction between a full length of RHD3 and its middle domain (Fig.2. 4, row 3). More importantly, mutations in 3HB-1 (A285P) and 3HB-2 (F382P) significantly reduced the interaction between RHD3 and its middle domain (MID) (Fig.2. 4, compare the interaction in row 3 with row 4,5). The yeast-based ER fusion assay also showed that RHD3(A285P) and RHD3(F382P) mutants had a reduced ER fusion efficiency (Fig.2. 2, column 8 and 9 respectively), suggesting that this dimerization through 3HB-1 and 3HB-2 is also required for efficient ER fusion mediated by RHD3 *in vivo*.

RHD3-1(A575V), located in the fourth 3HB, is showed to have reduced protein stability (Zhang et al., 2013). Because of the faint YFP signal produced by mutations in 3HB-3 and 3HB-4 of RHD3, we developed an RY (red and yellow) vector to quantify the expression level of the 3HB-3 and 3HB-4 RHD3 mutants. The RY vector can express mCherry-HDEL and YFP-RHD3 simultaneously (Supplemental Fig.S2.3A) so that mCherry-HDEL can be used as a reference for the expression of RHD3 (Zhang et al., 2015). With this system, we found that the 3HB-3 mutants RHD3(L461P) and RHD3(L465P), and 3HB-4 mutants RHD3(A575P) and RHD3(L580P) including RHD3-1, again showed a faint YFP signal in the form of small punctates (Supplemental Fig.S2.3B). The fluorescence quantification showed that the YFP signal of these RHD3 mutants was dramatically lower than that of wild type RHD3 (Fig.2. 5A). Western blot confirmed that the 3HB-3 and 3HB-4 RHD3 mutants had a reduced protein level (Fig.2. 5B), while at the transcription level, different 3HB-3 and 3HB-4 RHD3 mutants did not have significant difference compared to wild type RHD3 (Fig.2. 5C). These results indicate that both 3HB-3 and 3HB-4 of RHD3 play a role in the protein stability of RHD3.

2.2.3. The transmembrane domains play an important role in targeting and retention of RHD3 in the ER

RHD3 is an ER localized membrane protein (Chen et al., 2011). RHD3 with a point mutation (P701S) between the two TMs was present in some large structures, which were different from the ER network distribution of wild-type RHD3 (Stefano et al., 2012). We therefore wondered what determines the ER localization of the RHD3 protein. To this end, the two putative TMs (aa677-721) were deleted to create RHD3(ΔTM) and then RHD3(ΔTM) was fused to either YFP or RFP. We found that RHD3(ΔTM) was present largely in the cytosol (Fig.2. 6A-C). In addition,

occasional reticulum-like structures (Fig.2. 6A, arrows) and many punctates (Fig.2. 6B-C) were also visible. Co-expression with RFP-HDEL indicated that those reticulum-like structures were ER tubules (Fig.2. 6A, arrows), while co-expression with ERD2-GFP or ST-RFP indicated that those punctates were cis-Golgi (Fig.2. 6B-C). The results suggested that TMs of RHD3 play an important role in targeting and retention of RHD3 in the ER.

Atlastin-1 undergoes oligomerization in the same membrane through its TMs (Liu et al., 2012), so we wondered if the TMs of RHD3 has a similar mechanism. SUS test showed that the TMs of RHD3 could efficiently interact with each other (Fig.2. 6D, row 3), which suggested that RHD3 could also form oligomerization through TMs. These results indicate that in addition to determining the ER localization of RHD3, the TMs of RHD3 can also facilitate homotypic interaction of RHD3.

2.2.4. The amphipathic helix of the C-terminal RHD3 has an ability for membrane targeting

Although the TMs of RHD3 play an important role in targeting and retention of RHD3 in the ER, the unexpected ER and Golgi membrane association of RHD3(ΔTM) also suggests that, there are membrane targeting sequences outside of the TMs of RHD3. To determine this, the GD of RHD3, the N-terminal cytosolic part of RHD3 (RHD3(ΔTMΔCT)), and the CT of RHD3 were fused with YFP or RFP and transiently expressed in tobacco leaves. The GD of RHD3 or RHD3(ΔTMΔCT) was seen only in the cytosol (Fig.2. 7A-B). Interesting, although The GD of RHD3 or RHD3(ΔTMΔCT) was seen only in the cytosol, the expression of both parts of RHD3 has a negative effect on the formation of the polygonal ER network as indicated by RFP-HDEL (Fig.2. 7A-B, arrows). On the other hand, the CT of RHD3, like RHD3(ΔTM), was localized to the ER membrane and Golgi, in addition to the cytoplasm (Fig.2. 7C-D). This indicates that the CT of RHD3 contains a membrane targeting sequence(s). To gain deeper insight into what determines

the membrane targeting in the CT of RHD3, a multiple sequence alignment was performed within the CT of proteins in the Dynamin-like Atlastin GTPase protein family (Fig.2. 7E). We revealed that there were an conserved amphipathic helix and a divergent sequence (DS) in the end. The DS is involved in the phosphorylation of RHD3 (Ueda et al., 2015). When the divergent sequence (DS) was deleted, the membrane targeting of the CT of RHD3 was not abolished (Fig.2. 7F). This indicated that the amphipathic helix of RHD3 has an ability for membrane targeting.

2.2.5. The amphipathic helix of the C-terminal RHD3 is required for efficient ER membrane fusion

To understand how this amphipathic helix of RHD3 could direct a membrane targeting of a portion of RHD3(ΔTM) or the CT of RHD3 as well as the biological function of the amphipathic helix of RHD3, the possible arrangement of the helix (AA727-744) was first predicted using HeliQuest and PEP-FOLD (Fig.2. 8A). There was an obvious hydrophobic face in the helix and four of them (V731, L735, L738 and F742) are facing to the same surface, while F727 was not (Fig.2. 8A). When the hydrophobic residues were replaced by the acidic residue, Asp(D), all the mutations on the hydrophobic face, V731D, L735D, L738D, F742D, abolished the membrane anchoring ability of the CT of RHD3 (Fig.2. 8B), as indicated by the lack of punctate Golgi labelling. On the other hand, the F727D mutation did not change the membrane localization of the CT of RHD3 (Supplemental Fig.S2.4A). This suggests that the hydrophobic residues in the hydrophobic face are important for the membrane anchoring of the CT of RHD3. Moreover, changing V731 into the other hydrophobic residues (V731A, V731L and V731I) did not significantly diminish the membrane association of the CT of RHD3 (Fig.2. 8C), suggesting that the hydrophobic property of the hydrophobic face in the amphipathic helix is more important than the amino acid sequence specificity.

The potential biological function of the amphipathic helix was then tested in the yeast ER fusion assay. We found that RHD3 with single mutation RHD3(L735D) and EHD3(L738D) in the amphipathic helix had a reduction in the efficiency of rescuing *ΔSey1p* (Fig.2. 2, column 10 and 11, respectively), and RHD3 with double mutations EHD3(L735D, L738D) in the amphipathic helix had severe reduction in the efficiency of rescuing *ΔSey1p* (Fig.2. 2, column 12, the p-value between RHD3(L735D) and RHD3(L735D, L738D) is $0.019<0.05$ and the p-value between RHD3(L738D) and RHD3(L735D, L738D) is $0.016<0.05$). When transiently expressed in the tobacco leaves, the double mutant RHD3(L735D, L738D) and quadruple mutant RHD3(F727D, V731D, L735D, L738D) created thick and bundled ER tubules (Fig.2. 8E-F, arrows). Furthermore, the CT deleted mutant RHD3(ΔCT) and the quadruple mutant RHD3(F727D, V731D, L735D, L738D) could not rescue the ER defects revealed in the *rhd3-8* mutant (Supplemental Fig.S2.4B). Taking all together, the membrane anchoring mediated by the amphipathic helix of RHD3 is required for the efficient ER fusion mediated by RHD3.

2.3. DISCUSSION

As a member of the Atlastin GTPase family functioning in mediating the fusion of different ER tubules in plant cells, the mechanistic basis of the action of RHD3 in the ER membrane fusion is still not well studied. Previous studies showed that RHD3 undergoes a GTP-dependent homotypic interaction, which can be enhanced by phosphorylation on the divergent sequences of the CT of RHD3 (Chen et al., 2011; Ueda et al., 2015). Although the structure of RHD3 has not been resolved, based on the high structure similarity between RHD3 and Sey1p, a yeast member of the Atlastin GTPases, we simulated the structure of the cytosolic N-terminus of RHD3. The simulated cytosolic structure of RHD3 suggests that the GDs and the first two 3HBs of two RHD3 monomers could twist together to form a dimer. Consistent with this simulation, we find that a full length RHD3 can form homotypic interactions with its GD as well as its middle domain. When the potential polar linkage between D185 of one RHD3 monomer and R101 of another monomer in the interface of the dimer is disrupted, the interaction between a full length RHD3 and the GD of RHD3 is weakened. Similarly, mutations in the first two 3HBs in the middle domain could also reduce the interaction between a full length RHD3 and its middle domain. We suggest that the dimerization of RHD3 mediated by its GD and 3HBs is highly likely. Interestingly, when we expressed the GD or cytosolic N-terminus of RHD3 in plant cells, the expression has a negative effect on the formation of the polygonal ER network, suggesting that the function of endogenous RHD3 is affected. This influence is possibly through the interaction between the GD or cytosolic N-terminus of RHD3 and full length, endogenous RHD3. In animal cells, it is believed that, to facilitate the fusion between two different membranes, the cytosolic N-terminus of Atlastin-1 in two different ER membranes first undergo a dimerization between GDs to tether different ER membrane together, this dimerization is then stabilized by 3HBs in the middle domain, after which

a GTP-hydrolysis dependent conformational change occurs to fuse the ER membranes. Because the interaction between a full length RHD3 and its GD or first two 3HBs was required for the efficient ER fusion, we think that a similar mechanism may exist for RHD3.

A majordifference between RHD3 and Atlastin-1 is that, the predicted helical bundle enriched middle domain of RHD3 is much longer than that of Atlastin-1 (Stefano and Brandizzi, 2014). Like RHD3, Sey1p also has a middle domain longer than Atlastin-1. It has been shown that the deletion of 3HB-3 and 3HB-4 inactivates Sey1p (Yan et al., 2015). Here we find that, in RHD3, 3HB-3 and 3HB-4 play a vital role in the protein stability of RHD3. Although both 3HB-1 and 3HB-2 are required for possible dimerization of RHD3, it is interesting to note that 3HB-1 mutants RHD3(A285P) and RHD3(L355P), localized to thick bundled ER tubules, while 3HB-2 mutants RHD3(L379P) and RHD3(A434P), form punctates and aggregations on the ER tubules. This suggests that the mutations in 3HB-2 (L379P and A434P) may also influence the distribution of RHD3 on ER tubules.

RHD3 is an ER localized protein. Our results indicate that the TMs of RHD3 are important for the targeting and retention of RHD3 in the ER. The TMs not only serve as an ER membrane anchor, they are also able to interact with each other. Atlastin-1 in animal cells undergoes a GTP-independent association through its TMs. This TM-mediated association is proposed to increase the density of Atlastin-1 at the site of membrane tethering (Liu et al., 2012; Yan et al., 2015), so multiple cycles of dimerization of Atlastin-1 in the different membranes can occur for the efficient ER membrane fusion. Likely, RHD3 may also undergo a TM-mediated association for the efficient ER membrane fusion in plant cells.

Although the TMs are important for the targeting and retention of RHD3 in the ER, we also found the amphipathic helix located in the CT of RHD3 has an ability for the ER and Golgi targeting.

Given the fact that a large portion of RHD3(ΔTM) or the CT of RHD3 is in the cytosol, we think a portion of RHD3(ΔTM) or the CT of RHD3 is anchored to the membrane of the ER and Golgi. When the hydrophobic residues on the same hydrophobic face in the amphipathic helix are replaced by the acidic residues, all the mutations abolished the membrane attachment ability of the CT of RHD3, however different hydrophobic residue replacement did not compromise the membrane association of the CT of RHD3. Thus, it is highly likely that the membrane anchoring of RHD3(ΔTM) or the CT of RHD3 is due to an hydrophobic interaction between the amphipathic helix and membrane lipids. The amphipathic helix of Atlastin-1 has been proposed to facilitate the ER membrane fusion by providing the driving force for outer leaflet mixing of two different membranes through interacting with and destabilizing the lipid bilayer (Liu et al., 2012). The mutations in the hydrophobic residues on the same hydrophobic face in the helix not only abolish the membrane attachment ability of the CT of RHD3, the full length RHD3 with such mutations in the amphipathic helix also has reduced ability to rescue *ΔSey1p* and *rhd3-8* mutants. This indicates that membrane anchoring mediated by the amphipathic helix of RHD3 also plays a role in efficient ER membrane fusion, possibly through its interaction with lipid bilayers, like the amphipathic helix of Atlastin-1.

It is interesting to note that a portion of RHD3(ΔTM) or the CT of RHD3 is not only anchored to the ER membrane, but also the Golgi membrane. This is probably a reflection of the specific organization of the ER-Golgi interface in plant cells that Golgi is physically linked to the ER (Sparkes et al., 2009). However, when the CT of yeast Sey1p was expressed in plant cells, no Golgi targeting wasrevealed (Supplemental Fig.S2.5A) but replacing the amphipathic helix in the CT of yeast Sey1p with the amphipathic helix of RHD3 will target YFP to the Golgi or ER membrane (Supplemental Fig.S2.5B), so the Golgi targeting of RHD3(ΔTM) or the CT of RHD3

is RHD3 specific and is determined by the amphipathic helix of the CT of RHD3. However, the full length RHD3 is ER localized (Chen et al., 2011), so the physiological relevance of this Golgi membrane preference of the CT of RHD3 is not clear.

2.4. CONCLUSIONS

Based on our systemic structure-function analysis of RHD3, we hypothesize that, to mediate different ER membrane fusion, different RHD3 molecules in different ER membranes need to undergo homotypic interaction through their GDs and middle domains. Likely, RHD3 may also undergo a TM-mediated association to increase the density of RHD3 in the same ER membrane for efficient ER membrane fusion. Meanwhile, the amphipathic helix of the C-terminus of RHD3 would attach to the ER membrane to disturb the lipid bilayer to facilitate the membrane fusion.

2.5. MATERIALS AND METHODS

2.5.1. Molecular Cloning

RHD3 was first cloned into pCR™8/GW/TOPO® entry vector (Invitrogen). RHD3(ΔTM) was generated by overlap PCR. RHD3(ΔTM), GD of RHD3, RHD3(ΔTMΔCT), CT of RHD3 and CT of Sey1p were cloned into pCR™8/GW/TOPO®. All the point mutations were performed in pCR™8/GW/TOPO® by Quick Change Site-Directed Mutagenesis kit (Agilent Technologies). The RHD3 mutants were gateway cloned into pEarleyGate104 to produce YFP tagged RHD3 mutants. RY vectors were created based on pEarleyGate104 YFP-RHD3 with AQUA Cloning assay (Beyer et al., 2015). The original Basta resistance gene in pEarleyGate104 was replaced by mCherry-HDEL. To express in plants, all the constructs were transformed into *Agrobacterium tumefaciens* GV3101. For split-ubiquitin system (SUS), all the mutated RHD3 or different domains were gateway cloned into pNCW-GWRFC to generate N-terminal Cub fusion, or pNX32-DEST to generate N-terminal NubG fusion. For yeast ER fusion assay, endogenous Sey1p promoter and terminator were amplified from yeast genome and cloned into a p416GPD vector (URA3) with KpnI-SacI sites. All the RHD3 mutants were cloned between Sey1p promoter and terminator with BamHI-XbaI sites. All the ER and Golgi markers were described by Zheng et al., (Zheng et al., 2005).

2.5.2. Structure Simulation

The N-terminal sequence (AA1-668) of RHD3 or D185N sequence was used in Swiss-Model and Sey1p homo-dimer (5CA9, binding with GDPAlF4-) was used as the template for modeling. Multiple sequence alignment was analyzed by MUSCLE. Sequences were from RHD3: AA722-802, RHD3-LIKE2(RL2): AA729-834, RHD3-LIKE1(RL1): AA728-795, Sey1p: AA727-776,

ATL1: AA493-558. The possible arrangement of the amphipathic helix (AA727-744) was predicted by HeliQuest. 3D model of the short peptide was generated by PEP-FOLD. All the predicted structures were analyzed by PyMOL.

2.5.3. Mating based split-ubiquitin system (SUS)

The Cub tagged RHD3 mutants and NubG tagged RHD3 mutants were transformed into haploid yeast strains THY.AP4 and THY.AP5, respectively (Obrdlik et al., 2004). After transformation, colonies were picked and inoculated in SC selection medium (-leu for AP4 and -trp for AP5) for overnight at 28 ℃. The THY.AP4 (Cub) and THY.AP5 (NubG) suspensions were mixed and plated on YPD plates. After 6-8 hrs at 28 ℃, mated cells were streaked on -LT(-Leu-Trp) selection plates and incubated at 28℃for 2 days. Diploid cells were collected and inoculated in -LT liquid medium and incubate at 28℃ overnight. Yeast cells were resuspended in water and measured the OD600 value. Suspensions were diluted into OD600=2, 1, 0.1 and 0.01 or OD600=1, 0.1, 0.01 and 0.001. 15ul per spot was dropped on -LT plates for mating control or -LTH (-Leu-Trp-His) plates for interaction test. Plates were incubated at 28℃ for 2-3 days. The interaction efficiency was evaluated by counting the number of yeast colonies on -LTH plates.

2.5.4. Yeast ER fusion assay

Yeast ER fusion test was performed as previously described (Anwar et al., 2012). Different RHD3 mutants were transformed into two different *Δsey1p* mutant haploid cells, ACY53(ss-RFP-HDEL) and ACY54 (free GFP). Cells were grown to an OD (600nm) of 0.1-0.4, mixed and concentrated in YPD medium. 5ul cell suspension was dropped on a 1-mm-thick SC medium pad and grown at 30℃ for 40-60 mins. Then images were taken at 20s intervals.

2.5.5. Transient expression in *Nicotiana tabacum* and *Nicotiana benthamiana*

Plants (*Nicotiana tabacum* or *Nicotiana benthamiana*) with three or four leaves were used for infiltration. *Agrobacterium* with different constructs was grown at 28℃ overnight and resuspended in infiltration buffer (100μM acetosyringone and 10 mM $MgCl_2$). The final OD600 of agrobacterium was 0.01. Results were checked 2-3 days after infiltration.

2.5.6. Western blot

Two days after infiltration of RY constructs, total proteins were extracted with 1×SDS loading buffer from *Nicotiana benthamiana*. Samples were boiled for 5mins. After 2min 13,000 rpm centrifuge, the supernatants were loaded on 10% SDS-PAGE gel. SDS-PAGE was performed on a Protean III apparatus (Bio-Rad) and separated proteins were transferred onto a PVDF membrane. Western blotting was carried out with a rabbit anti-GFP antibody (Abcam, ab32146) at 1:5000 dilution or anti-RFP (Abcam, ab34771) at 1:2000 dilution. The secondary anti-Rabbit IgG-peroxidase (Sigma-Aldrich) was used at 1:5000 dilution. Signals were detected using Invitrogen Novex ECL (HRP Chemiluminescent Substrate Reagent Kit) according to the manufacturer's recommendations.

2.5.7. Confocal microscopy

The infiltration results were observed with a Leica SP8 point-scanning confocal system, on a Leica DMI6000B inverted microscope equipped with spectral fluorescent light detectors (three PMT, one HyD high sensitivity detector). 63x/1.4 oil objective was used for all the imaging. The 488nm laser was used to excite GFP or YFP, and the 552nm laser was used to excite RFP or mCherry. Two channels were excited sequentially. Emission filter was set as 490nm-560nm for GFP or YFP, and 580-660nm for RFP or mCherry. For post image editing and fluorescence signal quantification, Fiji (Fiji is just Image J) was used (Schindelin et al., 2012).

2.6. ACCESSION NUMBERS

Sequence data from this article can be found in the Arabidopsis Genome Initiative database under the following accession numbers: AtRHD3 (At3g13870).

2.7. ACKNOWLEDGEMENTS

We thank Sylvie Lalonde (Carnegie Institution, Stanford, CA, USA) for pNX32 and pXN22 mbSUS Gateway vectors; David Bird (University of Manitoba, Winnipeg, Canada) for pNCW-GWRFC.1; William A. Prinz (National Institute of Diabetes and Digestive and Kidney Diseases, NIH, Bethesda, MD, USA) for providing the yeast cells (ACY53 and ACY54 strains) for Yeast ER fusion test; the Cell Imaging and Analysis Network (CIAN) in McGill Biology department for microscopy imaging support. J.S was supported by a scholarship from the Chinese Scholarship Council. This research was supported by a grant from the Natural Sciences and Engineering Research Council (NSERC) of Canada to H.Z..

2.8. REFERENCES

Anwar, K., Klemm, R.W., Condon, A., Severin, K.N., Zhang, M., Ghirlando, R., Hu, J., Rapoport, T.A., and Prinz, W.A. (2012). The dynamin-like GTPase Sey1p mediates homotypic ER fusion in S. cerevisiae. J Cell Biol *197*, 209-217.

Beyer, H.M., Gonschorek, P., Samodelov, S.L., Meier, M., Weber, W., and Zurbriggen, M.D. (2015). AQUA Cloning: A Versatile and Simple Enzyme-Free Cloning Approach. PloS one *10*, e0137652.

Bian, X., Klemm, R.W., Liu, T.Y., Zhang, M., Sun, S., Sui, X., Liu, X., Rapoport, T.A., and Hu, J. (2011). Structures of the atlastin GTPase provide insight into homotypic fusion of endoplasmic reticulum membranes. Proc Natl Acad Sci U S A *108*, 3976-3981.

Brady, J.P., Claridge, J.K., Smith, P.G., and Schnell, J.R. (2015). A conserved amphipathic helix is required for membrane tubule formation by Yop1p. P Natl Acad Sci USA *112*, E639-E648.

Breeze, E., Dzimitrowicz, N., Kriechbaumer, V., Brooks, R., Botchway, S.W., Brady, J.P., Hawes, C., Dixon, A.M., Schnell, J.R., Fricker, M.D.*, et al.* (2016). A C-terminal amphipathic helix is necessary for the in vivo tubule-shaping function of a plant reticulon. P Natl Acad Sci USA *113*, 10902-10907.

Chen, J., Stefano, G., Brandizzi, F., and Zheng, H. (2011). Arabidopsis RHD3 mediates the generation of the tubular ER network and is required for Golgi distribution and motility in plant cells. J Cell Sci *124*, 2241-2252.

Grefen, C., Lalonde, S., and Obrdlik, P. (2007). Split-Ubiquitin System for Identifying Protein-Protein Interactions in Membrane and Full-Length Proteins. In Current Protocols in Neuroscience (John Wiley & Sons, Inc.).

Hu, J., and Rapoport, T.A. (2016). Fusion of the endoplasmic reticulum by membrane-bound GTPases. Semin Cell Dev Biol *60*, 105-111.

Hu, J., Shibata, Y., Voss, C., Shemesh, T., Li, Z., Coughlin, M., Kozlov, M.M., Rapoport, T.A., and Prinz, W.A. (2008). Membrane proteins of the endoplasmic reticulum induce high-curvature tubules. Science *319*, 1247-1250.

Hu, J., Shibata, Y., Zhu, P.P., Voss, C., Rismanchi, N., Prinz, W.A., Rapoport, T.A., and Blackstone, C. (2009). A class of dynamin-like GTPases involved in the generation of the tubular ER network. Cell *138*, 549-561.

Liu, T.Y., Bian, X., Romano, F.B., Shemesh, T., Rapoport, T.A., and Hu, J. (2015). Cis and trans interactions between atlastin molecules during membrane fusion. Proc Natl Acad Sci U S A.

Liu, T.Y., Bian, X., Sun, S., Hu, X., Klemm, R.W., Prinz, W.A., Rapoport, T.A., and Hu, J. (2012). Lipid interaction of the C terminus and association of the transmembrane segments facilitate atlastin-mediated homotypic endoplasmic reticulum fusion. Proc Natl Acad Sci U S A *109*, E2146-2154.

Obrdlik, P., El-Bakkoury, M., Hamacher, T., Cappellaro, C., Vilarino, C., Fleischer, C., Ellerbrok, H., Kamuzinzi, R., Ledent, V., Blaudez, D.*, et al.* (2004). K+ channel interactions detected by a genetic system optimized for systematic studies of membrane protein interactions. Proc Natl Acad Sci U S A *101*, 12242-12247.

Orso, G., Pendin, D., Liu, S., Tosetto, J., Moss, T.J., Faust, J.E., Micaroni, M., Egorova, A., Martinuzzi, A., McNew, J.A.*, et al.* (2009). Homotypic fusion of ER membranes requires the dynamin-like GTPase atlastin. Nature *460*, 978-983.

Schiefelbein, J.W., and Somerville, C. (1990). Genetic Control of Root Hair Development in Arabidopsis thaliana. Plant Cell *2*, 235-243.

Schindelin, J., Arganda-Carreras, I., Frise, E., Kaynig, V., Longair, M., Pietzsch, T., Preibisch, S., Rueden, C., Saalfeld, S., Schmid, B.*, et al.* (2012). Fiji: an open-source platform for biological-image analysis. Nat Methods *9*, 676-682.

Sparkes, I., Hawes, C., and Frigerio, L. (2011). FrontiERs: movers and shapers of the higher plant cortical endoplasmic reticulum. Curr Opin Plant Biol *14*, 658-665.

Sparkes, I., Tolley, N., Aller, I., Svozil, J., Osterrieder, A., Botchway, S., Mueller, C., Frigerio, L., and Hawes, C. (2010). Five Arabidopsis reticulon isoforms share endoplasmic reticulum location, topology, and membrane-shaping properties. Plant Cell *22*, 1333-1343.

Sparkes, I.A., Ketelaar, T., de Ruijter, N.C., and Hawes, C. (2009). Grab a Golgi: laser trapping of Golgi bodies reveals in vivo interactions with the endoplasmic reticulum. Traffic *10*, 567-571.

Stefano, G., and Brandizzi, F. (2014). Unique and conserved features of the plant ER-shaping GTPase RHD3. Cellular logistics *4*, e28217.

Stefano, G., Renna, L., Moss, T., McNew, J.A., and Brandizzi, F. (2012). In Arabidopsis, the spatial and dynamic organization of the endoplasmic reticulum and Golgi apparatus is influenced by the integrity of the C-terminal domain of RHD3, a non-essential GTPase. Plant J *69*, 957-966.

Ueda, H., Yokota, E., Kuwata, K., Kutsuna, N., Mano, S., Shimada, T., Tamura, K., Stefano, G., Fukao, Y., Brandizzi, F.*, et al.* (2015). Phosphorylation of the C-terminus of RHD3 Has a Critical Role in Homotypic ER Membrane Fusion in Arabidopsis. Plant Physiol.

Voeltz, G.K., Prinz, W.A., Shibata, Y., Rist, J.M., and Rapoport, T.A. (2006). A class of membrane proteins shaping the tubular endoplasmic reticulum. Cell *124*, 573-586.

Wang, H., Lockwood, S.K., Hoeltzel, M.F., and Schiefelbein, J.W. (1997). The ROOT HAIR DEFECTIVE3 gene encodes an evolutionarily conserved protein with GTP-binding motifs and is required for regulated cell enlargement in Arabidopsis. Genes Dev *11*, 799-811.

Wang, J., Wang, Y., Yang, J., Ma, C.L., Zhang, Y., Ge, T., Qi, Z., and Kang, Y. (2015). Arabidopsis ROOT HAIR DEFECTIVE3 is involved in nitrogen starvation-induced anthocyanin accumulation. J Integr Plant Biol *57*, 708-721.

Yamada-Okabe, T., and Yamada-Okabe, H. (2002). Characterization of the CaNAG3, CaNAG4, and CaNAG6 genes of the pathogenic fungus Candida albicans: possible involvement of these genes in the susceptibilities of cytotoxic agents. Fems Microbiol Lett *212*, 15-21.

Yan, L., Sun, S., Wang, W., Shi, J., Hu, X., Wang, S., Su, D., Rao, Z., Hu, J., and Lou, Z. (2015). Structures of the yeast dynamin-like GTPase Sey1p provide insight into homotypic ER fusion. The Journal of Cell Biology *210*, 961-972.

Zhang, B., Karnik, R., Wang, Y., Wallmeroth, N., Blatt, M.R., and Grefen, C. (2015). The Arabidopsis R-SNARE VAMP721 Interacts with KAT1 and KC1 K+ Channels to Moderate K+ Current at the Plasma Membrane. Plant Cell *27*, 1697-1717.

Zhang, M., Wu, F., Shi, J., Zhu, Y., Zhu, Z., Gong, Q., and Hu, J. (2013). ROOT HAIR DEFECTIVE3 family of dynamin-like GTPases mediates homotypic endoplasmic reticulum fusion and is essential for Arabidopsis development. Plant Physiol *163*, 713-720.

Zhao, X., Alvarado, D., Rainier, S., Lemons, R., Hedera, P., Weber, C.H., Tukel, T., Apak, M., Heiman-Patterson, T., Ming, L.*, et al.* (2001). Mutations in a newly identified GTPase gene cause autosomal dominant hereditary spastic paraplegia. Nat Genet *29*, 326-331.

Zheng, H., Camacho, L., Wee, E., Batoko, H., Legen, J., Leaver, C.J., Malho, R., Hussey, P.J., and Moore, I. (2005). A Rab-E GTPase mutant acts downstream of the Rab-D subclass in biosynthetic membrane traffic to the plasma membrane in tobacco leaf epidermis. Plant Cell *17*, 2020-2036.

Zheng, H., and Chen, J. (2011). Emerging aspects of ER organization in root hair tip growth: lessons from RHD3 and Atlastin. Plant signaling & behavior *6*, 1710-1713.

Zheng, H., Kunst, L., Hawes, C., and Moore, I. (2004). A GFP-based assay reveals a role for RHD3 in transport between the endoplasmic reticulum and Golgi apparatus. Plant J *37*, 398-414.

Figures

Figure 2.1. Mutations in the interface of the dimer influence the homotypic interaction of RHD3. A, The overall structure of full-length RHD3. The numbers indicate the corresponding amino acid positions. B, The predicted cytosolic dimer structure of RHD3. B1, the side view of cytosolic dimer structure of RHD3, B2, the top view of cytosolic dimer structure of RHD3. One RHD3 monomer is shown in grey and the other one in shown in different colors. RHD3 forms a dimer through its GTPase domain (red) and middle domain. The middle domain contains 4 different 3HBs: 3HB-1 (orange), 3HB-2(yellow), 3HB-3 (blue) and 3HB-4 (cyan). The mutated amino acids in this paper are indicated as the highlighted spheres. The enlarged structure of the blue dash box is shown in supplemental Fig. S1B. C, Co-expressing YFP-RHD3 and RFP-HDEL in tobacco leaves. Scale bar =10 μm. D, Co-expressing YFP-RHD3(D185N) and RFP-HDEL in tobacco leaves. The ER bundles are indicated by the arrow. Scale bar =10 μm. E, Yeast mating based split-ubiquitin system (SUS) for the homotypic interaction of RHD3 and various mutated versions of RHD3 as indicated. Cub fused full-length RHD3 interacts with NubG fused full-length RHD3 (1), but not with NubG alone (2). Cub fused RHD3 interacts with NubG fused GTPase domain (GD) (3), but Cub fused mutant RHD3(D185N) (4), RHD3(R101E) (5) and RHD3(D185N, R101E) (6) have the reduced interaction with NubG fused mutant GD(D185N), GD(R101E) and GD(D185N, R101E), respectively. The interaction between RHD3 and its GD domain with reciprocal mutagenesis (R101D, D185R) (7) was restored. On the other hand, the interaction between RHD3(R101E) and GD(D185N) (8) was not significantly reduced compared to RHD3 and its GD (3). Mated diploid yeast cells were diluted into DO600=2, 1, 0.1 and 0.01.

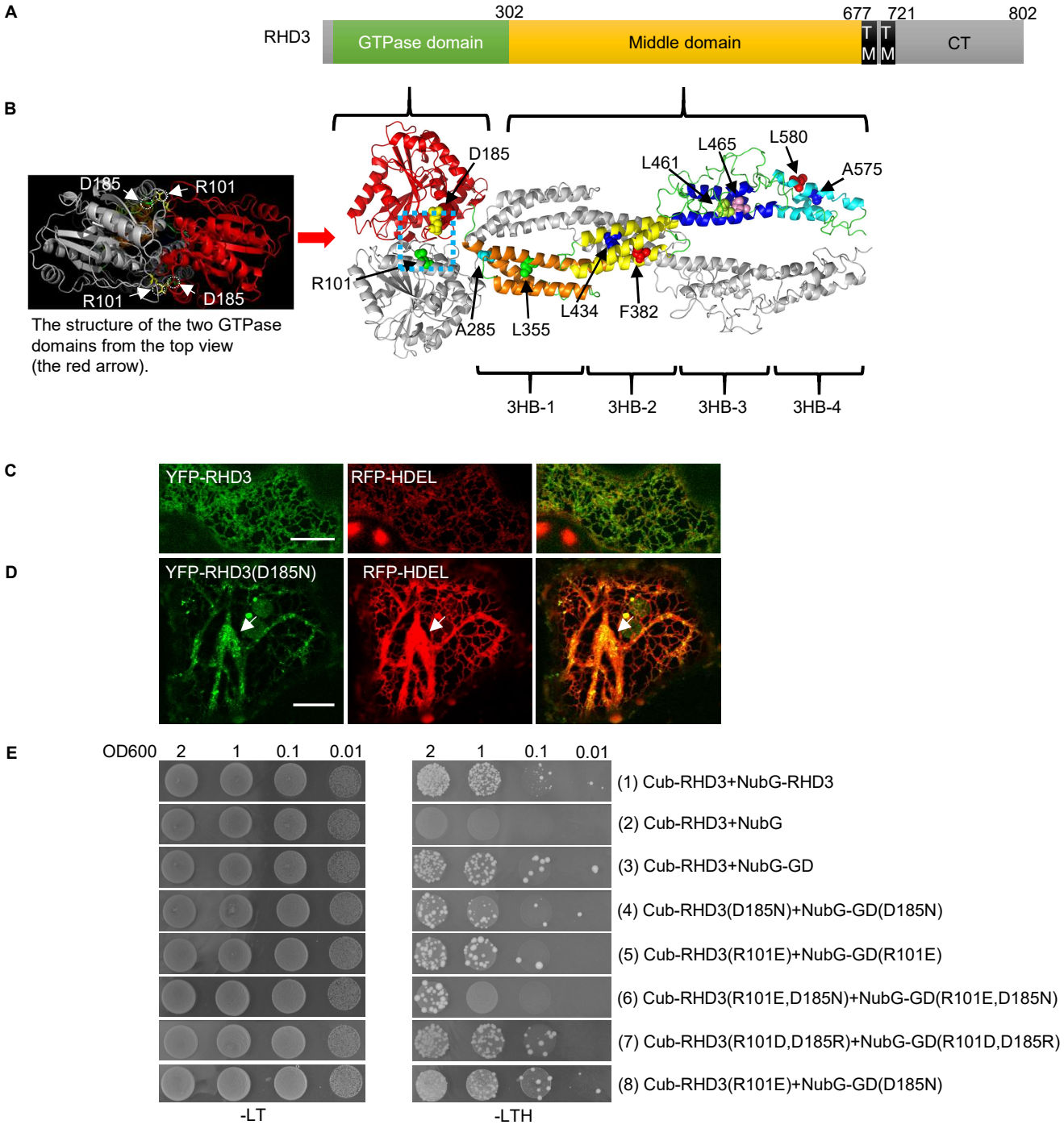
A
RHD3
302
677
721
802
GTPase domain
Middle domain
TM
TM
CT
B
D185
R101
R101
D185
The structure of the two GTPase domains from the top view (the red arrow).
D185
L465
L580
L461
A575
R101
A285
L355
L434
F382
3HB-1
3HB-2
3HB-3
3HB-4
C
YFP-RHD3
RFP-HDEL
D
YFP-RHD3(D185N)
RFP-HDEL
E
OD600
2
1
0.1
0.01
2
1
0.1
0.01
(1) Cub-RHD3+NubG-RHD3
(2) Cub-RHD3+NubG
(3) Cub-RHD3+NubG-GD
(4) Cub-RHD3(D185N)+NubG-GD(D185N)
(5) Cub-RHD3(R101E)+NubG-GD(R101E)
(6) Cub-RHD3(R101E,D185N)+NubG-GD(R101E,D185N)
(7) Cub-RHD3(R101D,D185R)+NubG-GD(R101D,D185R)
(8) Cub-RHD3(R101E)+NubG-GD(D185N)
-LT
-LTH

Figure 2.1.

Figure 2.2. Mutations in RHD3 compromise the ER fusion efficiency of RHD3. Sey1p, RHD3 and different RHD3 mutants as indicated were expressed in the Δ*sey1p* mutant and their average ER fusion time was quantified from 20-50 cells per sample. Each error bar represents mean ± standard deviation (SD). Student tests were used to check the significant difference between two groups of data and the corresponding p-values are shown. *** indicates significant difference from WT RHD3 (p-value<0.001, t-test).

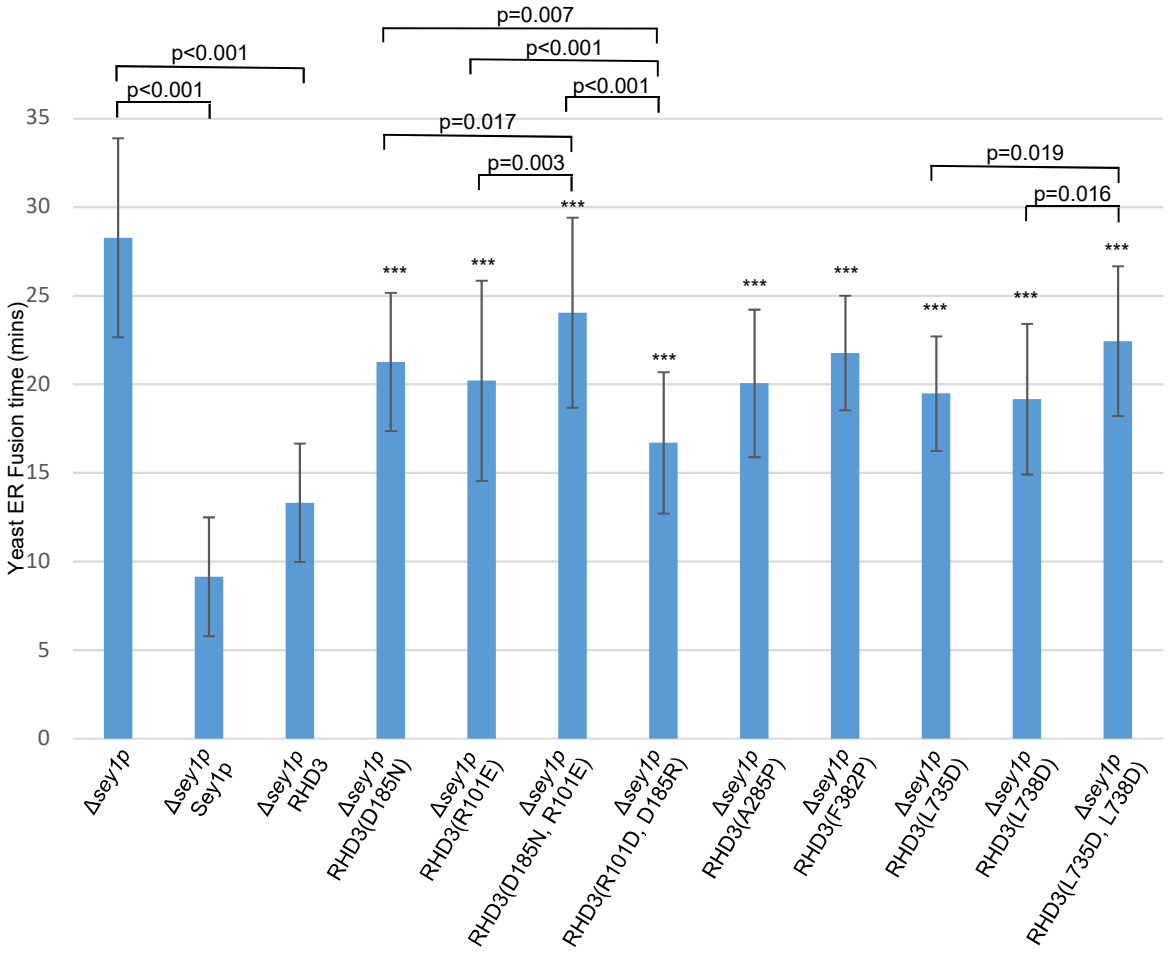
p=0.007
p<0.001
p<0.001
p<0.001
p=0.017
p=0.003
p=0.019
p=0.016
***
Yeast ER Fusion time (mins)
0
5
10
15
20
25
30
35
Δsey1p
Δsey1p Sey1p
Δsey1p RHD3
Δsey1p RHD3(D185N)
Δsey1p RHD3(R101E)
Δsey1p RHD3(D185N, R101E)
Δsey1p RHD3(R101D, D185R)
Δsey1p RHD3(A285P)
Δsey1p RHD3(F382P)
Δsey1p RHD3(L735D)
Δsey1p RHD3(L738D)
Δsey1p RHD3(L735D, L738D)

Figure 2.2.

Figure 2.3. Transient expression of RHD3 with mutations in the middle domain in tobacco leaves. A, Co-expressing YFP-RHD3 and RFP-HDEL. Scale bar = 10 μm. B, Expression of 3HB-1 mutant RHD3(A285P) generates thick ER bundles (arrows). Scale bar = 10 μm. C, Expression of 3HB-2 mutant RHD3(F382P) generates aggregations of ER tubules (arrowhead). Scale bar = 10 μm. D-E, Expression of 3HB-3 mutant RHD3(L461P) and 3HB-4 mutant RHD3(L580P) only marks weak punctates on the ER and have no influence on the formation of the ER indicated by RFP-HDEL. Scale bar = 10 μm.

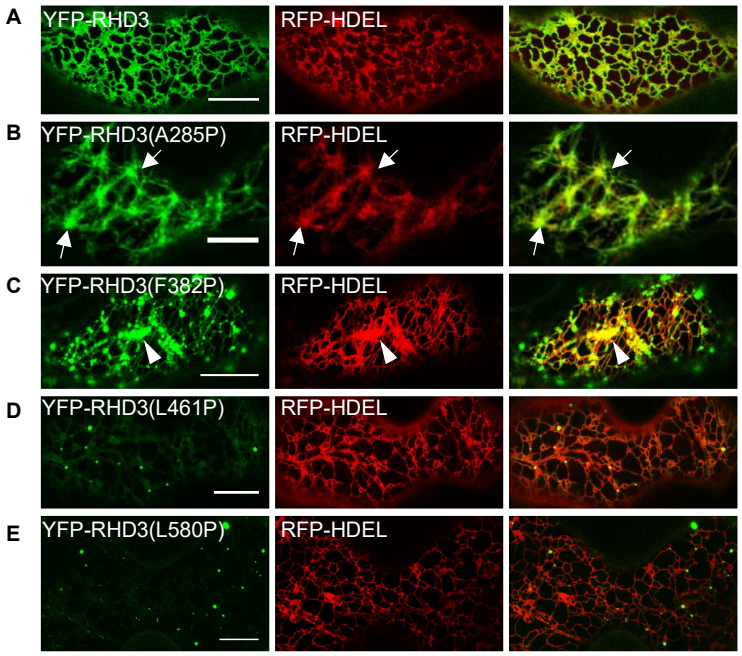
A
YFP-RHD3
RFP-HDEL
B
YFP-RHD3(A285P)
RFP-HDEL
C
YFP-RHD3(F382P)
RFP-HDEL
D
YFP-RHD3(L461P)
RFP-HDEL
E
YFP-RHD3(L580P)
RFP-HDEL

Figure 2.3.

Figure 2.4. 3HB-1 and 3HB-2 of RHD3 are important for the homotypic interaction of RHD3. (Row 1-5) Yeast mating based split-ubiquitin system (SUS) for interaction of RHD3 with its middle domain(MID) and mutated middle domains as indicated. Cub fused full-length RHD3 interacts with NubG-RHD3 (1) and NubG-MID (3), while the A285P or F382P mutations significantly compromised the interaction between RHD3 and its middle domain (4, 5, respectively). Mated diploid yeast cells were diluted into DO600 = 1, 0.1, 0.01 and 0.001.

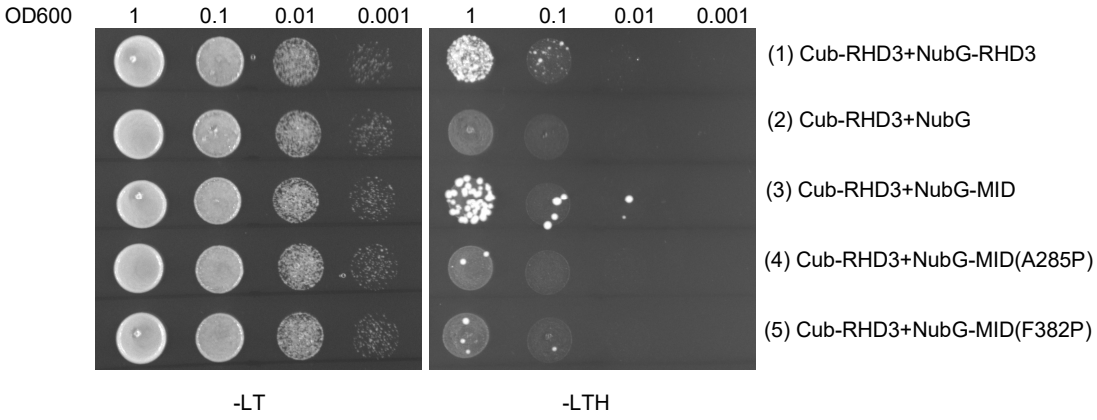
OD600
1
0.1
0.01
0.001
1
0.1
0.01
0.001
(1) Cub-RHD3+NubG-RHD3
(2) Cub-RHD3+NubG
(3) Cub-RHD3+NubG-MID
(4) Cub-RHD3+NubG-MID(A285P)
(5) Cub-RHD3+NubG-MID(F382P)
-LT
-LTH

Figure 2.4.

Figure 2.5. 3HB-3 and 3HB-4 of RHD3 are essential for the RHD3 protein stability. A, the ratio of YFP fluorescence of different YFP fused RHD3 mutants as indicated compared to mCherry-HDEL fluorescence intensity. The YFP/mCherry values of different RHD3 mutants were quantified relatively to the WT value set as 1. The fluorescent intensity from 20 cells was quantified for each mutant. Each bar represents mean ± standard deviation (SD). *** indicates significant difference from YFP-RHD3 (p-value<0.001, t-test). B, Western Blot for the protein expression level of YFP fused 3HB-3 (RHD3(L465P)) and 3HB-4 (RHD3(L580P)) mutants. Total proteins were extracted 48 hrs after the infiltration of respective constructs. Anti-GFP was used to detect YFP fused proteins and anti-RFP was used to detect mCherry-HDEL as the loading control. C, RT-PCR for the transcription of YFP fused 3HB-3 (RHD3(L465P)) and 3HB-4 (RHD3(L580P)) mutants. Compared to the transcription of the reference gene mCherry-HDEL, different RHD3 mutants as indicated have no significant difference at the transcription level.

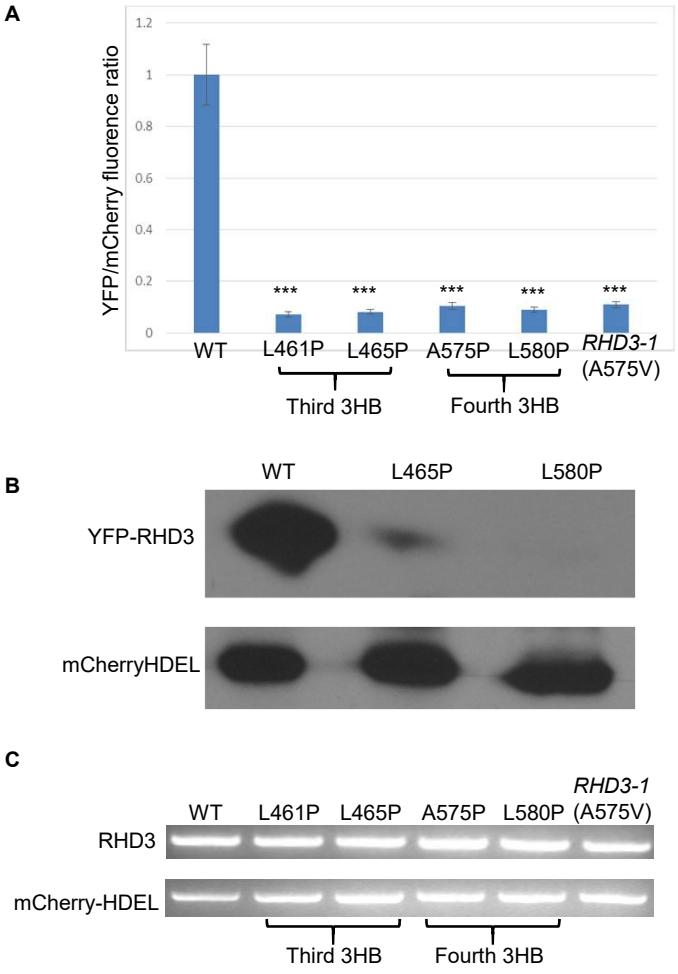
A
YFP/mCherry fluorence ratio
1.2
1
0.8
0.6
0.4
0.2
0
***
WT
L461P
L465P
A575P
L580P
RHD3-1
(A575V)
Third 3HB
Fourth 3HB
B
WT
L465P
L580P
YFP-RHD3
mCherryHDEL
C
RHD3-1
WT
L461P
L465P
A575P
L580P
(A575V)
RHD3
mCherry-HDEL
Third 3HB
Fourth 3HB

Figure 2.5.

Figure 2.6. Transmembrane segments of RHD3 determine the ER localization of RHD3 and can self-interact. A, Although largely cytosolic, YFP-RHD3(ΔTM) is occasionally co-localized with RFP-HDEL (Inset for A). The arrows in the inset of A point at ER tubules colocalized with mCherry-HDEL. B, Part of YFP-RHD3(ΔTM) is partially overlapped with ST-RFP (trans-Golgi). C, Part of RFP-RHD3(ΔTM) is fully overlapped with donut-shaped Cis-Golgi (ERD2-GFP). Scale bars = 10 μm except the scale bar in the inset of A = 5 μm. D, Yeast mating based split-ubiquitin system (SUS) for self-interaction of the TMs of RHD3. Note the Cub fused TMs of RHD3 can efficiently interact with the NubG fused TMs of RHD3 (3), but not with NubG alone (4).

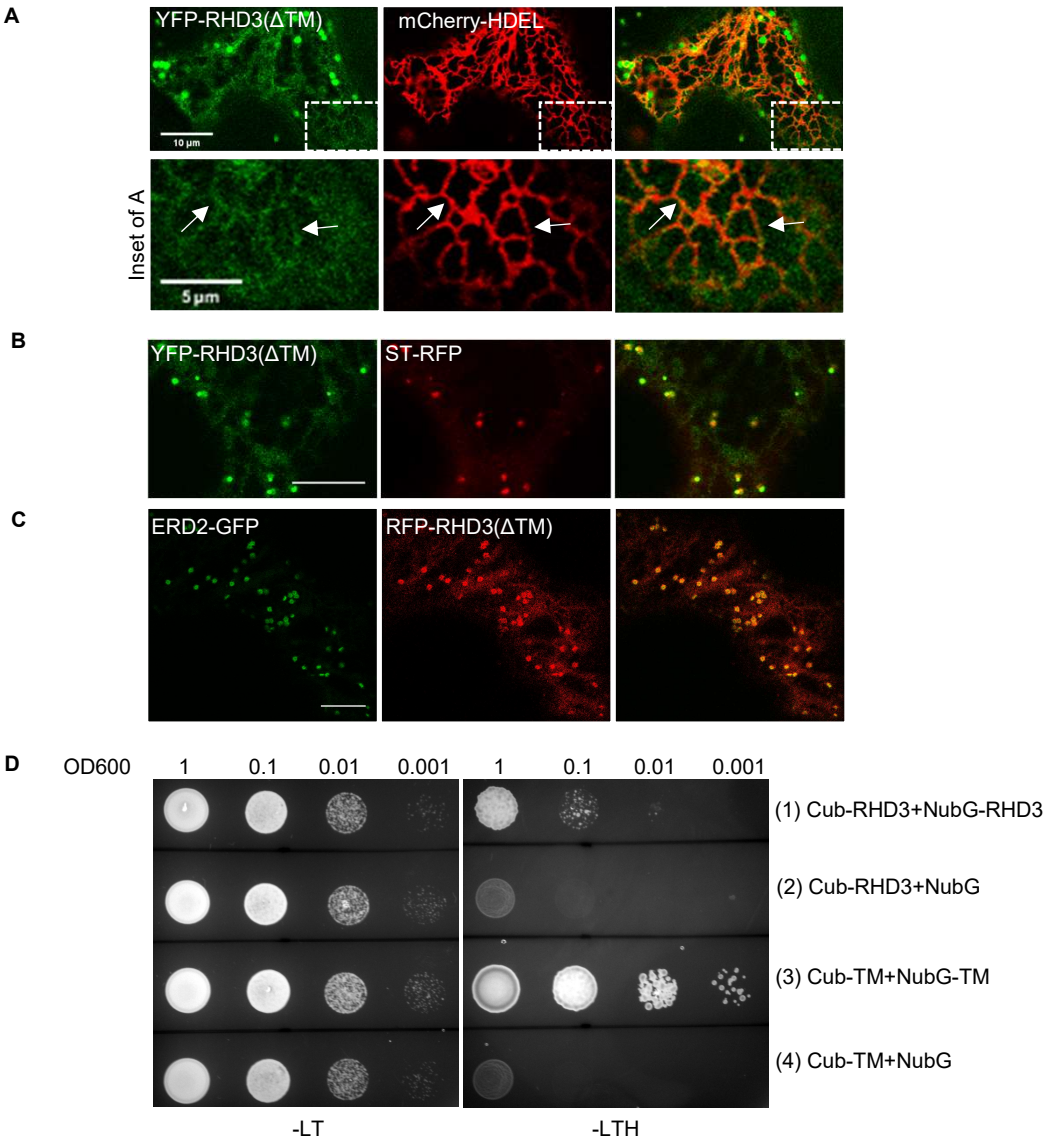
A
YFP-RHD3(ΔTM)
mCherry-HDEL
10 μm
Inset of A
5 μm
B
YFP-RHD3(ΔTM)
ST-RFP
C
ERD2-GFP
RFP-RHD3(ΔTM)
D
OD600
1
0.1
0.01
0.001
1
0.1
0.01
0.001
(1) Cub-RHD3+NubG-RHD3
(2) Cub-RHD3+NubG
(3) Cub-TM+NubG-TM
(4) Cub-TM+NubG
-LT
-LTH

Figure 2.6.

Figure 2.7. The amphipathic helix in the C-terminal tail of RHD3 has a membrane targeting ability. A, the YFP fused RHD3 GTPase domain (YFP-GD) is cytosolic and has a negative effect on the formation of the polygonal ER network as indicated by RFP-HDEL. The arrow indicates the thick and bundled ER tubules. Scale bar = 10 μm. B, the cytosolic N-terminal domain of RHD3(ΔTMΔCT) (AA1-676), is also in the cytosol and has a negative effect on the formation of the polygonal ER network. The arrow indicates the thick and bundled ER tubules. Scale bar = 10 μm. C, Co-expressing the RFP fused CT of RHD3 (RFP-CT) (AA722-802) and YFP-HDEL. Although largely cytosolic, the occasional tubular structure of RFP-CT is co-localized with YFP-HDEL. Scale bar = 10 μm. D, Co-expressing RFP-CT and ST-GFP. The punctate structure of RFP-CT is co-localized with ST-GFP. Scale bar = 10 μm. E, Multiple alignment of the cytosolic C-terminal sequences of the selected atlastin proteins. The alignment was analyzed by MUSCLE. Sequences used were from RHD3(AA722-802), RHD3-LIKE2(RL2)(AA729-834), RHD3-LIKE1(RL1)(AA728-795), Sey1p(AA727-776), ATL1(AA493-558). The amphipathic helix region and divergent sequence are highlighted. F, Co-expression of the RFP fused CT(ΔDS) of RHD3 with YFP-HDEL and ST-GFP. Divergent sequence deleted RFP-CT(ΔDS) exhibits the same localization as full C-terminus of RHD3. Scale bar = 10 μm.

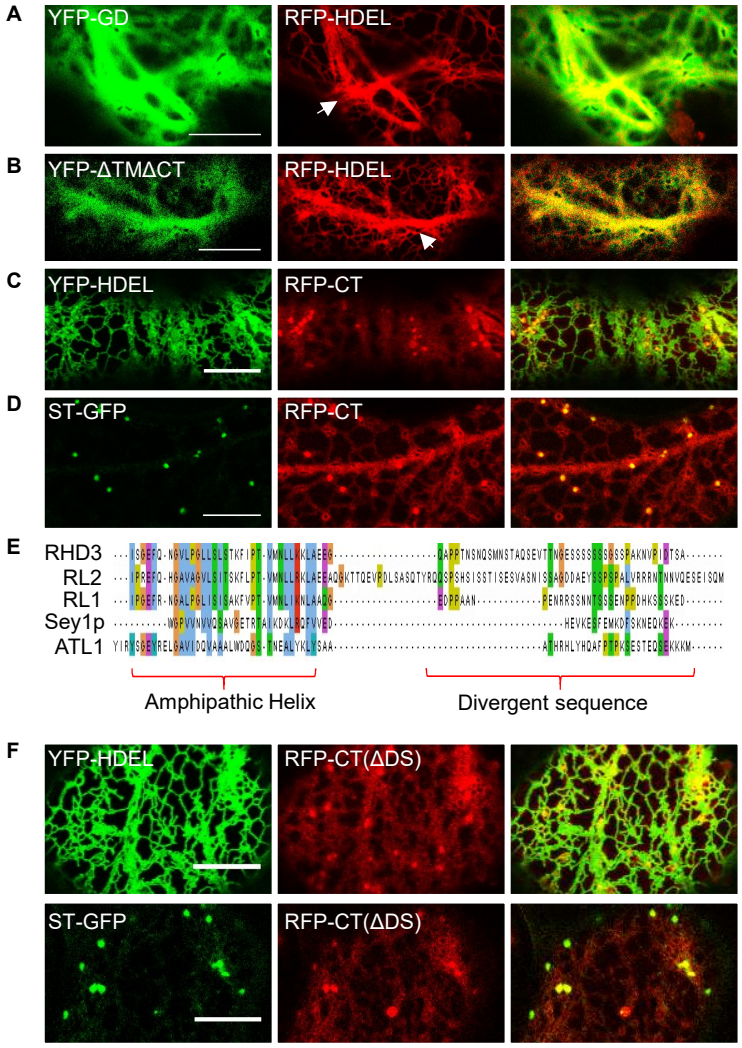
A
YFP-GD
RFP-HDEL
B
YFP-ΔTMΔCT
RFP-HDEL
C
YFP-HDEL
RFP-CT
D
ST-GFP
RFP-CT
E
RHD3
RL2
RL1
Sey1p
ATL1
Amphipathic Helix
Divergent sequence
F
YFP-HDEL
RFP-CT(ΔDS)
ST-GFP
RFP-CT(ΔDS)

Figure 2.7.

Figure 2.8. The hydrophobic face in the amphipathic helix of RHD3 is essential for membrane anchoring. A, Amphipathic helix model. Left: The possible arrangement of the amphipathic helix of RHD3, predicted by HeliQuest. The hydrophobic, positive charged and polar uncharged residues are shown in yellow, blue and magenta, respectively. Right: the 3D model of the amphipathic helix of RHD3 generated by PEP-FOLD. The hydrophobic residues are shown in red and their corresponding positions in the HeliQuest prediction are circled and pointed out. B, Acidic mutations in the hydrophobic face abolish the membrane association of the CT of RHD3. mCherry fused wild type CT of RHD3, and CT mutants (CT(V731D), CT(L735D), CT(L738D), and CT(F742D)) were transiently expressed in the tobacco leaves. All mutated CTs of RHD3 were localized in the cytoplasm. Scale bar = 10 μm. C, Different hydrophobic substations of V731 do not change the membrane association of the CT of RHD3. V731 was changed into alanine (V731A), leucine (V731L), or isoleucine (V731I), and all mutants show a similar membrane association as the wild type CT of RHD3, as indicated by punctate Golgi localization. Scale bar = 10 μm. D, Transient expression of wild type RHD3 and mCherry-HDEL in tobacco leaves. Scale bar = 10 μm.

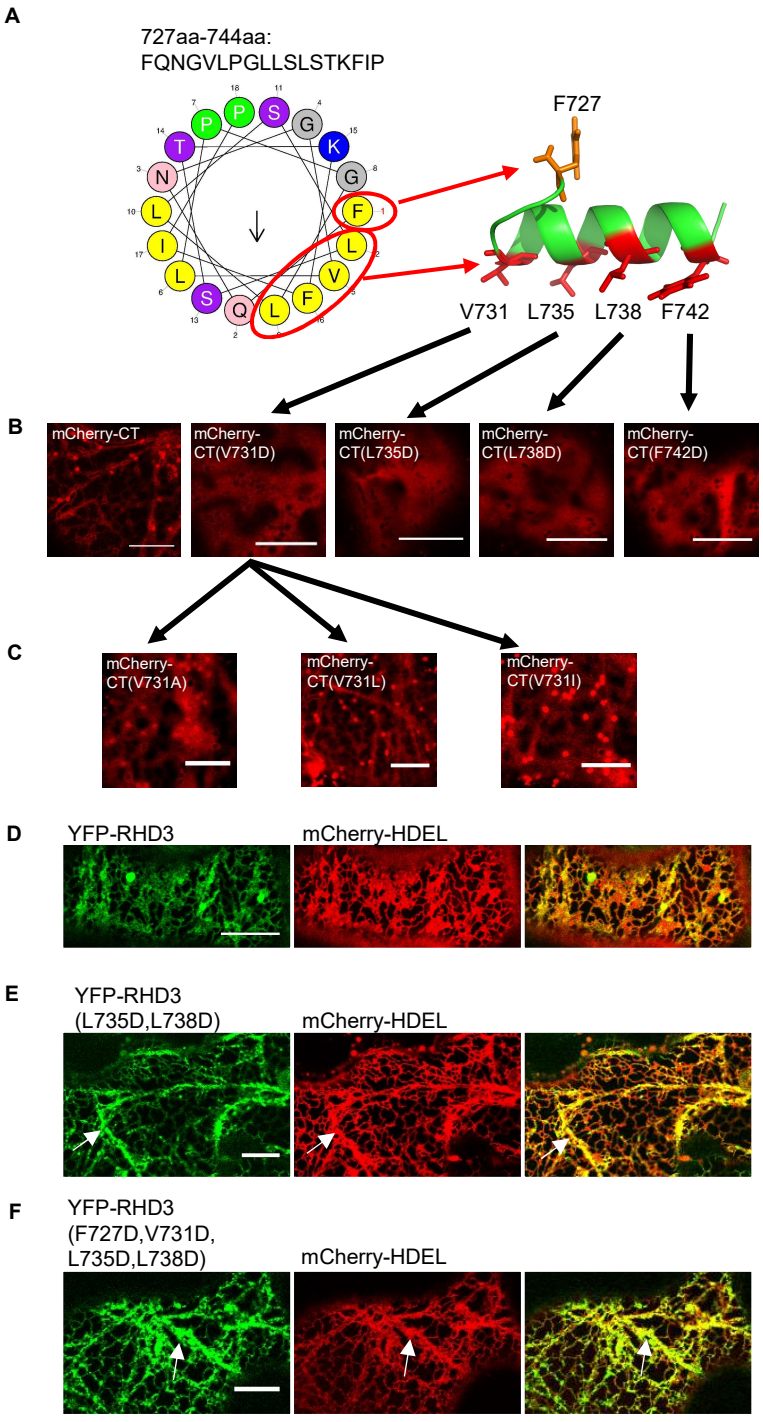
A
727aa-744aa:
FQNGVLPGLLSLSTKFIP
F727
V731
L735
L738
F742
B
mCherry-CT
mCherry-CT(V731D)
mCherry-CT(L735D)
mCherry-CT(L738D)
mCherry-CT(F742D)
C
mCherry-CT(V731A)
mCherry-CT(V731L)
mCherry-CT(V731I)
D
YFP-RHD3
mCherry-HDEL
E
YFP-RHD3 (L735D,L738D)
mCherry-HDEL
F
YFP-RHD3 (F727D,V731D, L735D,L738D)
mCherry-HDEL

Figure 2.8.

Supplemental Figures

Supplemental Fig.S2.1. A, The overall structure of full-length ATL1, caSey1p and RHD3. The numbers indicate the corresponding amino acid positions. B, The enlarged structure simulation of the interface in the highlighted box of Figure 1B. The potential polar contacts between D185 and R101 are indicated by arrowheads. C, The potential polar contacts are reduced from three to one with D185N mutation. The arrowhead points at the only remaining polar contact.

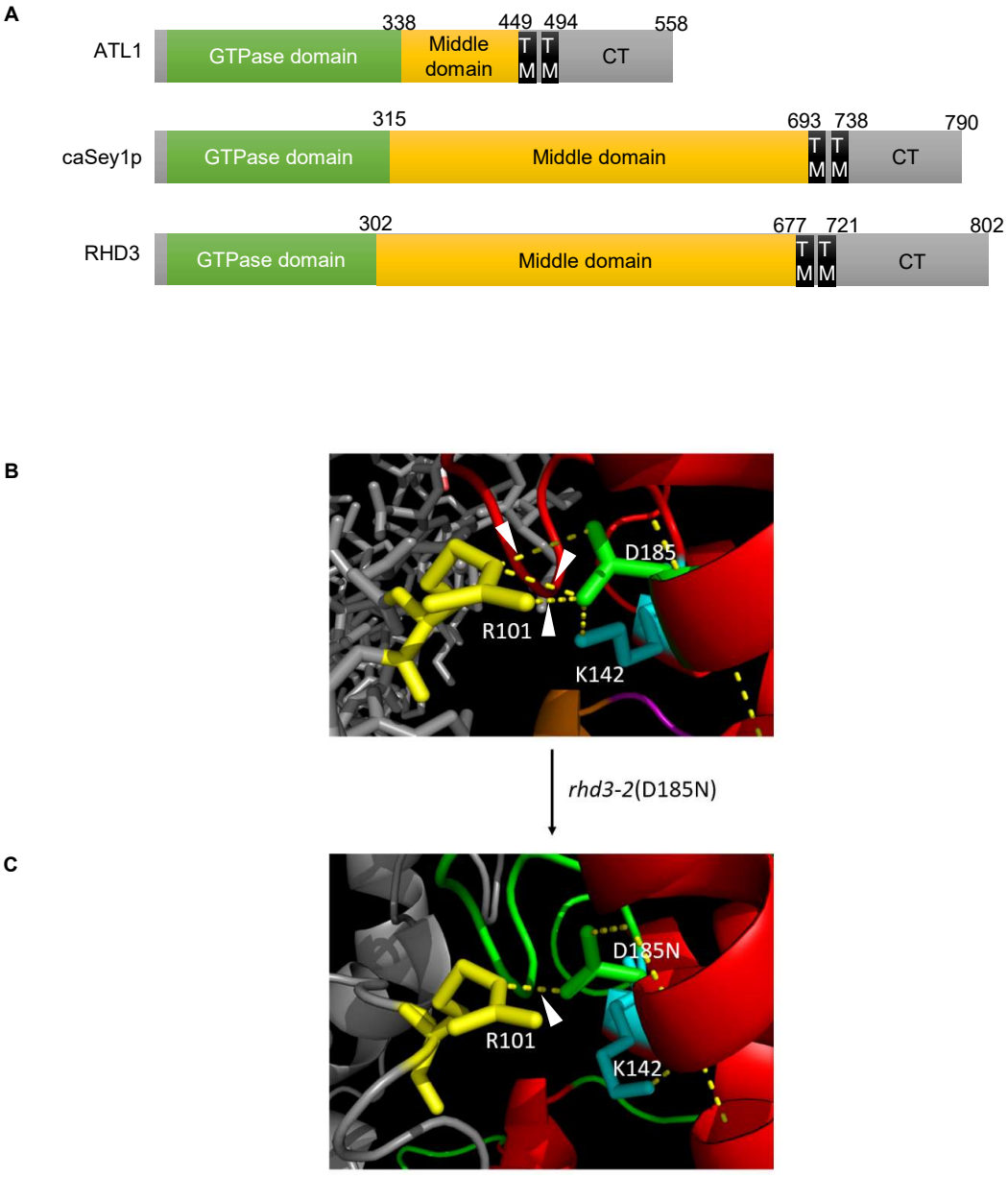

Supplemental Fig.S2.1.

Supplemental Fig. S2.2. Transient expression of RHD3 with mutations in the middle domain in tobacco leaves. A, Co-expression of YFP-RHD3(WT) and RFP-HDEL. B, Expression of 3HB-1 mutant RHD3(L355P) generates thick ER bundles (arrows). Scale bar = 10 μm. C, Expression of 3HB-2 mutant RHD3(L465P) generates aggregation of ER tubules (arrowhead). Scale bar = 10 μm. D-F, Expression of 3HB-3 mutant RHD3(L465P), and 3HB-4 mutants RHD3(A575P) and RHD3-1(A575A) only mark weak punctates on the ER and have no influence on the formation of the ER indicated by RFP-HDEL. Scale bar= 10 μm.

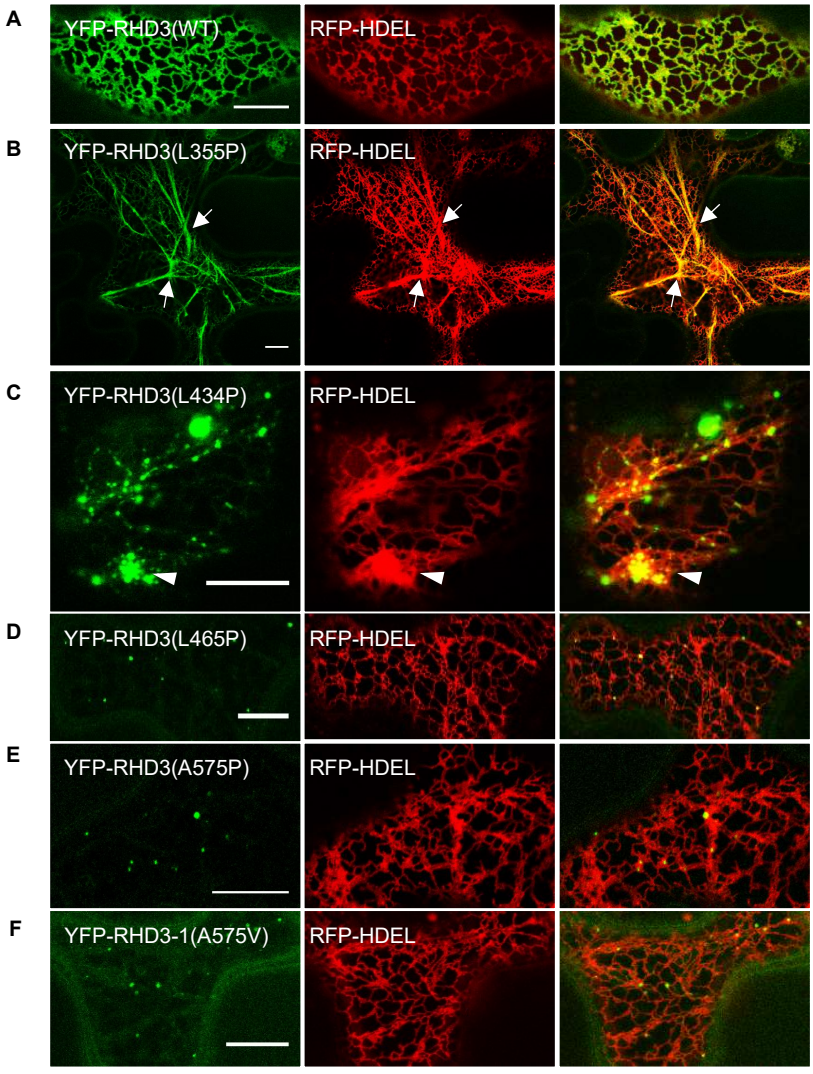

Supplemental Fig. S2.2.

Supplemental Fig.S2.3. Transient expression of different RY constructs in tobacco leaves. A, The organization of the RY vector used for the protein stability test for different RHD3 mutants. In the plasmid, there are two different ORFs, one is the lumen ER marker mCherry-HDEL and the another is different versions of YFP fused RHD3, and they can be expressed simultaneously. B, Expression of RY vectors containing WT RHD3, RHD3(L461P), RHD3(L465P), RHD3(A575P), RHD3(L580P) and RHD3-1(A575V) as indicated. Scale bar = 10 μm.

A

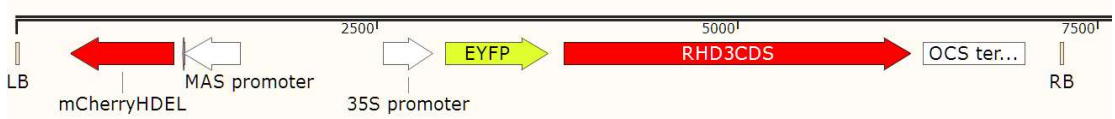

B

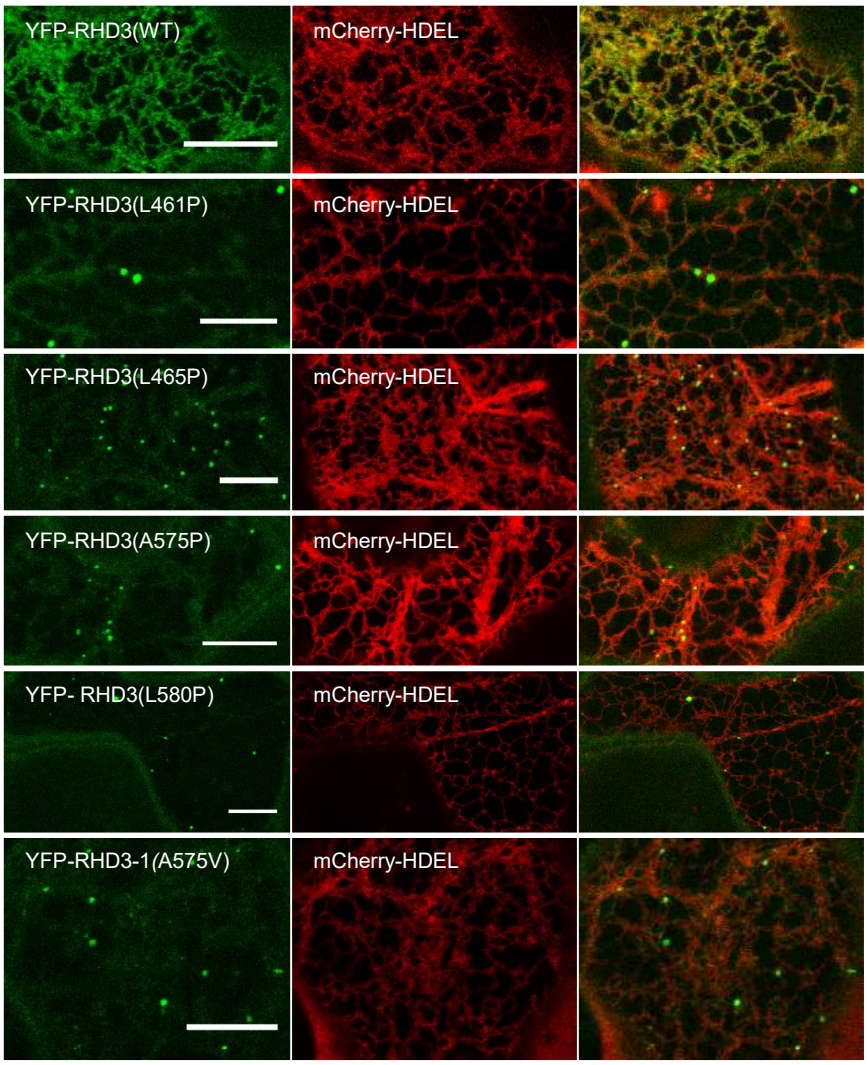

Supplemental Fig.S2.3.

Supplemental Fig. S2.4. A, Transient expression of mutated CT of RHD3 (CT(F727D)) in tobacco leaves. The mutation did not change the membrane attachment of the CT of RHD3 as indicated by the punctate Golgi localization. B, The expression of RHD3 with mutations in the CT of RHD3 in *rhd3-8* does not complement the ER defects of *rhd3-8* as indicated by thick and bundled ER tubules (arrows). YFP fused wild type RHD3, CT deleted RHD3 (RHD3(ΔCT)), and the quadruple RHD3 mutant (RHD3(F727D, V731D, L735D, L738D)) were expressed in the *rhd3-8* mutant driven by the 35S promoter. The leaves of 4-weeks old plants were taken for imaging. Scale bar= 10μm.

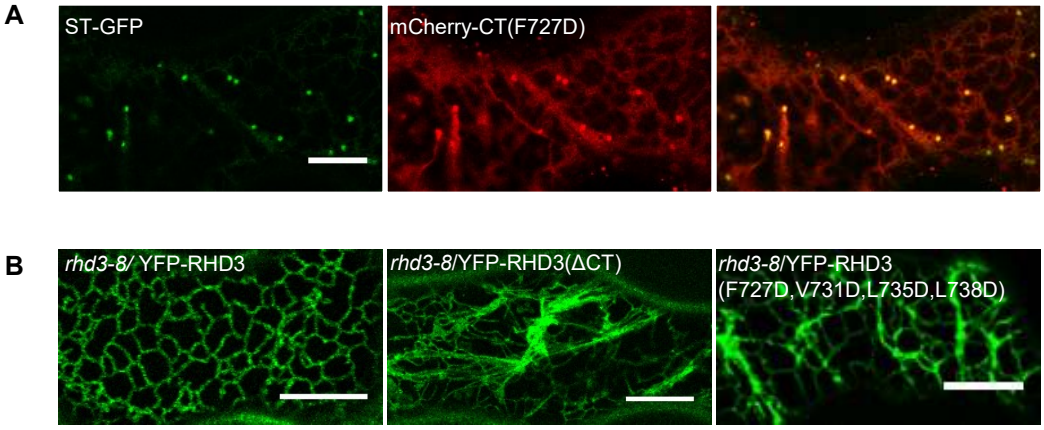

Supplemental Fig. S2.4.

Supplemental Fig. S2.5. Expression of the C-terminal tail of Sey1p (Sey1pCT) in plant cells. A, Co-expression of ST-GFP and RFP-Sey1pCT in tobacco leaves. B, Co-expression of GFP-HDEL and RFP-RHD3AH-Sey1pDS in tobacco leaves. The amphipathic helix in the C-terminal tail of RHD3 (RHD3AH) was fused with the divergent sequence of Sey1p (Sey1pDS). Scale bar = 10 μm.

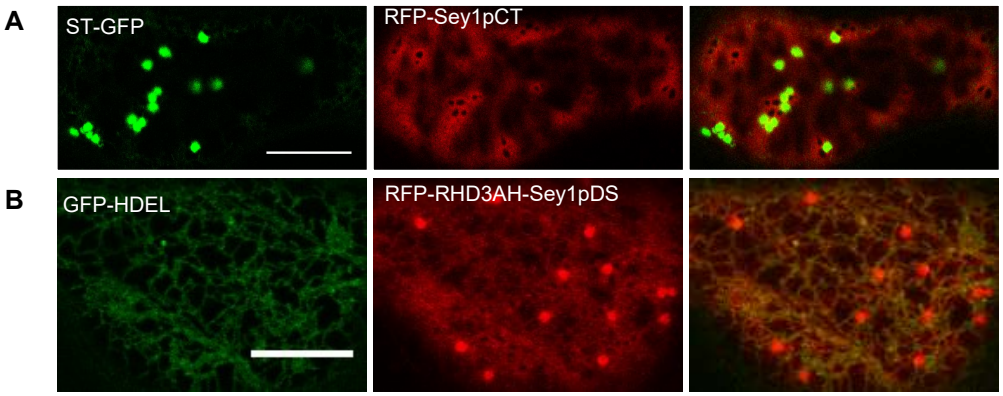

Supplemental Fig. S2.5

The link between Chapter II and Chapter III

In Chapter II, I studied the roles of different domains of RHD3 involved in mediating the ER membrane fusion. To maintain the ER homeostasis, the action of RHD3 must be regulated and balanced. Therefore, in Chapter III, I studied how Lunapark proteins regulate the activity of RHD3 in the plant cells.

CHAPTER III:

LUNAPARK INHIBITS FUSION ACTIVITY OF RHD3 IN GENERATION OF INTERCONNECTED TUBULAR ER NETWORK

Jiaqi Sun, Hugo Zheng

Nature Communications, submitted, 2018

ABSTRACT

The formation of the interconnected ER network requires homotypic fusion, which is mediated by Atlastin large GTPases, including RHD3 (ROOT HAIR DEFECTIVE 3) in *Arabidopsis*. To generate an interconnected ER network, the fusion activity of Atlastin proteins must be regulated. Such a regulation is, however, not well studied. We showed here that RHD3 physically interacts with two *Arabidopsis* Lunapark proteins (LNPs) LNP1 and LNP2 at 3-way junctions of the ER. We found that, recruited by RHD3 to newly formed 3-way junctions, LNPs stabilize the nascent 3-way junctions of the ER by inhibiting the fusion activity of RHD3. In *Arabidopsis lnp* mutant cells, the ER is often sheet-like with dense 3-way junctions. This phenotype is probably caused by the higher RHD3 protein level. We thus proposed the degradation of RHD3 is promoted by LNPs after the ER fusion is completed so newly formed 3-way junctions of the ER are stabilized.

3.1. INTRODUCTION

The endoplasmic reticulum (ER) is an interconnected network of membranous tubules and sheets that stretches throughout the cytoplasm of eukaryotic cells. The ER plays important roles in the biosynthesis and transport of proteins and lipids. The ER acts as an important architectural scaffold to maintain an ordered distribution of the other cellular organelles (English and Voeltz, 2013). The ER is also important for calcium signalling, general cellular homeostasis, plant growth and abiotic and biotic stress resistance (Angelos et al., 2017). Live-cell imaging has revealed that the ER is a highly dynamic organelle with continuous growth, retraction, sliding and fusion of tubules to enlarge and contract its highly dynamic polygonal tubular network (Sparkes et al., 2011). Such dynamics are important for the ER to perform various functions (Westrate et al., 2015). However, the mechanisms by which the structure of the ER is formed and maintained are not well studied.

Several evolutionarily conserved protein families have been implicated in shaping the interconnected ER network. The reticulons (Rtns) and DP1/Yop1p are proposed to shape the ER membranes, possibly through stabilizing the high membrane curvatures in tubules and sheet edges in mammalian, yeast and plant cells (Hu et al., 2008; Shibata et al., 2009; Sparkes et al., 2009). Recent work indicates that the fusion of ER tubules is mediated by a class of ER membrane-bound dynamin-like large GTPases, including the Atlastins (ATLs) in metazoans, Sey1p in yeast and RHD3 in plants (Anwar et al., 2012; Hu et al., 2009; Orso et al., 2009; Zhang et al., 2013). These dynamin-like GTPases tether opposing ER membranes through their dimerization and then fuse them together through a GTP hydrolysis-dependent conformational change (Bian et al., 2011; Sun and Zheng, 2017; Yan et al., 2015). Lunapark (LNP) proteins, a family of a conserved ER membrane proteins, are also known to play an important role in the maintenance of the

interconnected tubular ER network in yeast and mammalian cells by stabilizing nascent 3-way junctions formed by the fusion of different ER tubules (Chen et al., 2015; Wang et al., 2016). But how LNP proteins can stabilize 3-way junctions of the ER and the exact relationship between ATL and LNP are still unclear. In addition, as an important regulator of the ER morphology, the significance of LNPs on the organism development has not been studied. In the plant, the existence of functional LNP homologs is questioned and different mechanisms are proposed to play roles in stabilizing ER junctions and maintaining ER network (Stefano and Brandizzi, 2017).

Here we showed that, RHD3, a plant member of the atlastin GTPases, physically interacts with two evolutionally conserved LNPs, LNP1 and LNP2 in *Arabidopsis*. *Arabidopsis lnp1-1 lnp2-1* mutants grow short root hairs and have pleiotropic developmental growth defects with massive sheet-like ER which contains dense 3-way junctions in the cells. We demonstrated that LNPs are recruited by RHD3 to 3-way junctions of the ER and are required for stabilizing newly formed 3-way junctions. Our molecular and genetic evidence indicates that LNPs inhibit the fusion activity of RHD3. Furthermore, in *lnp* mutants, the RHD3 protein level is higher than that in wild type plants. We therefore proposed that there is a LNP-mediated RHD3 protein degradation whereby the action of RHD3 is inhibited after the formation of 3-way junctions so that the formed 3-way junctions can be stabilized.

3.2. RESULTS

3.2.1. LNPs physically interact with RHD3 in plants. To better understand how the action of RHD3 is regulated as well as the detailed mechanisms by which the tubular ER network is maintained, we developed a 3-in-1 Bimolecular Florescence Complementation (BiFC) based screening system (Fig. 3.1a) to identify the potential interacting proteins of RHD3 in the plant. In this system, there are three independent open reading frames (ORFs) in the construct. One ORF encodes the ER lumen marker mCherry-HDEL, and one ORF contains RHD3 fused with the N-terminal domain of Venus (nVenus). Potential RHD3 interacting proteins were fused to the C-terminal domain of Venus (cVenus) in the third ORF. Using this system, we identified two RHD3 interacting proteins, Lunapark1 (LNP1, AT4G31080) and Lunapark2 (LNP2, AT2G24330). We named so as both proteins shared a domain similarity with Lunapark proteins found in yeast and mammalian cells (Chen et al., 2015; Chen et al., 2012b; Wang et al., 2016) (Supplemental Fig 3.1).

Interestingly as indicated in Fig 3.1, in our BiFC assay, both of them interacted with RHD3 and on 3-way junctions of the ER indicated by mCherry-HDEL (Fig. 3.1b, c). As the negative control, RHD3 did not interact with p24 (Fig. 3.1d), which is an ER membrane protein involved in the transport between ER and Golgi (Chen et al., 2012a), and LNP1 or LNP2 did not interact with CER6 (Fig. 3.1e, f), encoding an ER localized condensing enzyme that catalyzes the elongation of C22 fatty acyl-CoAs or longer (Fiebig et al., 2000; Millar et al., 1999). To verify the interaction between RHD3 and LNP proteins, we used the mating based Split-Ubiquitin System (SUS) (Grefen et al., 2009). Both LNP1 and LNP2 interacted with RHD3 in the yeast cells (Fig. 3.2a, row 3 and 4). Consistent with the previous results (Chen et al., 2011), RHD3 could interact with itself (Fig. 3.2a, row 1, served as positive control), but not with NubG alone (Fig. 3.2a, row 2,

served as negative control). A GFP-trap bead based pull-down assay in *lnp2-1* plants expressing pLNP2:LNP2-YFP with mCherry-HDEL or mCherry-RHD3 were also conducted. As indicated in Fig. 3.2b, mCherry-RHD3 but not mCherry-HDEL was pulled down by GFP-trap beads. Taken all together, we concluded that LNP1 and LNP2 physically interact with RHD3.

3.2.2. LNPs are required for normal cell development and for maintenance of tubular ER network. Because LNPs interact with RHD3 which is required for normal root hair growth and cell development, we wondered whether LNP1 and LNP2 are also involved in normal plant cell development. To this end, we identified two T-DNA insertional knock-out *lnp1* mutant alleles *lnp1-1* (Salk_028863) and *lnp1-2* (Salk_100743) and two T-DNA insertional knock-down *lnp2* mutant alleles *lnp2-1* (GK607D07) and *lnp2-2* (SK2564) (Fig. 3.3a, b). Compared with WT seedlings, single *lnp1-1* and *lnp2-1* mutants had slightly shorter root hairs and double mutant *lnp1-1 lnp2-1* had much shorter root hairs (Fig. 3.3c). In the term of general plant architecture, single *lnp1-1* or *lnp2-1* mutant did not show any obvious defects, while the double mutant plants were much smaller than the wild type plants (Fig. 3.3d). The root hair defects and general developmental defects of the double mutant *lnp1-1 lnp2-1* could be rescued by the transformation of either LNP1-YFP or LNP2-YFP alone driven by their native promoters (Fig. 3.3c, d). These results suggested that that YFP-tagged LNP1 and LNP2 proteins are fully functional *in vivo*, and likely, LNP1 and LNP2 proteins have redundant functions in plant cell development. In *rhd3* mutants, the ER is bundled and unbranched, so we investigated whether *lnp* mutants are also defective in the ER morphology. YFP-HDEL was expressed in both wild type Col-0 and *lnp1-1 lnp2-1* double mutants. 3-days after germination, in the wild type cotyledon cells, the ER was viewed as a tubular network (Fig. 3.3e1,2). However, in the double mutant *lnp1-1 lnp2-1* cotyledon cells, there were massive

ER sheets (Fig. 3.3e3) under confocal microscopy. With Airyscan superresolution microscopy, we found that these ER sheets were actually ER networks with dense junctions (Fig. 3.3e4, enlarged image), similar to what is described in mammalian cells (Nixon-Abell et al., 2016) This result indicated that compared with WT, in *lnp1-1 lnp2-1* plants, there are increased number and densities of 3-way junctions, which are generated by homotypic ER fusion. All these results suggest that *Arabidopsis* LNPs are also involved in maintaining a normal tubular ER morphology.

3.2.3. LNPs are recruited by RHD3 to 3-way junctions of the ER network. In order to understand how LNPs are required for maintaining a normal tubular ER morphology, we first examined their subcellular localization. To this end, we made LNP1-YFP and LNP2-YFP driven by their native promoters and expressed them in *lnp1-1* and *lnp2-1* mutants. The expression of LNP1-YFP and LNP2-YFP were found to be overlapping in diverse tissues, including hypocotyl cells, the epidermal cells of cotyledons, the stomata cells, root tips and growing root hairs (Supplemental Fig. 3.2a, b), which further suggested that LNP1 and LNP2 have redundant functions in different cells types. A detailed confocal microscopy in cotyledon epidermal cells indicated that, LNP1-YFP and LNP2-YFP showed puncta localization (Fig. 3.4a). These puncta were confirmed to be 3-way junctions of the ER by expressing RFP-HDEL *in lnp1-1*::pLNP1:LNP1-YFP and *lnp2-1*::pLNP2:LNP2-YFP plants (Fig. 3.4b, c). Strikingly, in the epidermal cells of the *rhd3-8* mutant, LNP1 and LNP2 were seen on the ER tubules rather than in puncta (Fig. 3.4d). Similarly, in the presence of dominant negative RHD3 mutants YFP-RHD3(S51N) or YFP-RHD3(T75A) (Chen et al., 2011), LNP1-RFP (Supplemental Fig. 3.3a, b) and LNP2-RFP (Supplemental Fig. 3.3c, d) were also localized on ER tubules. These results suggested that the localization of LNP1 and LNP2 to 3-way junctions of the ER requires functional

RHD3. When LNP1 and LNP2 were transiently overexpressed in tobacco leaves, LNP1-RFP and LNP2 were observed in ER tubules in addition to the enrichment on 3-way junctions of the ER (Supplemental Fig. 3.3e, g, respectively) possibly own to the nature of transient overexpression (Sparkes et al., 2006). Interestingly, in the presence of YFP-RHD3, LNP1-RFP and LNP2-RFP were only seen on the 3-way junctions of the ER, most of which were co-localized with YFP-RHD3 (Supplemental Fig. 3.3f, h). These results suggested that LNP1and LNP2 can be recruited by RHD3 to 3-way junctions of the ER.

3.2.4. LNPs stabilize the nascent 3-way junctions of the ER in plant cells. In mammalian cells, a high correlation was found between the presence of LNPs and the stability of the nascent 3-way junctions (Chen et al., 2012b). The ER with dense 3-way junctions in *lnp1-1 lnp2-1* mutants and the localization of LNPs on 3-way junctions of the ER in plant cells prompted us to examine if there is a similar mechanism exists in plant cells. To this end, we transiently co-expressed LNP2-RFP with YFP-HDEL in the tobacco leaves. We observed the stability of nascent 3-way junctions of the ER within 200 seconds and assessed their existing time. We defined starting time when a tubule fuse together with another tubule to form a 3-way junction, and the end time when the junctions disappear after the ring closure. We found that in the absence of LNP2-RFP, most of the nascent junctions disappeared in 25s (Fig. 3.5a, c), while in the presence of LNP2-RFP, these nascent junctions would exist over 80s (Fig. 3.5b, c). This result indicated that *Arabidopsis* LNPs also stabilize the nascent 3-way junctions in plant cells.

3.2.5. LNPs inhibit the fusion activity of RHD3. Since LNPs interact with the RHD3 protein, we wondered if LNPs stabilize nascent 3-way junctions by regulating the fusion action of RHD3. It is known that, similar to the overexpression of Atlastin (Nixon-Abell et al., 2016), overexpression of RHD3 leads to the formation of massive sheet ER with dense junctions revealed by Airyscan superresolution microscopy (Supplemental Fig. 3.4) as a result of excessive fusion of ER membranes (Zheng and Chen, 2011). When YFP-HDEL was expressed alone in tobacco leave cells, only 10% of cells were found with the sheet-like ER (Fig. 3.6a, e), but when mCherry-RHD3 was co-expressed together with YFP-HDEL, massive sheet ER was found in over 60% cells (Fig. 3.6b, e), Intriguingly, the co-expression of LNP1-YFP or LNP2-YFP with mCherry-RHD3, the percentage of cells with sheet-like ER was decreased to about 30% (Fig. 3.6b, c, e). This implied that LNPs inhibit the excessive fusion activity of RHD3 that caused the formation of the sheet ER.

To further confirm that LNPs can inhibit the fusion activity of RHD3, we used a yeast ER fusion assay (Anwar et al., 2012). Consistent with a previous study (Sun and Zheng, 2017; Zhang et al., 2013), *Δsey1p* mutant cells exhibited slow ER fusion progress (about 23 mins) (Fig. 3.6f, column 1), and the expression of RHD3 or Sey1p significantly improved the ER fusion efficiency (Fig. 3.6f, column 2 and 5). However, co-expression RHD3 with LNP1 or LNP2 together did not rescue the ER fusion defects in the *Δsey1p* mutant (Fig. 3.6f, column 3 and 4), suggesting that LNPs can inhibit the fusion activity of RHD3. It is interesting to note that *Arabidopsis* LNP1 or LNP2 did not supress the fusion activity of Sey1p when LNP1 or LNP2 was co-expressed with Sey1p in the *Δsey1p* yeast cells (Fig. 3.6f, column 5, 6 and 7). This indicated that this inhibition is specific to RHD3.

If LNPs inhibit the action of RHD3, it would be expected that knock-out of LNPs in *rhd3* mutants could at least partially rescue developmental defects observed in *rhd3*. To this end, we crossed

rhd3-8 with *lnp1-1* or *lnp2-1*. We found that the root hairs of double mutants *rhd3-8 lnp1-1* or *rhd3-8 lnp2-1* were longer than the root hairs of *rhd3-8* mutant, and the plants of the double mutants were also larger than *rhd3-8* mutant (Fig. 3.7a, b). On the contrary, overexpression of LNP1-YFP and LNP2-YFP in *rhd3-8* mutant significantly reduced the root hair length (Fig. 3.7c, d). Taken all together, we conclude that LNPs inhibit the activity of RHD3 in plant cells.

3.2.6. LNPs promote the protein degradation of RHD3 in plant cells. Next, we wondered how LNPs could inhibit the action of RHD3. Recently in mammalian cells, Lnp was identified as an interacting protein of a ubiquitin ligase gp78, a component of the Hrd1-related protein mediated ER-associated degradation (ERAD) (Zhao et al., 2016) but it does not have a broad function in degradation of misfolded ER proteins (Zhao et al., 2016). Following this clue, we wondered if *Arabidopsis* LNPs could promote the degradation of RHD3. We checked the protein expression level of RHD3 in WT and *lnp1-1 lnp2-1* mutant plants with the anti-RHD3 antibody. The specificity of this anti-RHD3 antibody was confirmed by checking the expression of RHD3 in the *rhd3-8* mutant (Fig. 3.7e). We found that there was more RHD3 protein accumulated in *lnp1-1 lnp2-1* mutant than that in WT plants (Fig. 3.7e), while there was no significant difference at the RNA level (Fig. 3.7f). The results indicate that LNPs promote the protein degradation of RHD3 in plant cells.

3.3. DISCUSSION

Herein we identified two novel plant LNP homologs, LNP1 and LNP2, which interact with RHD3. *Arabidopsis* mutants with deletions in LNP1 and LNP2 exhibit sheet-like ER with dense 3-way junctions, indicating that *Arabidopsis* LNPs are required for the maintenance of a normal tubular ER morphology. Because single mutant *lnp1* or *lnp2* do not have obvious defects on plant development, but double mutant *lnp1-1 lnp2-1* show significantly reduced cell growth with massive sheet-like ER in the cells, there should be a functional redundancy between LNP1 and LNP2. In support of this notion, we found that the expression of LNP1 and LNP2 are highly overlapped in diverse cell types.

To generate an interconnected tubular ER network, the fusion activity of Atlastin proteins must be regulated or balanced after the fusion of different ER tubules. It has been shown that LNP1 in yeast and mammalian cells can antagonize the action of Sep1p and Atlastin-1, respectively (Chen et al., 2015; Chen et al., 2012b). But how LNP1 antagonizes the action of Sep1p or Atlastin-1 is not clear. For example, LNP1 was shown to interact with Sey1p in yeast cells (Chen et al., 2012b), but no physical interaction is detected between LNP1 and Atlastin-1 in mammalian cells (Chen et al., 2015). Our BiFC, SUS and Co-IP results indicated that *Arabidopsis* LNP1 and LNP2 directly interact with RHD3 in plant cells. Both *Arabidopsis* LNP1 and LNP2 are localized on 3-way junctions of the ER. Interestingly, their localization to 3-way junctions of the ER is lost in plants without RHD3 or in the presence of dominant negative RHD3 mutant proteins. In addition, when transiently expressed in the tobacco leaves alone, LNP1 and LNP2 are also seen on the ER tubules but when co-expressed with RHD3, both are only localized on 3-way junctions. Given the fact that

RHD3 physically interacts with both LNPs, it is likely that LNPs could be recruited to 3-way junctions of the ER by RHD3, once a 3-way junction of the ER is formed by tubular fusion.

Similar to what is described in mammalian cells (Chen et al., 2015), in the presence of LNP2, newly formed 3-way junctions of the ER are stable, while in the absence of LNP2, newly formed 3-way junctions of the ER is less stable. Because the expression of *Arabidopsis* LNP1 or LNP2 can 1) inhibit the fusion activity of RHD3 in yeast cells; 2) inhibit the formation of sheet-like ER caused by overexpression of RHD3 in plant cells, 3) synthetically enhance the root hair defects of *rhd3-8*, a RHD3 knockout mutants (Zhang et al., 2013), while knockout of LNP1 or LNP2 in *rhd3-8* can partially supress the root hair and developmental defects of *rhd3-8*, and *lnp1-1 lnp2-1* plants have massive sheet-ER in the cells phenocopying the overexpression of RHD3, we conclude that, LNP1 and LNP2, if it is recruited successfully to newly formed 3-way junctions of the ER, can inhibit the fusion activity of RHD3. This inhibition could prevent excessive fusion of ER tubules, thereby results in a stable 3-way junction of the ER.

How could LNPs inhibits the fusion activity of RHD3? In this study, we revealed that in *lnp1-1 lnp2-1* mutants, the protein level of RHD3 is higher than that in wild type Col-0. The massive ER sheets with dense 3-way junctions in *lnp1-1 lnp2-1* plants are likely cause by the elevated protein level of RHD3. Recently, mammalian Lnp1 was shown to interact with a ubiquitin ligase and has a novel ubiquitin ligase motif in the N-terminus (Zhao et al., 2016). Despite of these facts, Lnp does not seem to have a broad function in promoting the degradation of misfolded ER proteins (Zhao et al., 2016). Although this novel ubiquitin ligase motif in the N-terminus is not yet defined (Zhao et al., 2016), the N-terminus of the Lunapark family across the different species is relatively conserved (Supplemental Fig. 1b). It is therefore attempted to suspect here that *Arabiodpsis* LNPs may possess a specific role in promoting the degradation of RHD3. In supporting this, we noted

that in *Arabidopsis* either LNP1 or LNP2 does not inhibit fusion activity of Sey1p but RHD3 in the yeast cells. Likely, the inhibition of RHD3 is through a specific LNPs mediated ubiquitin based protein degradation pathway. If this also holds true for mammalian cells, it can explain why in a liposome-based *in vitro* assay, the soluble domain of the mammalian Lnp1 has no significant effect on the fusion activity of Atlastin *in vitro* (Chen et al., 2015). Because the ubiquitin based protein degradation requires the 26s protein proteasome and autophagy-based protein degradation systems in the cell, which are absent in the *in vitro* system.

Based on what we found here, we proposed a model by which how LNPs work together with RHD3 to regulate the formation of a tubular ER network. RHD3 molecules localized on two different ER membranes tether different ER tubules together by a dimerization (Sun and Zheng, 2017). After a GTP hydrolysis dependent conformational change, RHD3 molecules will pull and fuse tethered ER membranes together to form a junction, after which LNPs are recruited to 3-way junctions through its interaction with RHD3. Then RHD3 on a newly formed junction will be removed by LNP-dependent protein degradation to avoid excessive fusion. In this way, the nascent junction will be stabilized without supernumerary RHD3 molecules on the junctions. In *lnp1 lnp2* mutant or overexpression of RHD3, due to the paucity of LNPs, excessive RHD3 molecules accumulate on the junctions, whose fusion activity will cause unnecessary membrane fusion and sliding, resulting in a sheet-like ER with dense junctions in the cell.

3.4. METHODS

3.4.1. Molecular cloning

The 3 in 1 BiFC vectors were modified based on pDOE03 or pDOE04 vector(Gookin and Assmann, 2014). The original P19 fragment was replaced by mCherry-HDEL sequence within KpnI-NruI cutting sites. LNP1 and LNP2 were first cloned into pCR8/GW/TOPO entry vector (Invitrogen). Then these two entry vectors were performed gateway reactions with pNX22-DEST to generate LNP1-NubG and LNP2-NubG, or with pEarleyGate 101 to generate 35S:LNP1-YFP and 35S:LNP2-YFP. For the constructs of yeast ER fusion assay, RHD3 vector was created as previous described (Sun and Zheng, 2017). The yeast endogenous Lnp1p promoter was cloned into p413PGD vector (HIS3) and followed by LNP1 or LNP2 gene sequences. The promoters of LNP1 and LNP2 were amplified from *Arabidopsis* Genome and cloned into pCamiba 1300 together with LNP1-YFP or LNP2-YFP, which was amplified from 35S:LNP1-YFP and 35S:LNP2-YFP.

3.4.2. Plant Materials and Growth Conditions

All the seeds of the mutants, including *lnp1-1* (SALK_028863), *lnp1-2* (SALK_100743), *lnp2-1* (GK607D07), *lnp2-2* (SK2564) and *rhd3-8* (SALK_025215), were ordered from the Arabidopsis Biological Resource Center (ABRC). PCR and RT-PCR were used to identify homozygous lines. The primer sets for PCR and RT-PCR are listed in Supplemental Table S1.

pLNP1:LNP1-YFP and pLNP2:LNP2-YFP were transformed into *lnp1-1*, *lnp2-1* or *lnp1-1 lnp2-1* mutants correspondingly, to generate transgenic plants, *lnp1-1*::pLNP1:LNP1-YFP, *lnp2-1*::pLNP2:LNP2-YFP, *lnp1-1 lnp2-1*::pLNP1:LNP1-YFP and *lnp1-1 lnp2-1*::pLNP2:LNP2-YFP. RFP-HDEL, mCherry-HDEL and mCherry-RHD3 was transformed into *lnp1-1*::pLNP1:LNP1-

YFP and *lnp2-1*::pLNP2:LNP2-YFP to generate two fluorescent protein containing transgenic plant. *rhd3-8*::pLNP1:LNP1-YFP, *rhd3-8*::pLNP2:LNP2-YFP, *rhd3-8 lnp1-1* and *rhd3-8 lnp2-1* plants were made by crossing *rhd3-8* with *lnp1-1*::pLNP1:LNP1-YFP, *lnp2-1*::pLNP2:LNP2-YFP, *lnp1-1* and *lnp2-1* plants. *rhd3-8*::35S:LNP1-YFP and *rhd3-8*::35S:LNP2-YFP were made by transforming 35S:LNP1-YFP and 35S:LNP2-YFP into *rhd3-8* plants. YFP-HDEL was transformed into Col-0 wild type and *lnp1-1 lnp2-1* plants to generate Col-0 YFP-HDEL and *lnp1-1 lnp2-1* YFP-HDEL transgenic lines.

Seedlings were grown on AT (*Arabidopsis thaliana*) medium(Haughn and Somerville, 1986) with 1% sucrose at 22 to 24 ℃ under continuous light (80-100 μE m^{-1} s^{-1} photosynthetically active radiation).

3.4.3. Transient Expression in *Nicotiana tabacum* Leaves

Nicotiana tabacum plants with three or four leaves were used for infiltration. Agrobacterium carrying different constructs was grown in LB liquid medium at 28 ℃ for overnight. Then the agrobacterium was resuspended in infiltration buffer (100 μM acetosyringone and 10 mM $MgCl_2$). The final OD (600nm) was 0.01 or 0.1. Results were checked 2 days after infiltration.

3.4.4. Confocal Microscopy

Most images were observed with a Leica SP8 point-scanning confocal system on a Leica DMI6000B inverted microscope equipped with spectral fluorescent light detectors (three PMT, one HyD high sensitivity detector). A 63X/1.4 oil objective was used for all the imaging. The 488-nm laser was used to excite YFP, and the 552-nm laser was used to excite RFP/mCherry. Two

channels were excited sequentially. Emission filters were set as 490 to 560 nm for YFP and 580 to 660 nm for RFP/mCherry.

For observing the stability of 3-way junctions, a quorum WaveFX-X1 spinning disk confocal system and a 63X/1.4 numerical aperture oil lens were used. A 491 nm laser was used to excite YFP and a 568 nm laser was used to excite RFP/mCherry. Time-lapse images were taken every second.

3.4.5. Airyscan super-resolution microscopy

A ZEISS LSM 880 microscope with an Airyscan module was used for super-resolution microscopy imaging. 3 days seedlings were picked and mounted in the water for imaging, under a 63× oil immersion objective. YFP and mCherry were excited at 514 nm and 561 nm, respectively. Resolution vs. Sensitivity (RS) Airyscan mode was used for imaging. Airyscan processing was performed with ZEN imaging software. For post image editing, Fiji (Fiji is just ImageJ) was used (Schindelin et al., 2012).

3.4.6. Mating Based SUS

The Cub tagged RHD3 and NubG tagged proteins were transformed into haploid yeast strains THY.AP4 and THY.AP5, respectively (Obrdlik et al., 2004). After transformation, colonies were picked and inoculated in Synthetic Complete (SC) selection liquid medium (-Leu for AP4 and -Trp for AP5) for overnight at 28°C. The AP4 (Cub) and AP5 (NubG) suspensions were mixed and plated on YPD plates for mating. After 6 to 8 hrs at 28 °C, mated cells were streaked on -LT(-Leu) selection plates and incubated at 28 °C for 2 days. Diploid cells were collected, inoculated in -LT liquid medium and incubated at 28 °C for overnight. Then the cells were resuspended in water and

the OD (600nm) values were measured. Suspensions were diluted into OD = 1, 0.1, 0.01. Then 15 µl per spot was dropped on -LT plates for mating control, or -LTH (-Leu-Trp-His) plates for interaction test. Plates were incubated at 28 ℃ for 2 days.

3.4.7. Yeast ER Fusion Assay

Different constructs were transformed into two different *Δsey1p* mutant haploid cells, ACY53 (ss-RFP-HDEL) and ACY54 (free GFP). Cells were grown to an OD (600nm) of 0.1 to 0.4, mixed and concentrated in YPD medium. 5 µl cell suspension was dropped on a 1-mm-thick SC medium pad and grown at 30 ℃ for 40 to 60 mins. Then images were taken at 20-second intervals.

3.4.8. Co-immunoprecipitation

Transgenic seedlings were ground into a powder in liquid nitrogen and extracted with the extraction buffer (50 mM Tris-HCl pH 7.5, 150 mM NaCl, and 10% (v/v) glycerol, and 0.5% IGEPAL® CA-630 (#I8896, sigma), 1/100 volume of Protease Inhibitor Cocktail (#P9599, sigma)). The solution should be homogenized to an even mixture and centrifuged at 17,000g for 10 mins at 4℃. Then the supernatant was collected. 25 µl GFP-Trap®_MA beads (#gtma-20, Chromotek) was washed three times with wash buffer (10 mM Tris-HCl pH 7.5; 150 mM NaCl). The protein lysate was added to the washed beads and incubated for 1 hour at 4℃. The beads were magnetically separated and washed 3 times with wash buffer. Then the beads were resuspended in 50 µl 2X SDS-loading buffer and boiled for 10 mins. The solution was centrifuged and the supernatant was used for western blot.

3.4.9. Western Blot

4 days after germination, the total proteins were extracted with 1X SDS loading buffer from WT and *lnp1-1 lnp2-1* seedlings. Samples were boiled for 5 mins. After 2 mins centrifuge at 13,000 rpm, the supernatants were loaded on 10% SDS-PAGE gel. At 1:10,000 dilution, a rabbit Anti-RHD3CT antibody (PhytoAB, PHY0765S) was used for the western blot. For the blotting after immunoprecipitation, a rabbit anti-GFP antibody (Abcam, ab32146) at 1:5000 dilution or a rabbit anti-RFP (Abcam, ab34771) at 1:2000 dilution was used. The secondary anti-rabbit IgG-peroxidase (Sigma) was used at 1:5,000 dilution.

3.5. ACKNOWLEDGMENTS

We thank the Cell Imaging and Analysis Network (CIAN) and the Advanced BioImaging Facility(ABIF) at McGill University for confocal microscopy imaging support; the Neuro Microscopy Imaging Centre, McGill for Airyscan microscopy imaging support. J.S was supported by a scholarship from the Chinese Scholarship Council. This research was supported by a discovery grant and Discovery Accelerator Supplement award from the Natural Sciences and Engineering Research Council (NSERC) of Canada to H.Z..

3.6. REFERENCES

Angelos, E., Ruberti, C., Kim, S.J., and Brandizzi, F. (2017). Maintaining the factory: the roles of the unfolded protein response in cellular homeostasis in plants. Plant J *90*, 671-682.

Anwar, K., Klemm, R.W., Condon, A., Severin, K.N., Zhang, M., Ghirlando, R., Hu, J., Rapoport, T.A., and Prinz, W.A. (2012). The dynamin-like GTPase Sey1p mediates homotypic ER fusion in S. cerevisiae. J Cell Biol *197*, 209-217.

Bian, X., Klemm, R.W., Liu, T.Y., Zhang, M., Sun, S., Sui, X., Liu, X., Rapoport, T.A., and Hu, J. (2011). Structures of the atlastin GTPase provide insight into homotypic fusion of endoplasmic reticulum membranes. Proc Natl Acad Sci U S A *108*, 3976-3981.

Chen, J., Qi, X., and Zheng, H. (2012a). Subclass-specific localization and trafficking of Arabidopsis p24 proteins in the ER-Golgi interface. Traffic *13*, 400-415.

Chen, J., Stefano, G., Brandizzi, F., and Zheng, H. (2011). Arabidopsis RHD3 mediates the generation of the tubular ER network and is required for Golgi distribution and motility in plant cells. J Cell Sci *124*, 2241-2252.

Chen, S., Desai, T., McNew, J.A., Gerard, P., Novick, P.J., and Ferro-Novick, S. (2015). Lunapark stabilizes nascent three-way junctions in the endoplasmic reticulum. Proceedings of the National Academy of Sciences *112*, 418-423.

Chen, S., Novick, P., and Ferro-Novick, S. (2012b). ER network formation requires a balance of the dynamin-like GTPase Sey1p and the Lunapark family member Lnp1p. Nat Cell Biol *14*, 707-716.

English, A.R., and Voeltz, G.K. (2013). Endoplasmic reticulum structure and interconnections with other organelles. Cold Spring Harb Perspect Biol *5*.

Fiebig, A., Mayfield, J.A., Miley, N.L., Chau, S., Fischer, R.L., and Preuss, D. (2000). Alterations in CER6, a gene identical to CUT1, differentially affect long-chain lipid content on the surface of pollen and stems. Plant Cell *12*, 2001-2008.

Gookin, T.E., and Assmann, S.M. (2014). Significant reduction of BiFC non-specific assembly facilitates in planta assessment of heterotrimeric G-protein interactors. Plant J *80*, 553-567.

Grefen, C., Obrdlik, P., and Harter, K. (2009). The determination of protein-protein interactions by the mating-based split-ubiquitin system (mbSUS). Methods Mol Biol *479*, 217-233.

Haughn, G.W., and Somerville, C. (1986). Sulfonylurea-Resistant Mutants of Arabidopsis-Thaliana. Mol Gen Genet *204*, 430-434.

Hu, J., Shibata, Y., Voss, C., Shemesh, T., Li, Z., Coughlin, M., Kozlov, M.M., Rapoport, T.A., and Prinz, W.A. (2008). Membrane proteins of the endoplasmic reticulum induce high-curvature tubules. Science *319*, 1247-1250.

Hu, J., Shibata, Y., Zhu, P.P., Voss, C., Rismanchi, N., Prinz, W.A., Rapoport, T.A., and Blackstone, C. (2009). A class of dynamin-like GTPases involved in the generation of the tubular ER network. Cell *138*, 549-561.

Millar, A.A., Clemens, S., Zachgo, S., Giblin, E.M., Taylor, D.C., and Kunst, L. (1999). CUT1, an Arabidopsis gene required for cuticular wax biosynthesis and pollen fertility, encodes a very-long-chain fatty acid condensing enzyme. Plant Cell *11*, 825-838.

Nixon-Abell, J., Obara, C.J., Weigel, A.V., Li, D., Legant, W.R., Xu, C.S., Pasolli, H.A., Harvey, K., Hess, H.F., Betzig, E.*, et al.* (2016). Increased spatiotemporal resolution reveals highly dynamic dense tubular matrices in the peripheral ER. Science *354*.

Obrdlik, P., El-Bakkoury, M., Hamacher, T., Cappellaro, C., Vilarino, C., Fleischer, C., Ellerbrok, H., Kamuzinzi, R., Ledent, V., Blaudez, D.*, et al.* (2004). K+ channel interactions

detected by a genetic system optimized for systematic studies of membrane protein interactions. Proc Natl Acad Sci U S A *101*, 12242-12247.

Orso, G., Pendin, D., Liu, S., Tosetto, J., Moss, T.J., Faust, J.E., Micaroni, M., Egorova, A., Martinuzzi, A., McNew, J.A.*, et al.* (2009). Homotypic fusion of ER membranes requires the dynamin-like GTPase atlastin. Nature *460*, 978-983.

Schindelin, J., Arganda-Carreras, I., Frise, E., Kaynig, V., Longair, M., Pietzsch, T., Preibisch, S., Rueden, C., Saalfeld, S., Schmid, B.*, et al.* (2012). Fiji: an open-source platform for biological-image analysis. Nat Methods *9*, 676-682.

Shibata, Y., Hu, J., Kozlov, M.M., and Rapoport, T.A. (2009). Mechanisms shaping the membranes of cellular organelles. Annu Rev Cell Dev Biol *25*, 329-354.

Sparkes, I., Hawes, C., and Frigerio, L. (2011). FrontiERs: movers and shapers of the higher plant cortical endoplasmic reticulum. Curr Opin Plant Biol *14*, 658-665.

Sparkes, I., Runions, J., Hawes, C., and Griffing, L. (2009). Movement and remodeling of the endoplasmic reticulum in nondividing cells of tobacco leaves. Plant Cell *21*, 3937-3949.

Sparkes, I.A., Runions, J., Kearns, A., and Hawes, C. (2006). Rapid, transient expression of fluorescent fusion proteins in tobacco plants and generation of stably transformed plants. Nat Protoc *1*, 2019-2025.

Stefano, G., and Brandizzi, F. (2017). Advances in plant ER architecture and dynamics. Plant Physiol.

Sun, J., and Zheng, H. (2017). Efficient ER fusion requires a dimerization and C-terminal tail mediated membrane anchoring of RHD3. Plant Physiol.

Wang, S., Tukachinsky, H., Romano, F.B., and Rapoport, T.A. (2016). Cooperation of the ER-shaping proteins atlastin, lunapark, and reticulons to generate a tubular membrane network. eLife *5*, e18605.

Westrate, L.M., Lee, J.E., Prinz, W.A., and Voeltz, G.K. (2015). Form follows function: the importance of endoplasmic reticulum shape. Annu Rev Biochem *84*, 791-811.

Yan, L., Sun, S., Wang, W., Shi, J., Hu, X., Wang, S., Su, D., Rao, Z., Hu, J., and Lou, Z. (2015). Structures of the yeast dynamin-like GTPase Sey1p provide insight into homotypic ER fusion. The Journal of Cell Biology *210*, 961-972.

Zhang, M., Wu, F., Shi, J., Zhu, Y., Zhu, Z., Gong, Q., and Hu, J. (2013). RHD3 family of dynamin-like GTPases mediates homotypic endoplasmic reticulum fusion and is essential for Arabidopsis development. Plant Physiol.

Zhao, Y., Zhang, T., Huo, H., Ye, Y., and Liu, Y. (2016). Lunapark Is a Component of a Ubiquitin Ligase Complex Localized to the Endoplasmic Reticulum Three-way Junctions. Journal of Biological Chemistry.

Zheng, H., and Chen, J. (2011). Emerging aspects of ER organization in root hair tip growth: lessons from RHD3 and Atlastin. Plant signaling & behavior *6*, 1710-1713.

Figures

Figure 3.1 | RHD3 interacts with LNP proteins in BiFC screening. (**a**) 3-in-1 BiFC system. Three different ORFs are in the same vector. One ORF contains mCherry-HDEL, one contains nVenus fused RHD3 and another contains the candidate protein fused with cVenus. (**b**) RHD3 interacts with LNP1 in 3-way junctions of the ER. (**c**) RHD3 interacts with LNP2 in 3-way junctions of the ER. (**d**) Negative control, RHD3 does not interact with p24. (**e, f**) Negative control, LNP1 and LNP2 do not interact with CER6. Scale Bars = 10 μm.

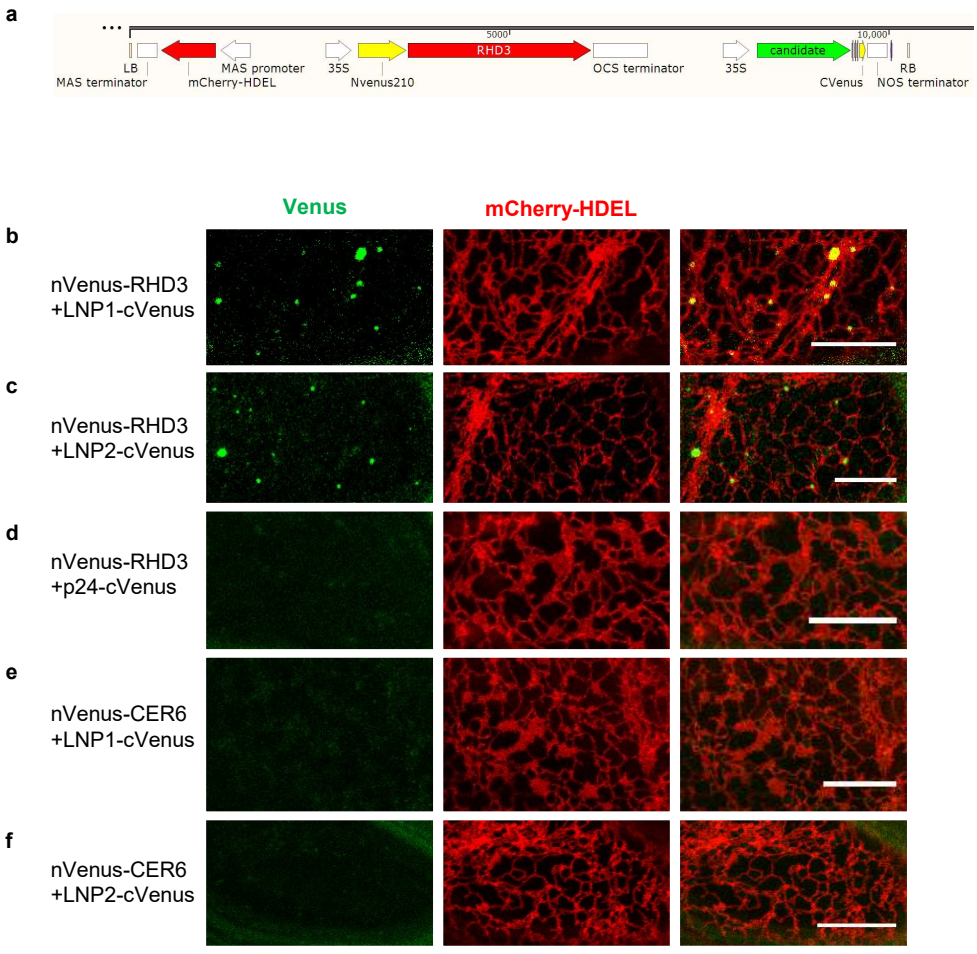
a
5000
RHD3
10,000
candidate
LB
MAS terminator
MAS promoter
mCherry-HDEL
35S
Nvenus210
OCS terminator
35S
CVenus
RB
NOS terminator
Venus
mCherry-HDEL
b
nVenus-RHD3
+LNP1-cVenus
c
nVenus-RHD3
+LNP2-cVenus
d
nVenus-RHD3
+p24-cVenus
e
nVenus-CER6
+LNP1-cVenus
f
nVenus-CER6
+LNP2-cVenus

Figure 3.1

Figure. 3.2 | RHD3 physically interact with LNP1 and LNP2. (**a**) The mating based Split-Ubiquitin System (SUS). (1) the positive control, Cub-RHD3 interacts with NubG-RHD3. (2) the Negative control, Cub-RHD3 does not interact with NubG. (3) Cub-RHD3 interacts with LNP1-NubG. (4) Cub-RHD3 interacts with LNP2-NubG. Mated diploid yeast cells were diluted into OD (600nm) =1, 0.1 and 0.01 as indicated. The diploid cells were dropped on SC medium without Leucine and Tryptophan (-LT) to verify the mating, and on SC medium without Leucine, Tryptophan and Histidine (-LTH) to verify the interaction. (**b**) Western blot of protein immunoprecipitated (IP) with GFP-trap beads. *lnp2-1* plants expressing pLNP2:LNP2-YFP with mCherry-HDEL or mCherry-RHD3 were used for IP.

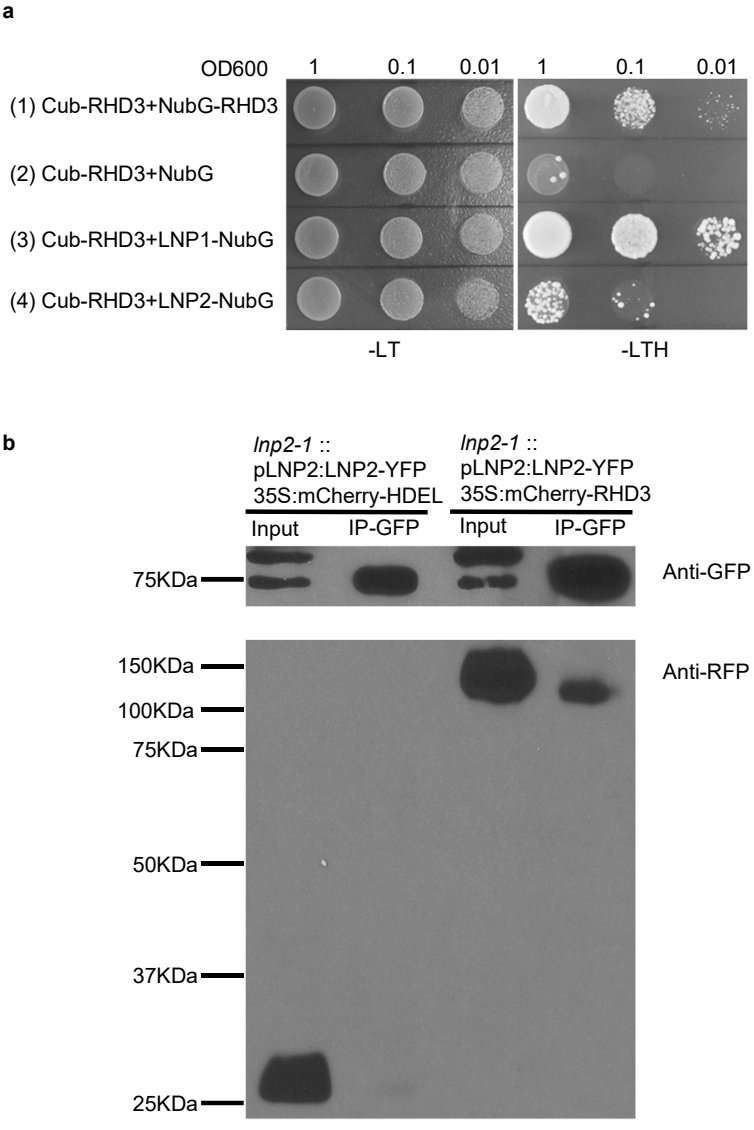
a
OD600
1
0.1
0.01
1
0.1
0.01
(1) Cub-RHD3+NubG-RHD3
(2) Cub-RHD3+NubG
(3) Cub-RHD3+LNP1-NubG
(4) Cub-RHD3+LNP2-NubG
-LT
-LTH
b
lnp2-1 ::
pLNP2:LNP2-YFP
35S:mCherry-HDEL
lnp2-1 ::
pLNP2:LNP2-YFP
35S:mCherry-RHD3
Input
IP-GFP
Input
IP-GFP
75KDa
Anti-GFP
150KDa
100KDa
75KDa
50KDa
37KDa
25KDa
Anti-RFP

Figure 3.2

Figure 3.3 | *LNPs* are required for normal plant cell development and formation of a normal tubular ER network. (**a**) *LNP1* and *LNP2* gene structures. The white boxes indicate untranslated regions (UTR), the blue boxes indicate exons, and the curved lines indicate the introns. The T-DNA insertion positions of *lnp1* and *lnp2* lines are shown in triangles. FP and RP are the primers used for RT-PCR. (**b**) RT-PCR of different *lnp1* (left) and *lnp2* (right) T-DNA mutants. EF1αA4 was used as the loading control. (**c**) Root hair phenotypes of *lnp1* and *lnp2* mutants. Scale bars = 100 μm. Right graph is the quantification of root hair length. *** indicates significant different from WT (p-value<0.001). (**d**) Developmental defects of *lnp1-1 lnp2-1* mutants and molecular complementation of *lnp1-1 lnp2-1.* (**e**) The ER morphology in WT and *lnp1-1lnp2-1* double mutant. (1-4) The confocal (1, 2) and Airyscan (3, 4) imaging of the ER network in hypocotyl cells of wild type (**1, 3**) or *lnp1-1 lnp2-1* (**2, 4**) seedlings expressing YFP-HDEL. The enlarged regions are indicated by dashed red squares. Compared with wild type, there are much more dense ER junctions in *lnp1-1 lnp2-1* mutant cells. Scale bars = 5 μm.

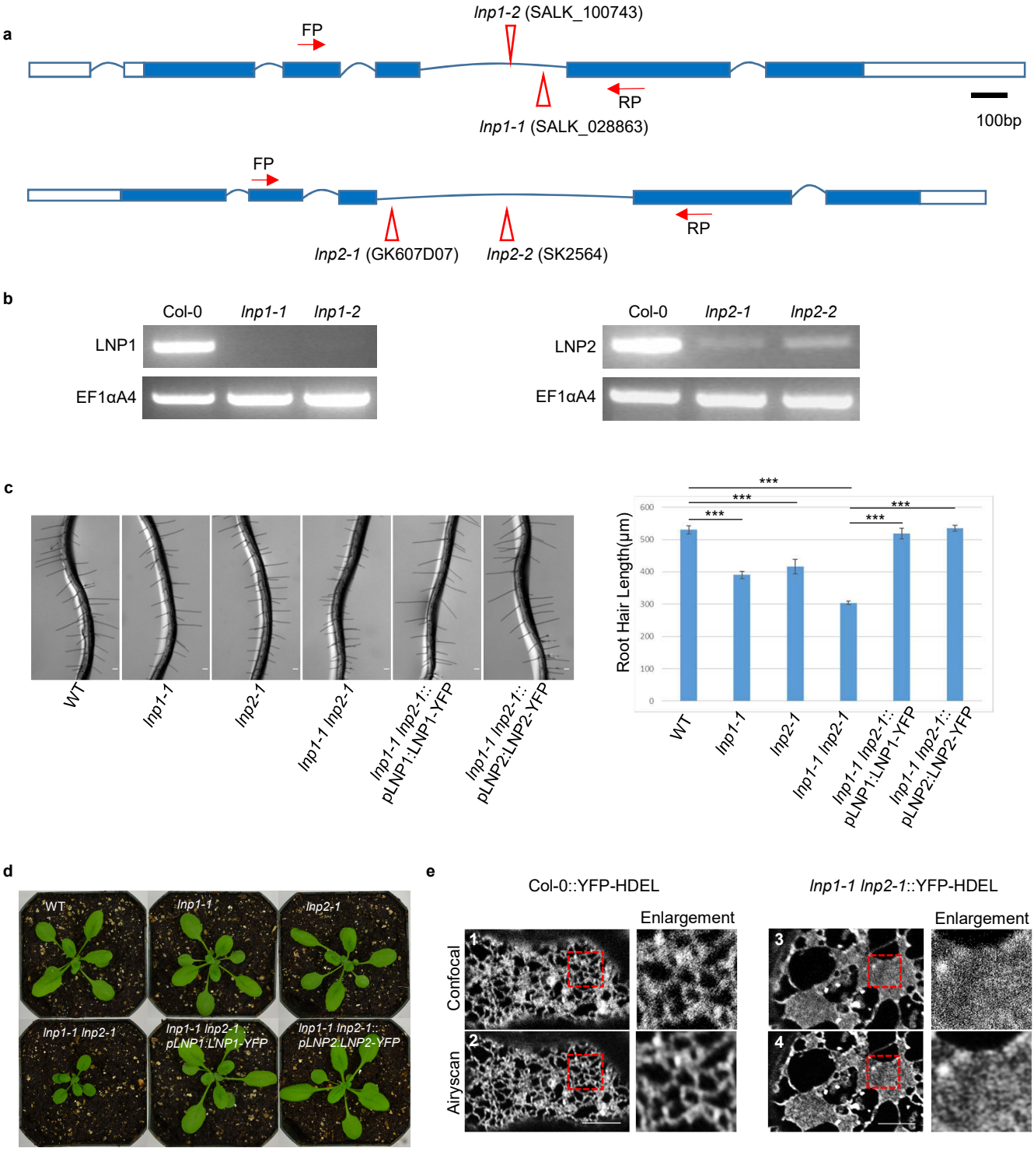
a
lnp1-2 (SALK_100743)
FP
RP
lnp1-1 (SALK_028863)
100bp
FP
RP
lnp2-1 (GK607D07)
lnp2-2 (SK2564)
b
Col-0
lnp1-1
lnp1-2
LNP1
EF1αA4
Col-0
lnp2-1
lnp2-2
LNP2
EF1αA4
c
WT
lnp1-1
lnp2-1
lnp1-1 lnp2-1
lnp1-1 lnp2-1:: pLNP1:LNP1-YFP
lnp1-1 lnp2-1:: pLNP2:LNP2-YFP
Root Hair Length(μm)
***
d
WT
lnp1-1
lnp2-1
lnp1-1 lnp2-1
lnp1-1 lnp2-1 :: pLNP1:LNP1-YFP
lnp1-1 lnp2-1:: pLNP2:LNP2-YFP
e
Col-0::YFP-HDEL
lnp1-1 lnp2-1::YFP-HDEL
Enlargement
Confocal
Airyscan
1
2
3
4

Figure 3.3

Figure 3.4 | The localization of Lunapark proteins to 3-way junctions of the ER requires RHD3. (**a**) The localization of LNP1 and LNP2 driven by their native promoter. Both showed punctate pattern. Scale bar = 5 μm. (**b-c**) LNP1 (b) and LNP2 (c) is localized on 3-way junctions of the ER. The cotyledon cells of *lnp1-1* or *lnp2-1* seedlings expressing LNP1-YFP or LNP2-YFP driven by its native promoter and RFP-HDEL were used for imaging. Scale bar = 10 μm. (**d**) LNP1 and LNP2 are mis-localized to ER tubules in *rhd3-8* mutant. Scale bar = 5 μm.

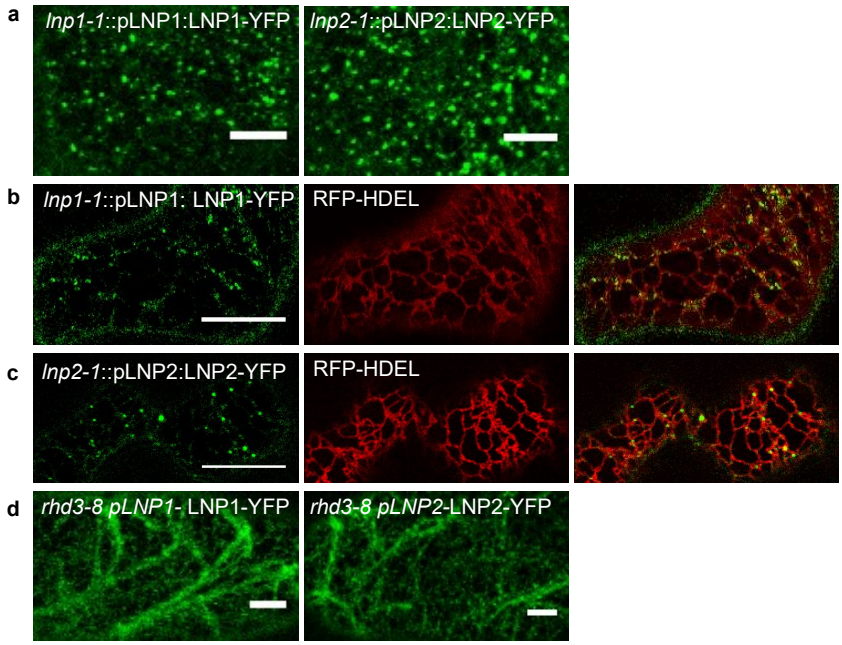
a
lnp1-1::pLNP1:LNP1-YFP
lnp2-1::pLNP2:LNP2-YFP
b
lnp1-1::pLNP1: LNP1-YFP
RFP-HDEL
c
lnp2-1::pLNP2:LNP2-YFP
RFP-HDEL
d
rhd3-8 pLNP1- LNP1-YFP
rhd3-8 pLNP2-LNP2-YFP

Figure 3.4

Figure 3.5 | Lunapark proteins stabilize newly formed junctions of the ER. (**a**) An example of an unstable newly formed ER junction lacking LNP2-RFP. (**b**) An example of a stable newly formed junction with LNP2-RFP. The arrows point at the newly formed junction. YFP-HDEL and LNP2-RFP were co-expressed in the tobacco leaves and observed 2-days after infiltration. (**c**) The numbers of junctions with or without LNP2 present in different time periods were quantified. 112 newly formed junctions without LNP2 and 58 newly formed junctions with LNP2 were quantified.

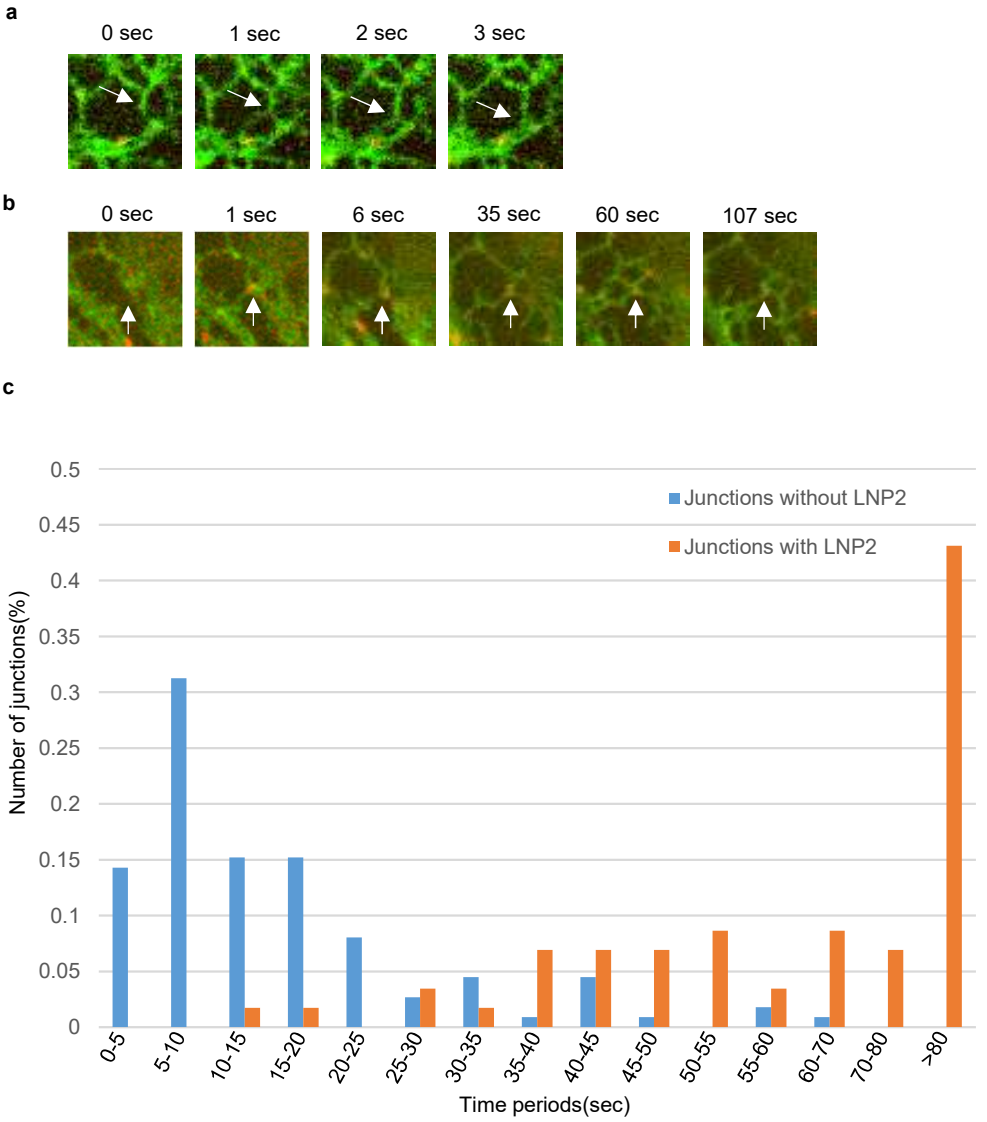
a
0 sec
1 sec
2 sec
3 sec
b
0 sec
1 sec
6 sec
35 sec
60 sec
107 sec
c
Junctions without LNP2
Junctions with LNP2
Number of junctions(%)
0.5
0.45
0.4
0.35
0.3
0.25
0.2
0.15
0.1
0.05
0
0-5
5-10
10-15
15-20
20-25
25-30
30-35
35-40
40-45
45-50
50-55
55-60
60-70
70-80
>80
Time periods(sec)

Figure 3.5

Figure 6 | LNP proteins inhibit fusion activity of RHD3. (**a-d**) The representative images of three different transient expressions in the tobacco leaves. (**a**) YFP-HDEL alone, OD=0.01; (**b**) YFP-HDEL (OD=0.01) and mCherry-RHD3 (OD=0.1); (**c**) LNP1-YFP (OD=0.01) and mCherry-RHD3(OD=0.1); (**d**) LNP2-YFP (OD=0.01) and mCherry-RHD3(OD=0.1). Scale bar = 10 μm. (**e**) Quantification of the number of cells with sheet ER in the total cell number examined in the three different infiltration conditions. Data was from three different repeats. *** represents p-value<0.001(t-test). (**f**) Yeast ER fusion test for different yeast strains indicated. *** represents p-value<0.001(t-test) and NS stands for no significant difference. The error bars represent standard deviation.

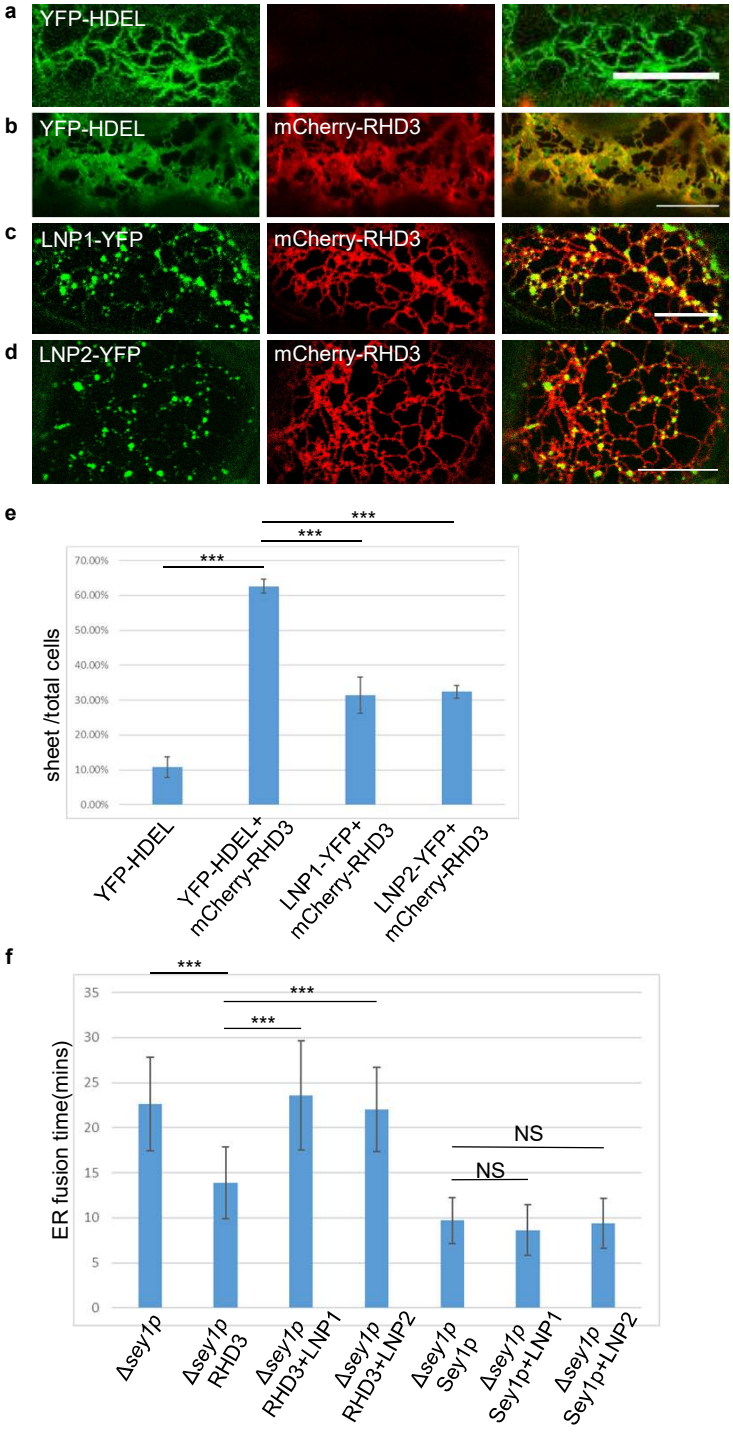
a
YFP-HDEL
b
YFP-HDEL
mCherry-RHD3
c
LNP1-YFP
mCherry-RHD3
d
LNP2-YFP
mCherry-RHD3
e
***
***
***
70.00%
60.00%
50.00%
40.00%
30.00%
20.00%
10.00%
0.00%
sheet /total cells
YFP-HDEL
YFP-HDEL+ mCherry-RHD3
LNP1-YFP+ mCherry-RHD3
LNP2-YFP+ mCherry-RHD3
f
***
***
***
NS
NS
35
30
25
20
15
10
5
0
ER fusion time(mins)
Δsey1p
Δsey1p RHD3
Δsey1p RHD3+LNP1
Δsey1p RHD3+LNP2
Δsey1p Sey1p
Δsey1p Sey1p+LNP1
Δsey1p Sey1p+LNP2

Figure 3.6

Figure 3.7 | LNPs promote the protein degradation of RHD3. (**a**) The root hair and plant phenotypes of *rhd3-8*, *rhd3-8 lnp1-1* and *rhd3-8 lnp2-1*. Deletion of *LNP1* and *LNP2* partially rescues *rhd3-8* mutant phenotype. (**b**) Quantification of root hair length of *rhd3-8*, *rhd3-8 lnp1-1* and *rhd3-8 lnp2-1*. *** represents p-value<0.001(t-test). (**c**) The root hair phenotypes of *rhd3-8*, *rhd3-8*::35S:LNP1-YFP and *rhd3-8*::35S:LNP2-YFP. Overexpression of LNP1 and LNP2 enhanced *rhd3-8* mutant phenotype. (**d**) Quantification of root hair length of *rhd3-8*, *rhd3-8*::35S:LNP1-YFP and *rhd3-8*::35S:LNP2-YFP. *** represents p-value<0.001(t-test). (**e**) The RHD3 protein expression levels in *rhd3-8*, WT and *lnp1-1 lnp2-1* mutant plants. Total proteins were extracted from 4-days seedlings and used for western blot. The protein expression of RHD3 is higher in *lnp1-1 lnp2-1* than that in WT. *rhd3-8* was used as the negative control for checking the specificity of the antibody. Coomassie blue staining is used as the loading control. (**f**) The RNA expression level of *RHD3* in WT and *lnp1lnp2* mutant plants. Total RNAs were extracted from 4-days seedings and used for RT-PCR. The RNA expression of *RHD3* is the same in WT and *lnp1-1 lnp2-1*. The expression of *Actin2* was used as the loading control.

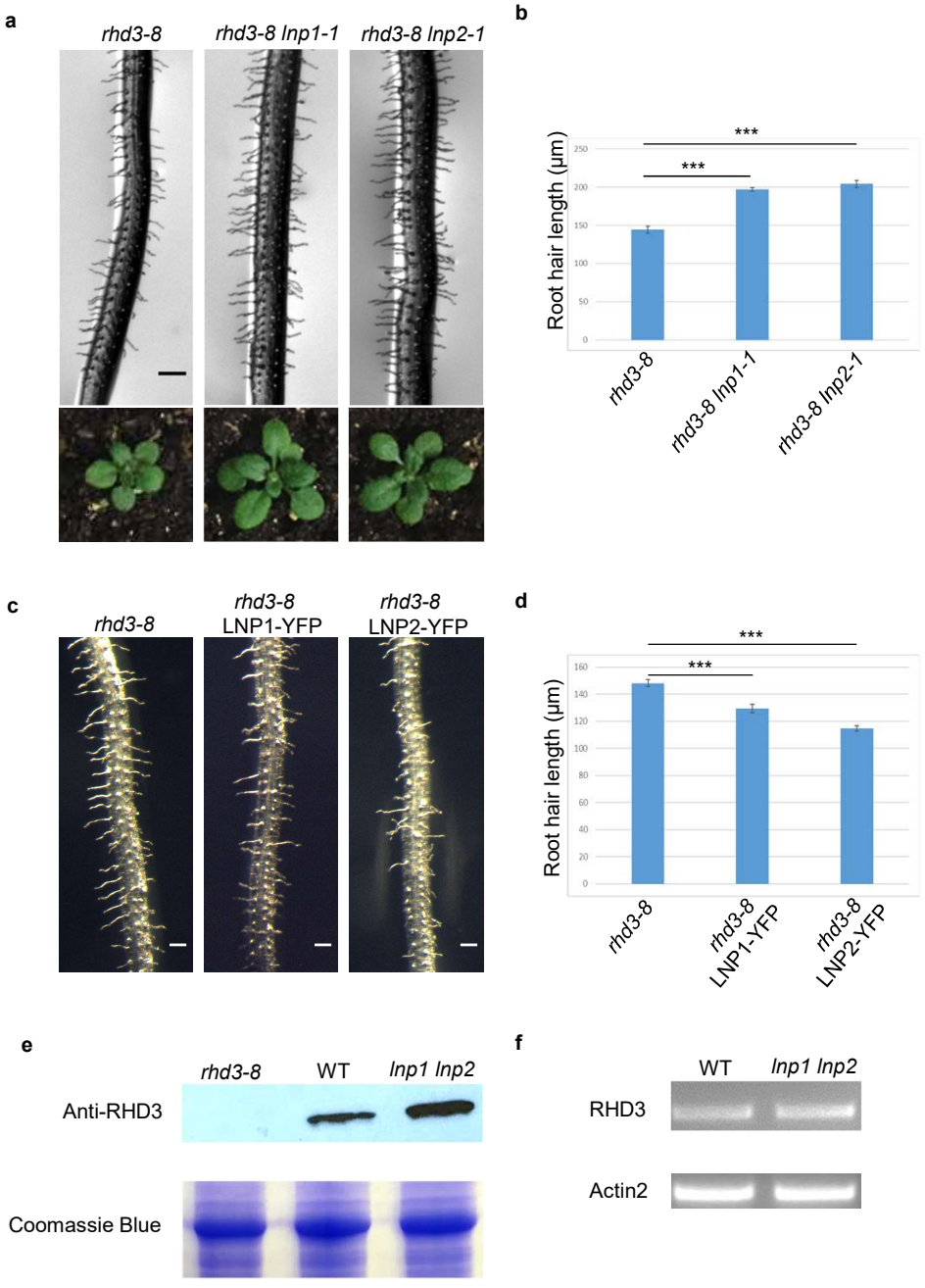
a
rhd3-8
rhd3-8 lnp1-1
rhd3-8 lnp2-1
b
Root hair length (μm)
***
***
rhd3-8
rhd3-8 lnp1-1
rhd3-8 lnp2-1
c
rhd3-8
rhd3-8 LNP1-YFP
rhd3-8 LNP2-YFP
d
Root hair length (μm)
***
***
rhd3-8
rhd3-8 LNP1-YFP
rhd3-8 LNP2-YFP
e
rhd3-8
WT
lnp1 lnp2
Anti-RHD3
Coomassie Blue
f
WT
lnp1 lnp2
RHD3
Actin2

Figure 3.7

Supplemental Figures

Supplemental Figure 3.1 | LNPs form an evolutionary conserved protein family. (**a**) The overall domain organization of LNPs. TM1 and TM2 stand for transmembrane domain 1 and 2. (**b**) The multiple sequence alignment of N-terminus, TM1, TM2 and Zinc finger motif within *Arabidopsis* LNP1 and LNP2, human LNP1 and yeast LNP1p. The multiple sequence alignment was done by MUSCLE. The hydrophobic residues are in blue, the positive charged residues are in red, the negative charged residues are in magenta, and the polar uncharged residues are in green. The conserved four cysteine residues are pointed by the arrows.

a

b

N-terminus

Transmembrane domains

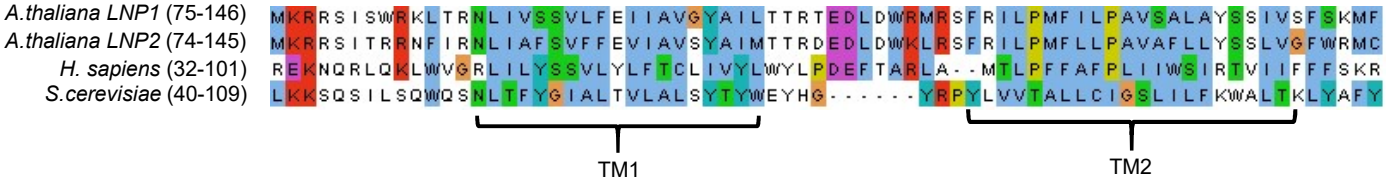

Zinc finger motif

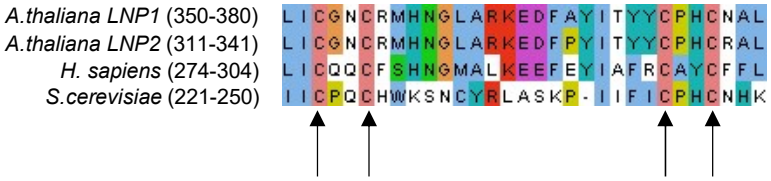

Supplemental Figure 3.1

Supplemental Figure 3.2 | *Arabidopsis* LNPs are ubiquitously expressed. (**a-b**) LNP1 (a) and LNP2 (b) are expressed in hypocotyl, cotyledon, stomata, root tips and growing root hairs. 4 days after germination, *lnp1-1*::pLNP1:LNP1-YFP and *lnp2-1*::pLNP2:LNP2-YFP seedlings were taken for imaging. Scale Bar = 10 μm. The Scale bar of root hair images is 5 μm.

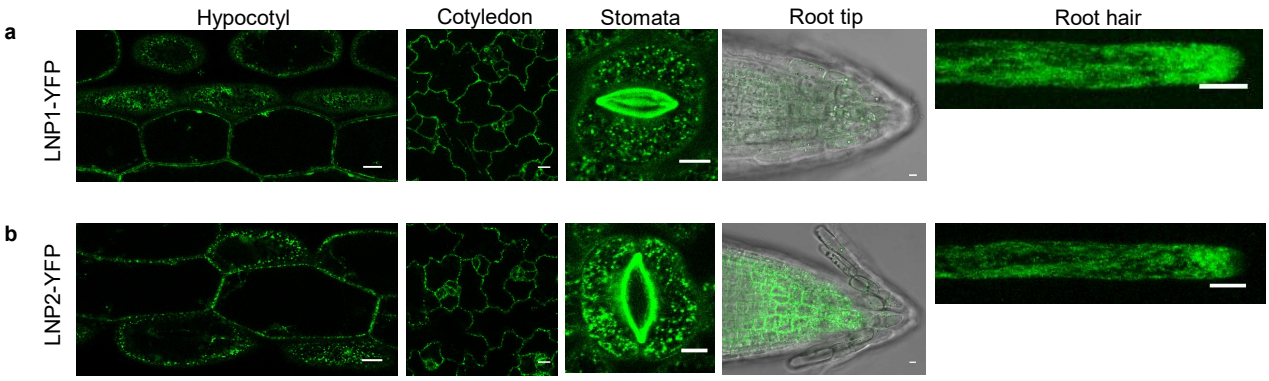

Supplemental Figure 3.2

Supplemental Figure 3.3 | The localizations of LNPs are dependent of RHD3. (**a-d**) The tubule localization of LNP1 (a, b) and LNP2 (c, d) in the presence of RHD3(S51N) (a, c) or RHD3(T75A) (b, d) in tobacco leave cells. (**e-h**) Expression of LNP1 (e, f) and LNP2 (g, h) in the absence (e, g) and presence (f, h) of RHD3 in tobacco leave cells. In the absence of RHD3, LNP1 (e) and LNP2 (g) was also observed in tubule ER in addition to 3-way junctions of the ER, but in the presence of RHD3, LNP1 (f) and LNP2 (h) was only observed in punctae colocalized with RHD3. The Scale Bar = 10 μm.

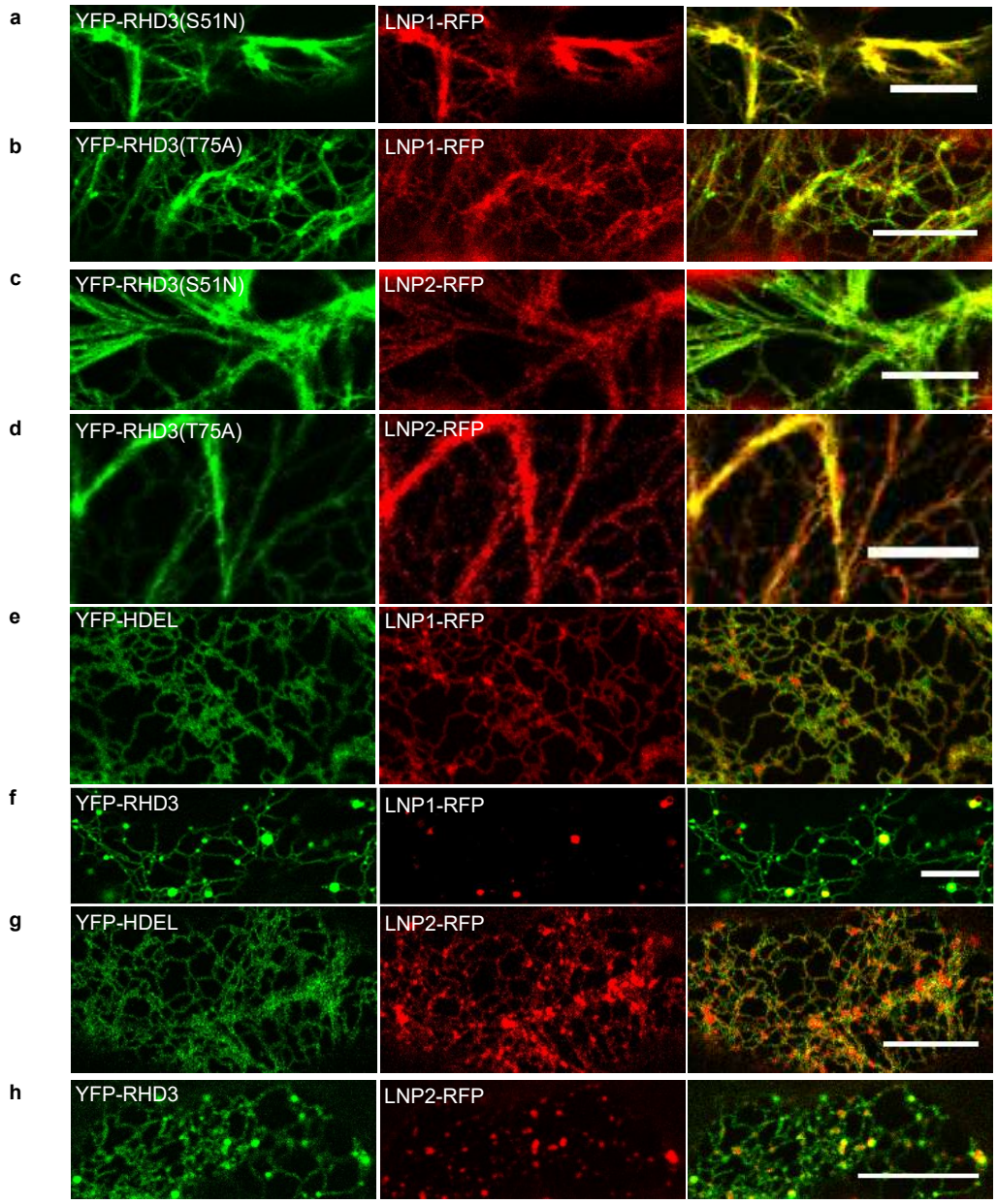

Supplemental Figure 3.3

Supplemental Figure 3.4 | Overexpression of RHD3 generates massive ER sheets with dense ER junctions. **(a-b)** The ER network labelled by YFP-HDEL in the absence (a) and presence (b) of RHD3 Airyscan images of ER sheets indicated that these sheets are actually ER with dense ER junctions. The enlarged regions are indicated by dashed red squares. Scale bar = 5 μm.

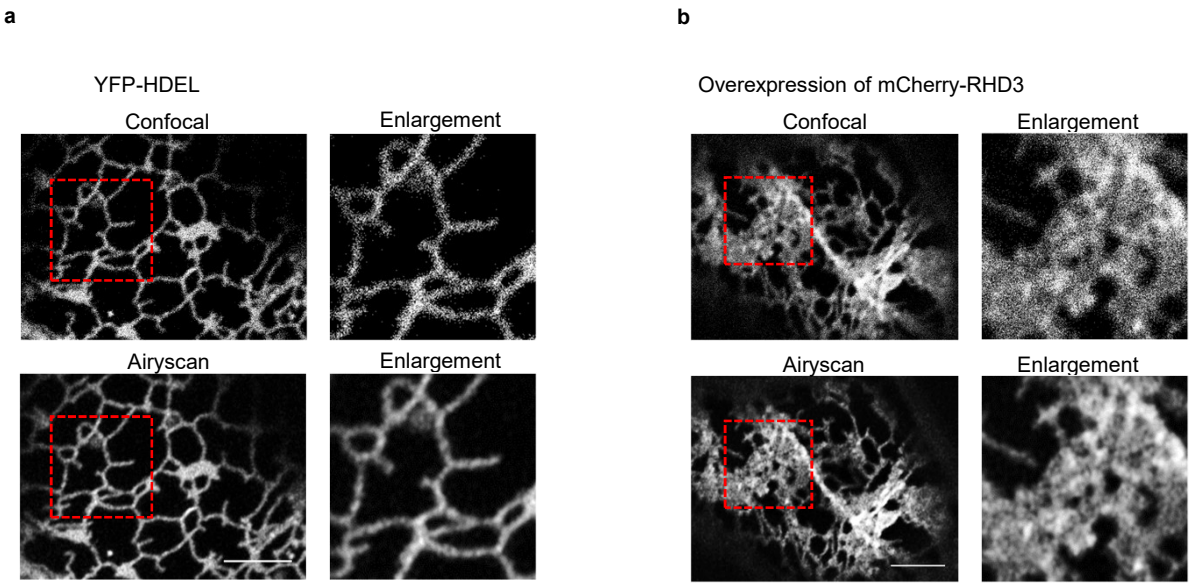

Supplemental Figure 3.4

CHAPTER IV:

CONCLUSIONS

In this thesis, I studied the action and regulation of RHD3 in the formation of interconnected tubular ER network in *Arabidopsis thaliana*.

4.1. Efficient ER membrane fusion mediated by RHD3 requires a dimerization of RHD3 through different domains and a membrane anchoring via C-terminal tail of RHD3

To date, the knowledge on how RHD3 is involved in mediating the ER membrane fusion is very limited. Based on the fact that the overall structure between RHD3 and Sey1p is very similar (Stefano and Brandizzi, 2014), in the first part of my study, I simulated the structure of cytosolic N-terminus of RHD3 based on the crystal structure of Sey1p (Yan et al., 2015). I noticed that the cytosolic N-terminus of RHD3 could form a dimer, with two GTPase domains facing to each other and a twisted arm of two middle domains composed of four 3HBs.

By mapping the previous reported mutations of RHD3 to this simulated structure, I found that a genetic mutation D185N(*rhd3-2*) (Wang et al., 1997) is within the interface of two RHD3 molecules. I proposed that D185N mutation may disrupt the two potential D185-R101 salt bridges in the interface, thereby reduce the efficiency of the ER membrane fusion mediated by RHD3. The results from yeast two hybrid, yeast ER fusion assay, transient expression of the mutated versions of RHD3, strongly supported that the dimerization via D185-R101 salt bridges in the GTPase domain is required for the efficient ER fusion mediated by RHD3.

The simulated structure suggests that the long middle domain of RHD3 contains four different 3HBs. To understand the roles of each 3HB, Proline substitutions were introduced into two

different conserved hydrophobic residues in each 3HB to disrupt the α-helix (Pendin et al., 2011). Transient expression of mutated RHD3 showed that mutations in the first and second 3HBs, exerted dominant negative effects on the formation of tubular ER network, however, mutations in the third and four 3HBs, converted RHD3 into puncta distribution on ER tubules without any effect on the formation of tubular ER network. The yeast two hybrid and yeast ER fusion assay suggested that the first and second 3HBs are involved in the dimerization of RHD3 and efficient ER fusion. With the fluorescent intensity quantification and western blot, I revealed that the third and fourth 3HBs are required for the stability of RHD3.

There are two predicted transmembrane domains (TMs) in the RHD3 protein. The depletion of two TMs in RHD3 shifts the localization of RHD3 from the ER membrane largely to the cytosol with the cis-Golgi and occasional ER tubules localization. The yeast two hybrid results suggest that in addition to the membrane anchoring ability, the TMs also facilitate homotypic interaction of RHD3.

With a detailed analysis of the sequence of C-terminal tail (CT) of RHD3, I found that there is a conserved amphipathic helix and a divergent sequence in the CT of RHD3. The CT fragment of RHD3 is able to localize to distinct membrane structures, including the ER membrane and Golgi, indicating a potential membrane targeting ability of the CT of RHD3. Introducing acidic substitutions, but not hydrophobic substitutions in the hydrophobic face of the conserved amphipathic helix of RHD3, disrupted the membrane targeting ability of the CT, as well as the efficient ER fusion mediated by RHD3, indicating that this amphipathic helix mediated membrane targeting is required for efficient ER fusion.

With these detailed structure-based mutagenesis analyses, it appears that ER fusion mediated by RHD3 requires a delicate coordinated action of different domains of RHD3. This study contributes to a better understanding of the molecular mechanism of how the evolutionarily conserved ER tubular network is formed in plant cells.

In the future, more research can be performed to better understand the mechanism how RHD3 is involved in mediating ER membrane fusion. For example, it will be necessary to study the real structure of RHD3 with GTP and GDP with cryo-electron microscopy or X-ray to confirm the RHD3 structure simulated here. As an ER fusogen, likely RHD3 will operate together with other proteins, it is important to find the possible RHD3 interacting proteins that cooperate with RHD3 in mediating ER membrane fusion with yeast two hybrid, mass spectrometry or BiFC screening. In yeast cells, independent pathways parallel to Sey1p has been proposed (Rogers et al., 2014), to fully understand the regulation of the formation of the tubular ER network in plant cells, it will be also interesting to study e.g. using genetic screen if in plants there are RHD3 independent parallel pathways involved in the ER membrane fusion, for example it will be interesting to test if plant SNAREs and Rabs GTPases are involved in the ER fusion. Last but not least, it is known that plants can adapt to different environments with a significant ER morphology change, it will be interesting to check if the function of RHD3 mediated ER membrane formation in plant response to different environmental stimuli.

4.2. Fusion activity of RHD3 is regulated by Lunapark proteins

As an ER membrane fusogen, the fusion actin of RHD3 should be regulated or balanced in a very dedicated way. Unfortunately, how the action of RHD3 is regulated is virtually unknown. To explore the potential regulators of RHD3, I built a 3-in-1 BiFC based system for screening protein interactors of RHD3. I found that LNP1 and LNP2, two Lunapark homologs (Chen et al., 2012) in *Arabidopsis*, interact with RHD3 on 3-way junctions of the ER. Their interactions are confirmed with yeast two hybrid and Co-IP experiments.

LNP1 and LNP2 have functional redundancy in root hair growth and plant cell development. Double mutant lnp1 lnp2 has short root hairs and pleiotropic developmental growth defects with massive sheet-like ER with condensed 3-way junctions in the cells. The expressions of LNP1 and LNP2 are overlapped in diverse tissues.

LNP1 and LNP2 under a native promoter localize to 3-way junctions of the ER network. This 3-way junction localization of LNP1 and LNP2 are dependent on RHD3, since in the *rhd3* mutant or in the presence of dominant negative RHD3 mutants, the localizations of LNP1 and LNP2 are evenly distributed on the ER tubules. With live imaging, I found that the stability of nascent 3-way junctions of the ER is highly correlated with the presence of LNPs, suggesting that LNPs can stabilize the nascent 3-way junctions in the plant cells.

Co-expression of LNPs with RHD3 in the tobacco leaves or yeast cells, the ER fusion activity of RHD3 was significantly inhibited. According to the western blot results in WT and *lnp1 lnp2* mutant, the protein expression level of RHD3 is much higher in *lnp1 lnp2* mutant, indicating that LNPs may promote the protein degradation of RHD3.

Taking all together, I proposed that there is a post-membrane fusion regulatory system in the plant cells. RHD3 mediates ER membrane fusion, after which LNPs will be recruited by RHD3 to 3-way junctions of the ER to inhibit the action of RHD3 by promoting the protein degradation of RHD3. With this action, the newly formed 3-way junctions will be stabilized and an interconnected ER network can be formed and maintained.

This work is the first report that there are functional Lunapark homologs in plants. It is also the first report of the functional significance of LNPs in cell and tissue development in eukaryotes. In the future, it will be very interesting to see if the actin of yeast Sey1p and mammalian Atlastin are also regulated by LNPs in yeast and mammalian cells, respectively. Furthermore, it will be important to examine how LNPs promote the protein degradation of RHD3 in the cells. For this, the interaction between RHD3 and components of ubiquitin ligases can be selectively tested, the ubiquitin level and degradation level of RHD3 in WT and *lnp1 lnp2* mutant plants can also be tested. A supernumerary of RHD3 could cause an excessive fusion of the ER, how does this excessive fusion relate to unstable 3-way junctions? The sliding speed of ER tubule and the stability of 3-way junctions can be checked after overexpression of RHD3. Because Lnp1 interacts with Rtn1p and Yop1p in yeast cells (Chen et al., 2012), it may be also important to examine the functional relationship between LNPs and Rtns and Yop1 e.g. whether LNPs can also regulate the action of these ER shaping proteins, or that these ER shaping proteins can somehow regulate the activity of LNPs. Finally, although I showed here that LNPs are an important regulator of the ER morphology, the loss of LNPs does not result in a severe cell developmental phenotype. This suggests that there must be plant specific pathway involved in the compensation of the loss of

LNPs in cell development in plants. To explore this, genetic screen for enhancers and/or suppressor of the *lnp* mutant could conducted. Once genes are identified, the detailed mechanisms can then be illustrated.

4.3. REFERENCES

Chen, S., Novick, P., and Ferro-Novick, S. (2012). ER network formation requires a balance of the dynamin-like GTPase Sey1p and the Lunapark family member Lnp1p. Nat Cell Biol *14*, 707-716.

Pendin, D., Tosetto, J., Moss, T.J., Andreazza, C., Moro, S., McNew, J.A., and Daga, A. (2011). GTP-dependent packing of a three-helix bundle is required for atlastin-mediated fusion. Proc Natl Acad Sci U S A *108*, 16283-16288.

Rogers, J.V., McMahon, C., Baryshnikova, A., Hughson, F.M., and Rose, M.D. (2014). ER-associated retrograde SNAREs and the Dsl1 complex mediate an alternative, Sey1p-independent homotypic ER fusion pathway. Mol Biol Cell *25*, 3401-3412.

Stefano, G., and Brandizzi, F. (2014). Unique and conserved features of the plant ER-shaping GTPase RHD3. Cellular logistics *4*, e28217.

Wang, H., Lockwood, S.K., Hoeltzel, M.F., and Schiefelbein, J.W. (1997). The ROOT HAIR DEFECTIVE3 gene encodes an evolutionarily conserved protein with GTP-binding motifs and is required for regulated cell enlargement in Arabidopsis. Genes Dev *11*, 799-811.

Yan, L., Sun, S., Wang, W., Shi, J., Hu, X., Wang, S., Su, D., Rao, Z., Hu, J., and Lou, Z. (2015). Structures of the yeast dynamin-like GTPase Sey1p provide insight into homotypic ER fusion. The Journal of Cell Biology *210*, 961-972.